CHALMERS
UNIVERSITY OF TECHNOLOGY

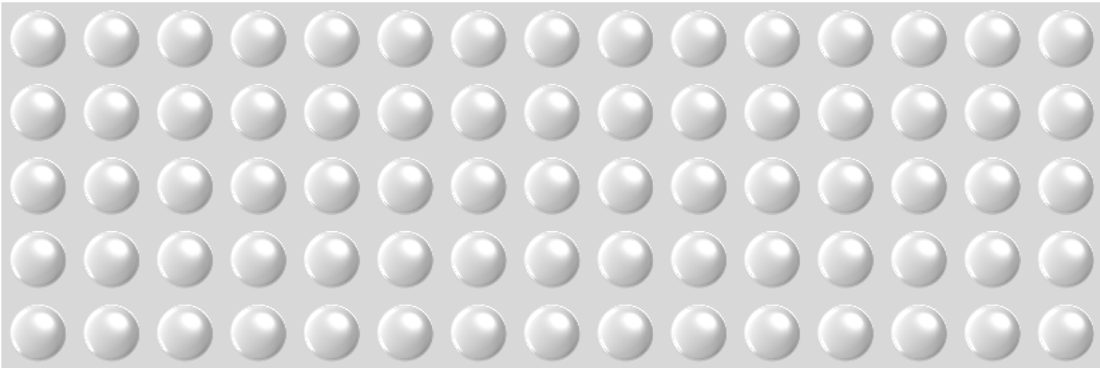

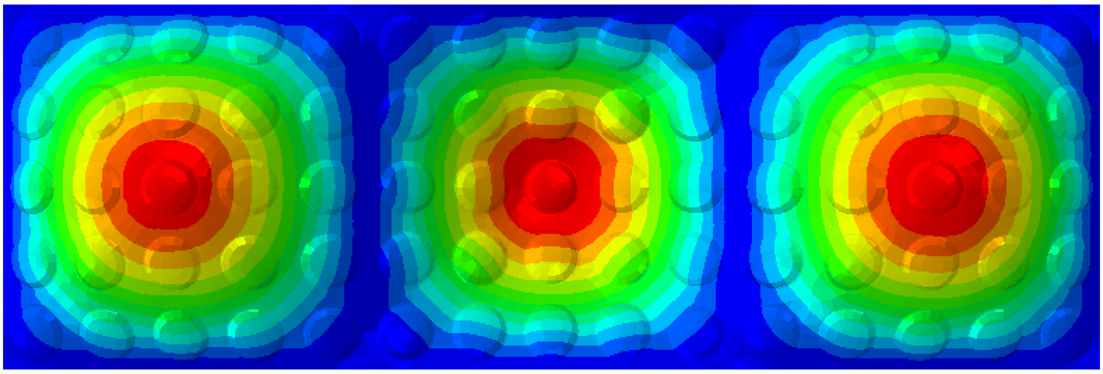

A novel concept for enhancement of the buckling capacity of thin plates via geometric modification.

Master's thesis in Master's Programme Structural Engineering and Building Technology

Maharaghni Chennapragada
Malik Sheraz Nazam

Architecture and Civil Engineering

CHALMERS UNIVERSITY OF TECHNOLOGY
Gothenburg, Sweden 2021
www.chalmers.se

Master's thesis 2021

A novel concept for enhancement of the buckling capacity of thin plates via geometric modification.

Maharaghni Chennapragada
Malik Sheraz Nazam

Department of Architecture and Civil Engineering
Chalmers University of Technology
Gothenburg, Sweden 2021

A novel concept for enhancement of the buckling capacity of thin plates via geometric modification.

Maharaghni Chennapragada
Malik Sheraz Nazam

Supervisor: Rasoul Atashipour, Architecture and Civil Engineering
Co-Supervisor: Mohammad Al-Emrani, Architecture and Civil Engineering
Examiner: Mohammad Al-Emrani, Architecture and Civil Engineering

Master's Thesis 2021
Department of Architecture and Civil Engineering
Structural Engineering and Building Technology
Lightweight Structures
Chalmers University of Technology
SE-412 96 Gothenburg
Telephone +46 31 772 1000

Cover: Stiffened Thin Plate with Circular Stiffeners and its Mode Shape under Uni-axial Compression.

Printed by Chalmers Reproservice
Gothenburg, Sweden 2021

A novel concept for enhancement of the buckling capacity of thin plates via geometric modification.
Maharaghni Chennapragada
Malik Sheraz Nazam
Department of Architecture and Civil Engineering
Chalmers University of Technology

Abstract

The extensive use of thin-walled structures in various field owing to their know advantages motivates the further research to mitigate their failure due to buckling. Thin-walled members are dominantly susceptible to failure due to the buckling, so, a great effort has been devoted in the past decades to postpone the buckling using different stiffening approaches. However, almost all these techniques result in additional weight which reduces their lightweight performance. So, this study deals with assessing an innovative idea of increasing the buckling performance by the introduction of multiple stiffening shapes of thin-walled panel without increasing the mass of the plate.Flat plates are strengthened based on the innovative concept with various geometrical configuration of augmented sub-surface areas and subjected to varying type of in-plane loads.

A comprehensive linear buckling parametric study is conducted over a wide range of varying dimensions, loading, and stiffening shapes to investigate their effect on critical buckling capacity and identify the optimal geometry. Thin plates with thickness ranging from 0.05% to 1% of their width are analysed for multiple stiffening shapes and pattern. Stiffening unit cell shapes include circular, square, triangle and capsule. The study is carried out by developing FE parametric models in a programming language known as Python relying on the use of finite element (FE) software ABAQUS-CAE, to run a large number of simulations and gather results in an efficient manner. Sensitivity analyses are conducted over multiple geometrical parameters in relation to critical buckling load, leading to recommendation of most optimal patterns according to the implemented shape stiffening concept.

FE method of analysis is validated through comparison with available analytical solution in the literature for flat buckling under uni-axial, bi-axial and shear loading. Over the specified thickness range, an extensive parametric study is conducted with circular-unit-cell shape stiffeners.About Two thousand and sixty models for each the three aspect ratios and three load case generates a total of more than eighteen thousand five hundred cases. Due to the time-consuming nature of the computations the parallel processing cluster computing facility at Chalmers is utilised to execute, gather and export results. Hence the obtained results constituted a large range of comparable parameters and their dependency on improvement of buckling capacity is assessed. The results highlight the importance of stiffener density and dimensions. This stiffening is observed to be most beneficial for thinner plates and as the thickness increased, the % improvement decreased. The study of the results also reflect upon the importance of careful selection of the most optimized pattern for a design

situation. In order to examine the unit-cell shape's potential for enhancement of the buckling load capacity, in addition of a large number of modeling and analyses of the circular stiffening shape, other geometric shapes are examined, including square, triangular and capsule shaped stiffeners. The square space with most surface area offered the best improvement compared to others.

Results from non-linear analysis reflect that geometric and material non linearity is affecting buckling strength of flat plate and stiffened plate in similar proportion. Non-linear analysis also indicate that stiffening shapes are leading to more uniform distribution of stress as compared to flat plate.

For varying plate thickness, recommended stiffening patterns yield 114% - 1143% of increase in buckling capacity, conclusively establishing enhanced buckling capacity by introducing stiffening shapes. The varying level of disturbance to the first buckling mode depending on the shape and size of stiffeners leads to an increase in buckling capacity. Study results lead to a new technique in the research area of strengthening thin-walled structures without increasing the consumed constituent materials or adding the structures total weight.

Keywords: Shape Stiffeners, Linear Buckling, ABAQUS, PYTHON, Thin Plates, Post Buckling

Acknowledgements

This research study is the culmination of our Master's degree experience at the Chalmers University of Technology. Experience has not only been academically rewarding but also offered a great learning curve in terms of our personal growth.

We would take this opportunity to extend immense gratitude to Dr. Rasoul Atashpour and Dr. Mohammad Al-Emrani for providing us with the opportunity to work on such an interesting and innovative project. As supervisor and co-supervisor respectively, their inputs and constructive feedback have kept us motivated despite the challenges we faced. Thank you for always being available at every step of this project. Working under your supervision has been an enriching experience. We would also like to acknowledge one another for being a complimenting team members to each other.

During this pandemic, our families have paid an immense price emotionally, and despite tough circumstance provided us perfect grounds to focus on our studies. We would always be indebted to our families for their unconditional love and support throughout this period.

Maharaghni Chennapragada
Malik Sheraz Nazam
Chalmers, June 2021

Contents

List of Figures

List of Tables

1

Introduction

1.1 Background

Thin-walled structures have extensive application in building construction, aviation, marine, automobile, and other industries due to their high strength-weight ratio. The ease of production and efficient analytical tools have also contributed to the versatility of thin-wall structures.

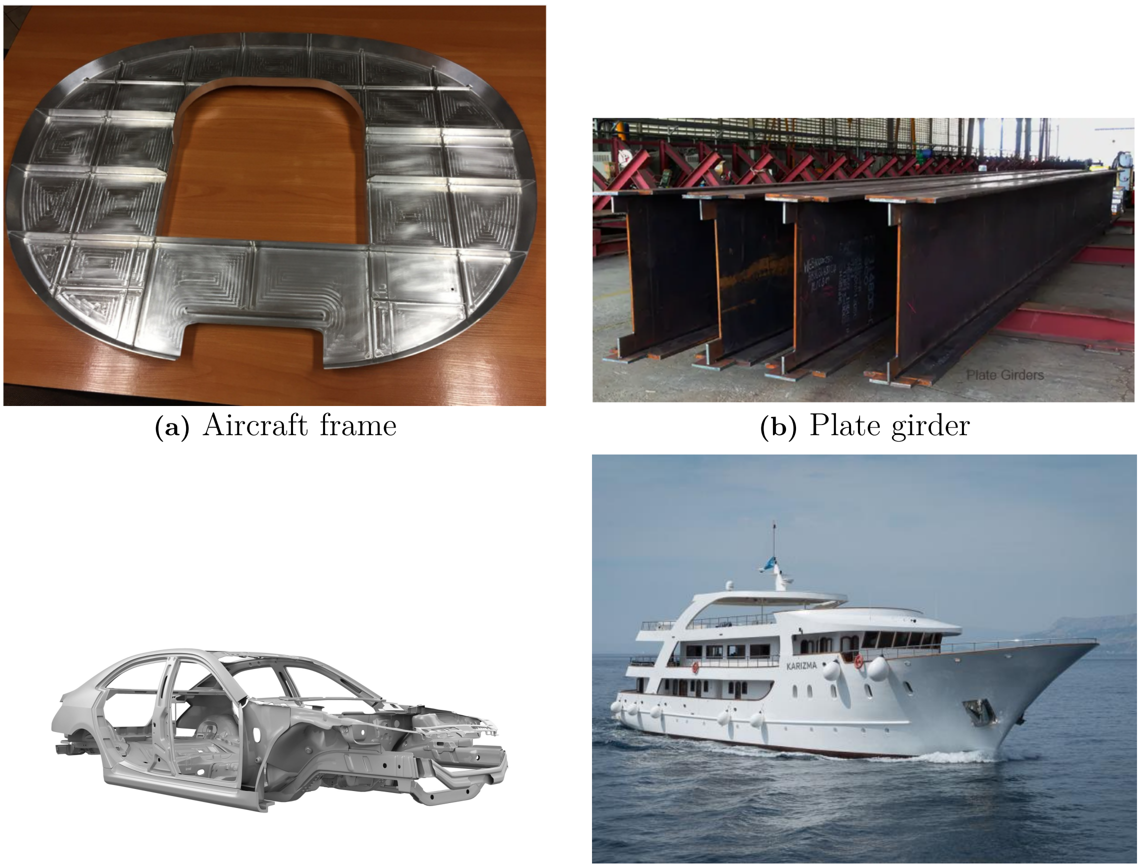

(a) Aircraft frame **(b)** Plate girder

(c) Car frame **(d)** Ship hull

Figure 1.1: Application of thin walled structures

However, using thin plates for structures also presents some inherent challenges because it is susceptible to buckling. Hence thin plates must be reinforced to mitigate the risk of buckling enabling the structure to maintain its shape and remain within acceptable deflection limits during its service life.

For quite a few centuries most straight forward solution of increasing rigidity of thin plates has been to add ribs or stiffeners like one illustrated in an example below.

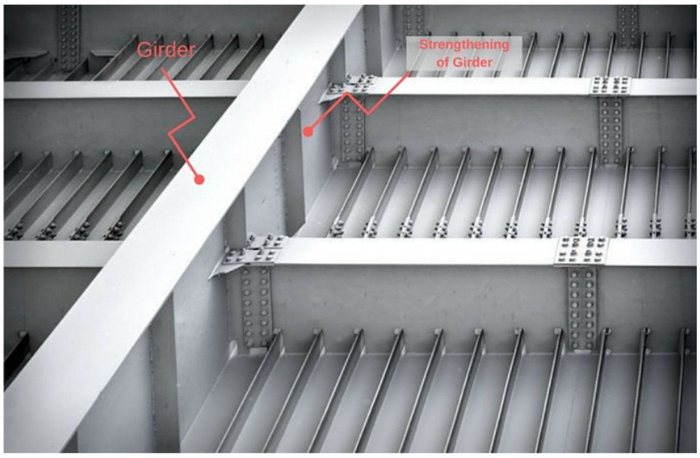

Figure 1.2: Stiffening thin plates

Design and spacing of such stiffeners is governed by structural requirement, hence global buckling strength of member can be increased, but they come with certain drawbacks. For example, strengthening stiffeners are added to main girder increasing the material consumption, manufacturing complexity and weight of the product. Considering the recent application of thin plates in space rockets, long span bridges and massive cargo ships etc., increasing weight might me an unacceptable trade off to increase the rigidity. Moreover, environmental footprint from increased material usage and life cycle cost associated with transportation of higher weight has motivated researchers to increase the structural strength without adding weight.

1.2 Core Concept

For a simply supported flat plate under uni-axial loading, the first buckling mode corresponds to mechanical energy absorbed by structure leading to buckling failure of the plate as shown in figure 1.3.

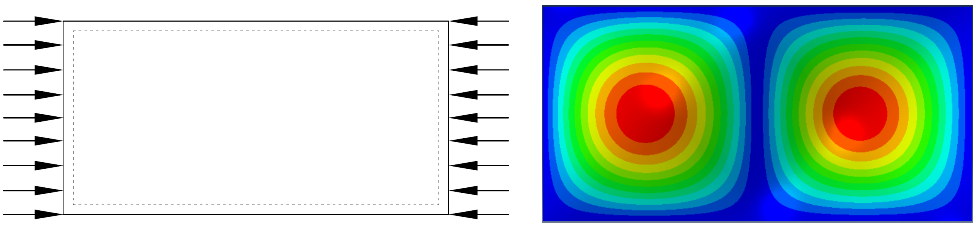

(a) Flat plate under uni-axial loading (b) First buckling mode

Figure 1.3: Buckling mode for simply supported flat plate under uni-axial compression load

Disturbing this buckling mode will lead to increased mechanical energy absorbed to failure. External stiffeners like ribs reduce the effective buckling width of the plate, disturbing the first buckling mode, hence increasing the rigidity of thin plates as illustrated in figure 1.4.

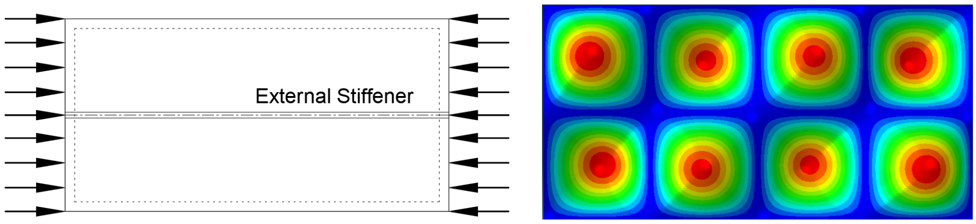

(a) Externally stiffened plate (b) First buckling mode

Figure 1.4: Buckling mode for simply supported externally stiffened plate under uni-axial compression load

Another logical approach to disturb the first buckling mode could be by making geometrical modifications on the plane of the plate. Such as introducing unit cells of different shapes and sizes, thus increasing buckling capacity of the plate. A plate modified by the proposed concept and different possible shapes of unit cells are shown in figure 1.5.

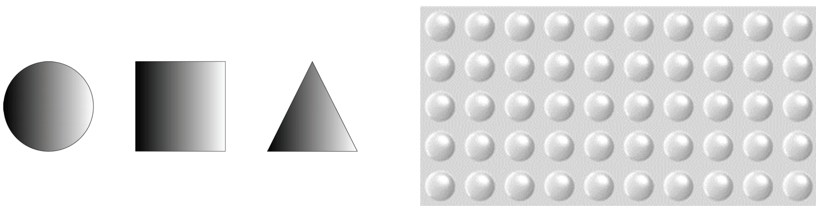

(a) Circular, rectangular and triangular unit cells (b) Plate modified with pattern of circular unit cells.

Figure 1.5: Different shapes of stiffening unit cells and geometrically modified plate by a pattern of circular unit cells.

1.3 Research Questions

The motivation behind the evolution of the proposal came from the thorough research and review of the contemporary methods. Therefore, these research questions drawn stimulated the idea.

- Production aspects:
  - The industrial demand to formulate a solution which has both structural and production value is growing. The manufacturing of the existing stiffeners require higher usage of material which lead to higher carbon footprints. Therefore, what modification can be made to the existing plate?
- Structural Behaviour:
  - Generally, the minimum thickness of thin plates for structural purpose is 4 mm. This is because of the high risk of buckling failure. Therefore there is a need to increase the efficiency of thinner plates to be suitable for a wider range of applications.Therefore, the behaviour of thin plate to structural loads is to be studied.
  - The early buckling failure is a result of concentration of resultant stresses (von misses stresses) to the central area. Therefore, pre-buckling stresses are needed to be distributed across the area of the member. We know that the load path is dependent of the stiffness properties. Therefore, by stiffening the plate allover its area, the stress area distributed to smaller sub areas. How can this be achieved?
  - The surface disturbances must be uniform over the area of flat plate. Yet, what effect does geometrical modification have of the buckling capacity of these thin steel plates?

1.4 Project Aim and Outline

The aim of this master's thesis is to explores a novel concept of geometrical modification by introducing multiple stiffening shapes on the surface of a flat plate to increase its stiffness. This enables stiffened plate to be able to have improved resistance against applied stresses and retain its shape.

Linear buckling response of stiffened plate with various shapes will be compared to flat plate response under uni-axial, bi-axial and shear loading. A brief structure of the report is as presented below:

> **Chapter 2** gives an insight into the research performed to analyse and upgrade the characteristics of a thin plate. This chapter presents critical review of the early work and theoretical conclusions made, which provide a basis for verification of the present work. The chapter also presents the failure criteria and the design stresses according to EN1993-1-5. Relevant studies performed are summarised which validate the motivation of the research.
>
> **Chapter 3** presents the methodology for using Finite Element Analysis. The

variables of this parametric study are explained and analysed to find the most optimized combination of all the defined parameters. It also presents a validation to the studies by comparing the numerical solutions to the theoretical solution of the flat plate. The method of modelings and its inputs like material properties, boundary conditions and loading were detailed.

Chapter 4 elaborates the results from parametric Eigen buckling analysis by relating them to the theoretical knowledge available. Followed, by results from post-buckling analysis reflecting on the behavior of the plate in terms of stress distribution and ultimate capacity.

Chapter 5 summarises the conclusions extracted from the extensive FE analysis. It also presents a scope for future investigations that could be made in this field.

1.5 Method

The current studies are conducted using "Eigen Value Buckling Analysis" of a thin plate. Thin plate considered falls under the Classification of Class lV (EN1993-1-5). The parameters of stiffening shapes introduced onto the plane of flat plate are varied over thickness ranging from 0.05% to 1% of plate width. These variations were automated using PYTHON Scripting. The work can be divided into three parts:

- The first part, which constitutes 80% of the thesis work is performed using Eigen Buckling Analysis on a plate with circular stiffeners. From the results of the first part, a validation of the advantage using this novel method is observed.
- A post buckling analysis is performed to observe the contribution of these shapes to the improvement of ultimate capacity.
- Various stiffener shapes such as square, capsule and triangle have been analysed using Linear Buckling Analysis for the third part of the work.

1.6 Limitations

The novelty of the concept meant limited literature to compare and validate the results. To study the effect of most critical parameters in given time, project had following limitations:

- Study is only limited to finite element analysis, as neither analytical solution nor experimental studies are available to validate the results for stiffened plate.
- Response of plate is only studied under pure uni-axial, bi-axial and shear loading. Interaction of multi-axial stresses in not studied.
- Simply supported boundary conditions are considered.
- At present, economically viable methods for mass production are not available, hence aspect related to production are not studied. These possibly could include spring back, plate thickness reduction and residual stresses.

2
Buckling of Thin-walled Members

2.1 Introduction

Recent advancement in metallurgy field of high strength steel has provided us with an opportunity to expand the horizon of application of thin steel plate to manufacture light weight products. Thin plate has its transverse dimension(thickness) much smaller in comparison to other two dimensions (length and width). Which can be written mathematically as

$$t/b << 1$$

Where "t" is plate thickness and "b" is plate width.
Owing to its economic advantages, reduced energy consumption and weight to strength ratio, light weight structures are experiencing burgeoning demand in construction industry, naval industry, automobile industry etc. The applicability of the thin plates in various sectors such as building, bridges, air crafts, ships, etc due to its light weight property has motivated many researches in the past to optimize and the strengthen plate is many diverse ways. Ultra-high strength steel of yield strength greater than 1780 MPa have been produced. However, high strength steel is vulnerable against buckling instability from compressive stresses generated under compressive loads, shear loads and combination of these loads at stresses much lower than yield strength. When the aforementioned loads are gradually applied on a structural member, a sudden out of plane deformation can be observed when the load reaches a critical value. This means that the member is buckled. This critical value could be more or less than the yield strength depending on the slenderness or stockiness of the member. For thin structural member, due to its low slenderness, the critical buckling load (N_{cr}) is generally less than its yield strength. This will cause sudden buckling failure in the member before it can reach the material failure.

2.2 Elastic Buckling

The compressive forces on a structural member can lead to instability and quick failure due to buckling. The parameters such as dimensions,loading and material properties have a major effect to determine the mode and critical buckling load of which can be seen in the later sections.

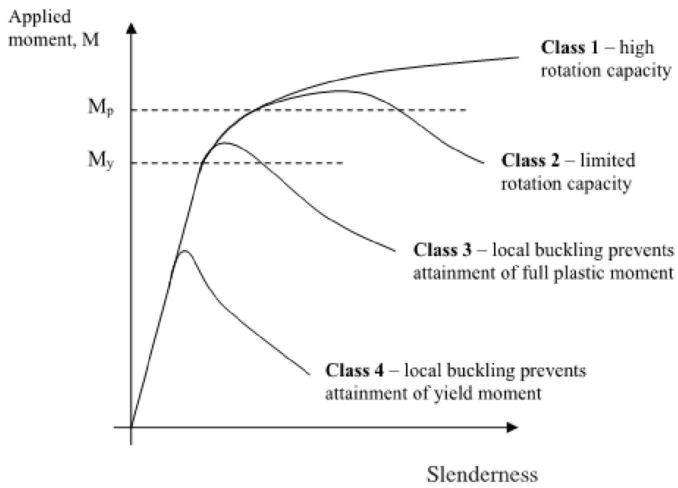

Figure 2.1: Effect of slenderness on moment capacity [1]

The major concern of all the factors is the slenderness of the compression member. Eurocode define four categories of classification, as shown in figure 2.1, to determine the risk of local buckling with respect to slenderness of the member.

Class l: This class corresponds to compact or a plastic cross-section(very low slenderness). The risk of local buckling is either none or very less. The stresses due to loading might cause progressive yielding until the section reaches ultimate capacity. These sections can develop a plastic hinge which has strength to attain complete failure mechanism.

Class ll: This class also corresponds to compact cross-section but the plastic hinge developed does not have enough strength to form a complete failure mechanism.

Class lll: This class also corresponds to semi compact section.There is a risk of local buckling which will not allow the section to develop plastic moment. The section develops only the yield moment.

Class lV: This class also corresponds to slender or thin walled section. The section will not attain yielding due to premature buckling locally before the linear elastic limit has reached.

Note 1: This thesis focuses of the Class lV sections. Substantially, the analysis carried out is **Linear Elastic Buckling Analysis** as the class lV sections generally tend to buckle even before reaching the elastic limit. Class lV members fail before the full cross-section yields as the generated compressive forces can buckle the section at one or more places.

Note 2: Material and geometric non-linearity is expected to have an effect on actual bifurcation load as compared to buckling load obtained from linear buckling analysis. Material and geometric non linearity will have effect on response of both flat and stiffened plate. However aim of this project is to explore how different stiffening shape patterns affect buckling capacity. Hence linear buckling analysis is a computationally effective method to assess the variation in buckling capacity between stiffened and flat plate.

Various possible load cases can generate the critical buckling stresses. Extensive research was performed to formulate the stresses caused due to buckling.

2.2.1 Uni-axial Buckling

Early research described linear buckling of slender columns which has an isotropic material by Euler [3]. In 1757, Leonhard Euler, a Swiss mathematician derived the famous Euler's critical load formula for columns.

$$P_{cr} = \frac{\pi^2 EI}{(KL)^2} \tag{2.1}$$

where:

P_{cr}=Euler's critical Load
E = young's modulus
I = weaker moment of inertia
L = unsupported length of column
K= effective length factor of column

He also observed that the corresponding lateral deformation of column(w) to P_{cr} is in the shape of a sine wave.

$$w(x) = B \sin \frac{\pi x}{L} \tag{2.2}$$

This sine wave shape is termed as a mode shape of the column under axial compressive load. The failure is generally assessed in terms of critical stress. For a pinned pinned column,critical stress is given by:

$$\sigma_{cr} = \frac{n^2 \pi^2 EI}{AL^2} \tag{2.3}$$

where:

σ_{cr}=Critical Buckling Stress
E = Young's modulus
I = weaker moment of inertia
L = unsupported length of column
A = Area of column
n = number of sine curves

To extend the Euler's theory of columns to plates, a plate strut can be considered as below. A uniform horizontal force causing uni-axial compression is considered as shown in the figure 2.2.

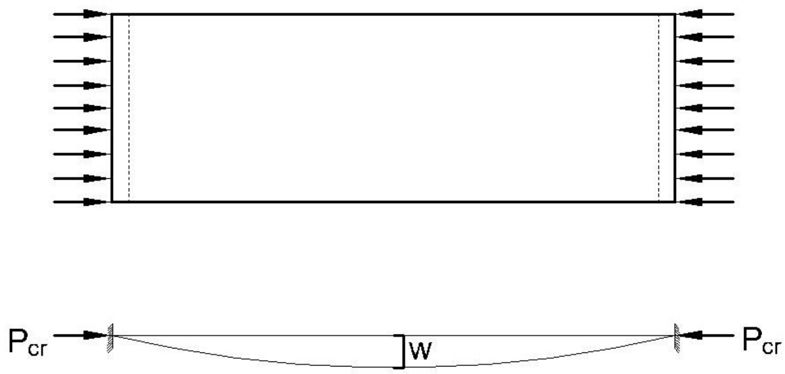

Figure 2.2: Buckling of plate strut under uni-axial loading

The critical buckling load for the plate strut becomes,

$$P_{cr} = \frac{\pi^2 EI}{a^2} . \frac{1}{(1 - v^2)} \tag{2.4}$$

Where $1/(1 - v^2)$ accounts for the free strain caused in the transverse direction in the central area of the plate. This free strain results in higher critical buckling loads for plates. Therefore, the critical stress of plate struts supported on two edges can be formulated as,

$$\sigma_{cr} = \frac{\pi^2 E}{12(1 - v^2)(\frac{a}{t})^2} \tag{2.5}$$

De Saint-Venant, Dubas & Gehri [2] construed the differential equation of the equilibrium state for in plane plate loading which is under small deformations.

$$\frac{\partial^4 w}{\partial x^4} + 2\frac{\partial^4 w}{\partial x^2 \partial y^2} + \frac{\partial^4 w}{\partial y^4} = \frac{1}{D}(N_x \frac{\partial^2 w}{\partial x^2} + N_y \frac{\partial^2 w}{\partial y^2} + N_{xy} \frac{\partial^2 w}{\partial x \partial y}) \tag{2.6}$$

where Flexural Rigidity of the plate:

$$D = \frac{Et^3}{12(1 - v^2)} \tag{2.7}$$

They assumed that the plate does not have initial imperfections and residual stresses. The early researcher Bryan [4] obtained the critical loads of plate using energy criterion. He analysed the cases of uni-axial and bi-axial compression to derive relations between number of corrugations obtained and the geometry of the plate. In the case of uni-axial compression, he concluded that the shape of corrugations could be nearly a square shape.

Timeshenko and Gere [5] assumed initial deformations or lateral loading to derive the critical values of loads. The critical loads on the plate are calculated in order to maintain the a slightly buckled shape. The plate is assumed to buckle in half sinusoidal waves along the direction of the compressive load. Upon introducing the suitable boundary conditions, the critical loads are calculated. The differential equation of an uni-axially compressed plate simply supported on all edges is expressed in equation 2.8

$$D(\frac{\partial^4 w}{\partial x^4} + 2\frac{\partial^4 w}{\partial x^2 \partial y^2} + \frac{\partial^4 w}{\partial y^4}) = -\sigma_{cr} t \frac{\partial^2 w}{\partial x^2} \tag{2.8}$$

The deflection can be written as double Fourier sine series as the two dimensional plate is dependent on two independent variables. The equation follows

$$\omega = A \sin\frac{m\pi x}{a} \sin\frac{n\pi y}{b} \tag{2.9}$$

Where,

ω =out-of-plane deflection
A= constant
m , n=the number of half-sine waves in the length and width direction
a=the length of the plate (unloaded edge)
b=the width of the plate (loaded edge)

Upon derivation and substituting the equation for deflection into the differential equation of an uni-axially compressed plate simply supported on all edges, the obtained expression for critical stress is,

$$\sigma_{cr} = \frac{\pi^2 D a^2}{t m^2}(\frac{m^2}{a^2} + \frac{n^2}{b^2})^2 \tag{2.10}$$

To find the least value of the critical stress, the case of only one half sine wave in the transverse direction(perpendicular to the direction of load) is considered, i.e. n=1, the above equation becomes

$$\sigma_{cr} = k\frac{\pi^2 E}{12(1-v^2)(\frac{b}{t})^2} \tag{2.11}$$

Where the buckling coefficient (k) is

$$k = (\frac{mb}{a} + \frac{a}{mb})^2 \tag{2.12}$$

The buckling coefficient can be written in terms of the aspect ratio η=a/b. Upon drawing graphical relationship between the buckling coefficient and aspect ratio in figure 2.3, we can observe that the minimum value of k is 4.

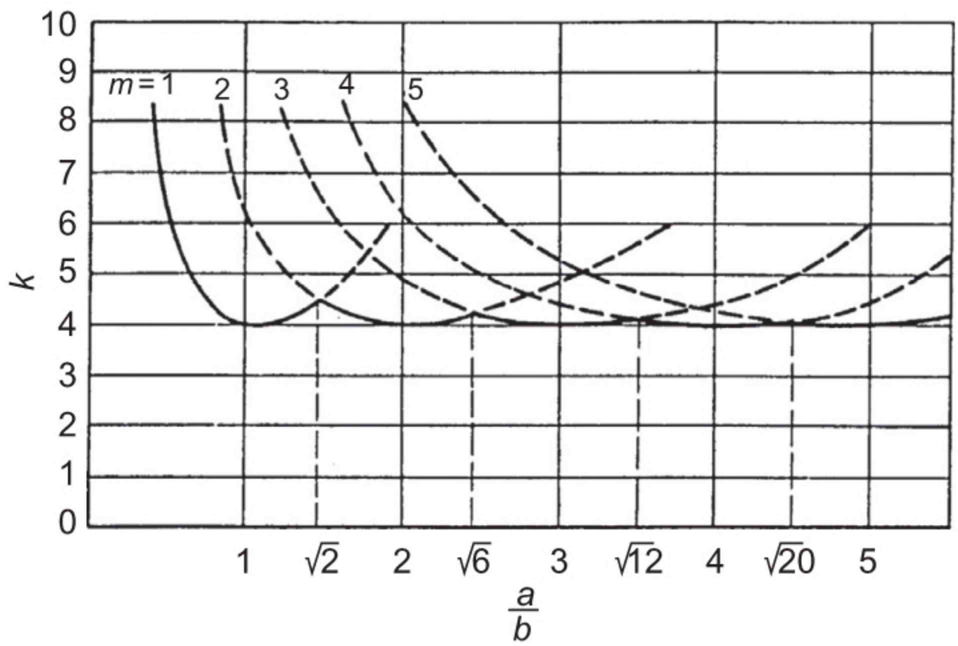

Figure 2.3: Buckling coefficient(k) vs aspect ratio(α) for a simply supported thin plate [5]

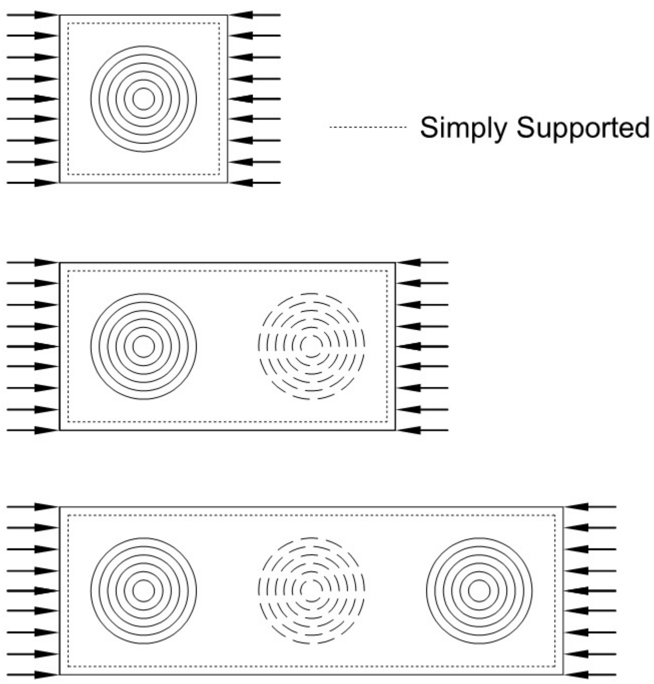

Figure 2.4: Mode shapes under to uni-axial compression

2.2.2 Bi-axial Buckling

Consider a thin rectangular plate of dimensions $a \times b$ with thickness t subjected to uniform longitudinal(σ_1) and transverse compression(σ_2).The stresses are at proportion β ($\beta = \sigma_2/\sigma_1$)

The theoretical stresses caused due to bi-axial buckling presented by Betten & Shin [6] are:

$$\sigma_{cr} = \frac{D\pi^2[(\frac{m}{a})^2 + (\frac{n}{b})^2]^2}{t[(\frac{m}{a})^2 + \beta(\frac{n}{b})^2]} \tag{2.13}$$

For the case under consideration i.e. $\sigma_1 = \sigma_2$, $\beta = 1$. For a thin plate with aspect ratio $\phi = a/b$ and assuming $b << a$ i.e number of half waves along shorter edge becomes $n = 1$, we have:

$$\sigma_{cr} = \frac{D\pi^2[m^2 + \phi^2]^2}{a^2 t[m^2 + \beta\phi^2]} \tag{2.14}$$

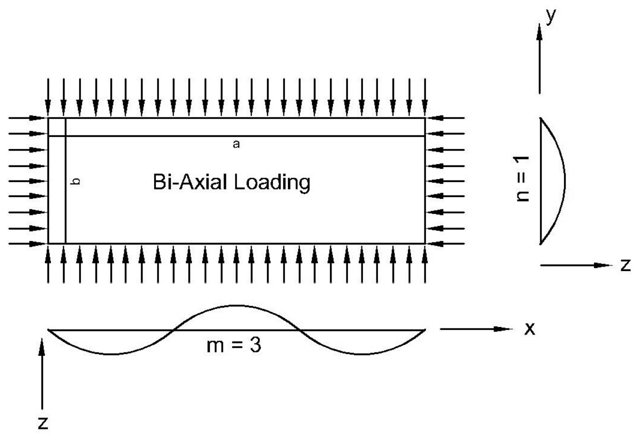

Figure 2.5: Buckling of thin plate under bi-axial loading

Therfore the biaxial buckling coefficient becomes

$$k = \frac{[(\frac{m}{a})^2 + (\frac{m}{b})^2]^2}{[(\frac{m}{a})^2 + \beta(\frac{m}{b})^2]} \tag{2.15}$$

If the aspect ratio $\alpha = a/b$, then the equation becomes,

$$k = \frac{[(\frac{m}{\alpha})^2 + n^2]^2}{[(\frac{m}{\alpha})^2 + \beta n^2]} \tag{2.16}$$

The dependency of the buckling coefficient k with aspect ratio α and the stress proportionality factor β is note worthy.This can be observed in figure 2.6.

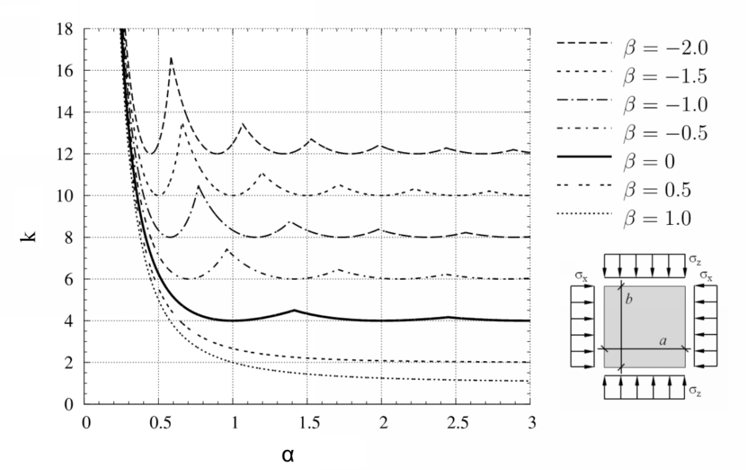

Figure 2.6: Dependency of buckling coefficient(k) on aspect ratio α and stress proportion β [7]

Some observations that can be made from figure 2.6 are:

- The buckling coefficient of bi-axial compression (positive β) is lesser than that of uni-axial compression.
- The buckling coefficient of bi-axial tension and compression (negative β) is higher than that of uni-axial compression
- The curves plotted with tension and compression stresses (negative β), have more number of half waves, whereas the plates loaded in compressive stress throughout the edges have no peaks.

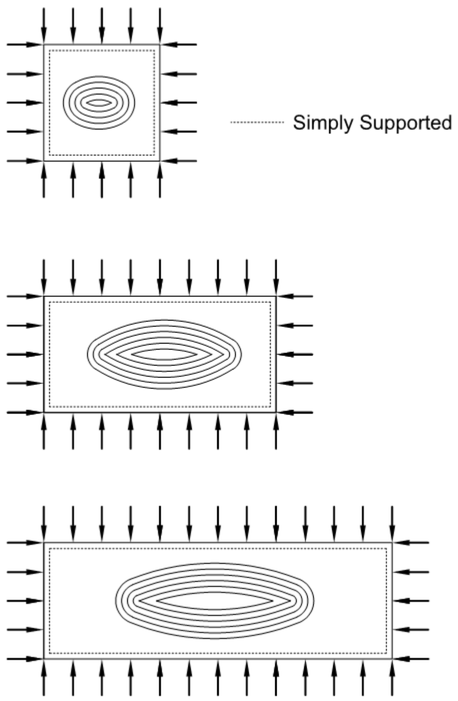

Figure 2.7: Mode shape under to bi-axial compression

2.2.3 Shear Buckling

Pure shear, when applied on a thin plate of dimensions $a \times b \times t$, the principle stress are produced along the direction of the diagonals as tensile and compressive stresses. This case can be observed to be very similar to the previously perceived bi-axial compression except, in this case, we have equal tensile and compressive stresses. Therefore, in the reversed direction stress makes $\beta = -1$.

$$\sigma_{cr} = \frac{D\pi^2[m^2 + \phi^2]^2}{a^2 t[m^2 - \phi^2]} \tag{2.17}$$

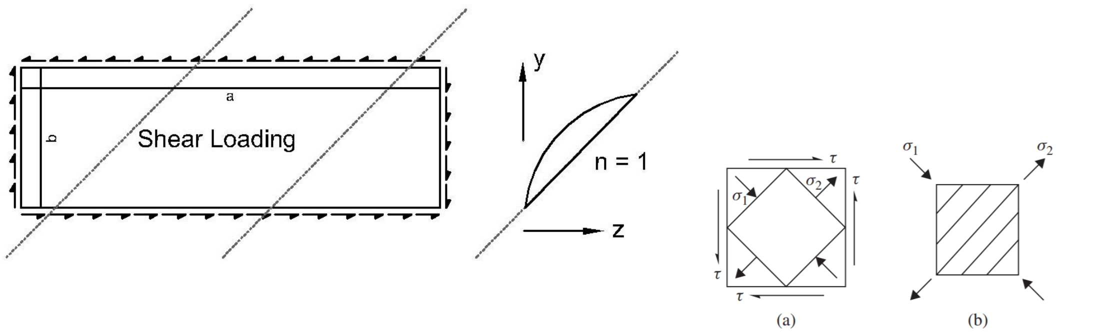

(a) Thin plate under pure shear **(b)** Principle shear stress σ_1

Figure 2.8: Thin plate under pure shear [8]

To evaluate shear buckling coefficients, Kuhlmann et al had observed that the simply supported boundary conditions must be considered while evaluating the critical shear buckling stress, if designed according to EN 1993-1-5 [9]. Euro-code recommends the shear buckling coefficient to be as shown in equation 2.18.

$$k_\tau = \begin{cases} 4.00 + \frac{5.34}{\alpha^2} & \alpha \leq 1 \\ 5.34 + \frac{4.00}{\alpha^2} & \alpha \geq 1 \end{cases} \tag{2.18}$$

To observe a range of aspect ratios, a plot between k_τ and $1/\alpha$ was made. This can be seen in figure 2.9. The figure 2.9 depicts the inverse proportionality of the shear buckling coefficient and the aspect ratio α.

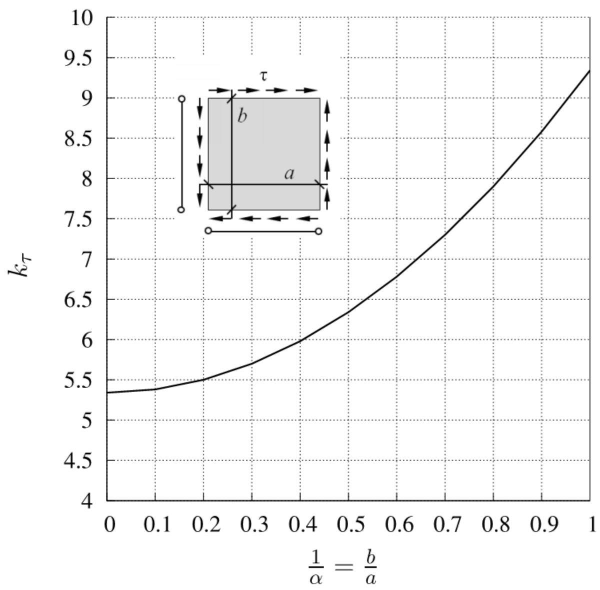

Figure 2.9: Coefficient of shear buckling (k_τ) with respect to aspect ratio (α) [7]

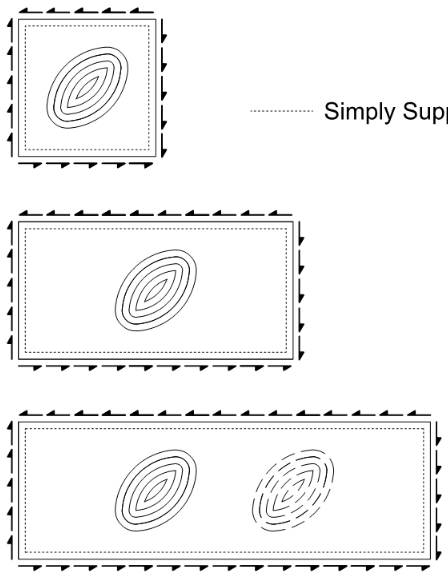

Figure 2.10: Mode shapes under to shear buckling

Continuing the research for optimization and design practices, various investigations were made with the theoretical stresses due to loading as basis. Batdorf & John [10] worked out a research on finding the critical combination of shear and transverse direct stress that can be applied on a long plate which is elastically restrained against rotation. One of the major outcomes of this research shows that the infinitely long plate can be loaded with a considerable amount of pure shear without limiting longitudinal compressive stress which is required to cause buckling of plate.
Stowell et al. [11] has also performed research on flat plates which have elastically

restrained edges against rotation and supported on all edges to find critical shear and compressive stress equations. The research continues to explore new methods such as Taylor-Mclaurin Shape function, double and single finite fourier sine integral transform method etc. Many researchers such as Ibearugbulem et al. [12], Nwoji et al. [13] etc have performed detailed elastic buckling analysis on simply supported thin plate. Riahi [14] presented the buckling behaviour of SSSS (all edges simply supported) and CCCC (all edges clamped) plates under shear and edge compression with variable parameters such as thickness, slenderness ratio and plate aspect ratio. The methods of part period balancing (PPB) and finite element method (FEM) were compared to find the discrepancies between them. The SSSS conditions showed lesser buckling coefficients compared to CCCC. Secondly the proportionality between buckling loads vs aspect ratio and buckling loads vs thickness were drawn graphically. Jana [15] has obtained an elasticity solution for each of the various types of non uniform edge loaded flat plates using approximate plane stress solutions. The investigation was aimed at interpreting the dependence of buckled shape on type of load distribution on the edge of flat plate. The stress equations were obtained from superimposition of three Airy stress functions into fourier series with appropriate boundary conditions. Further the buckling loads are obtained from Galerkin's approach.

2.2.4 Imperfection

Imperfection in a plate can be developed during production process or transportation or also due to processes such as welding.These imperfection lead to an added lever arm to the deflected shape resulting in higher bending stresses.However these imperfections are very small compared to the thickness of the plate. An experimental study of load displacement curves of a simply supported plate is shown in figure 2.11.The curves plotted represent a perfect plate and the lowering of load carrying capacity due to the inclusion of various levels imperfections can be observed.

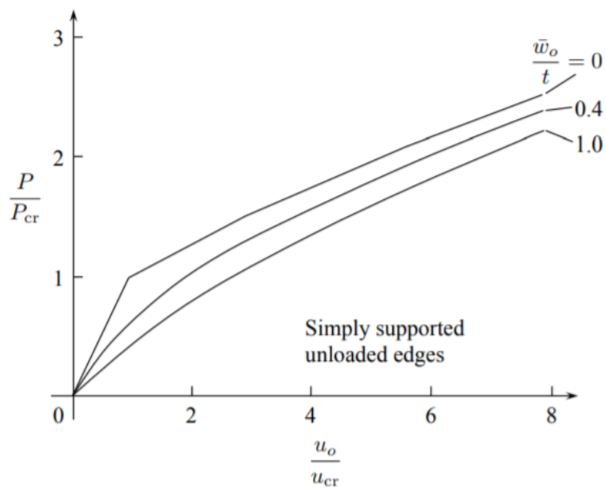

Figure 2.11: Load-Displacement curve comparison of a perfect plate to imperfect plate [19]

Arbocz [3] conducted experimental and theoretical study of effect of geometric imperfections on the critical buckling load on cylindrical shells. He observed the patterns of deformation pre and post buckling to investigate the effect of imperfection on lower and higher order modes. Following this work, Luo [17] presented a model to evaluate the critical buckling load and the worst case of imperfection patter in thin plates by using non probabilistic field model and also presented some numerical examples. Neale [16] examined effect of imperfections on plastic buckling of simply supported rectangular plates. In general, the initial imperfections are considered to be 1% of deformation.

2.2.5 Residual Stresses

Residual stresses exist in the structure without application of external load. Resultant force and moment produced from residual stresses must also be in equilibrium. Hence implying that stresses must be varying in magnitude along the profile to maintain equilibrium. All the members in civil and mechanical engineering application inherit residual stresses of different type and magnitude. Residual stress may arise from different stages in history of metallic materials. Most commonly residual stresses rise from manufacturing and fabrication process. However, residual stresses might also arise during the life cycle of structures through event such as ground settlement, repair work etc.Origin of residual stresses for steel structure can be characterized into group:

- Stresses due to structural mismatch
- Stresses caused by uneven distribution of thermal and plastic strains

Residual stresses from structural mismatch can be avoided by designing the joint region appropriately where different grade of steel meet.As only one material is used in this project residual stresses from structural mismatch are not significant. Although properties of cold formed region change slightly it will not be correct to say that stresses due to structural mismatch do not exist, however can be regarded negligible.

When material is heated or cooled under some degree of external restraint residual stresses due to thermal strain start to grow in the steel. Moreover, the uneven distribution of non-elastic strain also lead to residual stresses. Such are the stresses significant in the cold formed structures. During cold forming process thin steel plates undergo two events:

- Flat plat is deformed elastically and plastically
- The deformed shape is elastically unloaded

Excessive plastic deformation not recovered from elastic unloading lead to residual stresses [18].Number of experimental and numerical studies have been conducted to study the effect of residual stresses over the thickness of the profile. Effect of initial residual stresses is significant for thick and intermediate plates, however for the more slender-plates effect of initial imperfection surpass effect of initial residual stress.

However, in reality, the plate has imperfection and also the residual stresses. In an imperfect plate, out of plane deformation start to increase with increasing load. Such deformation leads to second-order forces and strains which must be accounted for. Secondly, residual stresses from the production might also cause the plate to be initially stressed to some degree. For columns, due to imperfection and residual stresses, the ultimate load is always lower than the elastic critical load. Imperfection and residual also cause reduction of ultimate load in plates, however other more prominent phenomena lead to an increase of the buckling capacity for plates. For plates supported on their edges fail at a load much larger than the critical buckling load. The difference between the ultimate load and critical buckling load is known as post-critical strength.

2.3 Post buckling behavior

Columns which are subjected to direst stresses,fail at a critical buckling load due to sudden increase in lever arm of the load.Yet due to some additional imperfections, the ultimate load becomes lesser than critical load. Unlike columns, plates tend to have a post critical capacity ,due to which the ultimate load becomes higher than elastic critical load.

Post buckling strength comes from the formation of tension field perpendicular to the direction of the loading. We can think of a plate composed of a grillage model shown in figure 2.12 , where the continuous plate is replaced by strips in the direction of loading and columns in the direction perpendicular to the loading. The columns in direction of loading will continue to buckle with no post-critical strength if they were not connected to perpendicular ties. The ties, however, are stretched as the columns buckle outward, and thus they tend to restrain motion and in turn provide a post-buckling reserve. Stretching of the retraining column leads to redistribution of stresses from the center to edges as shown in figure 2.13.

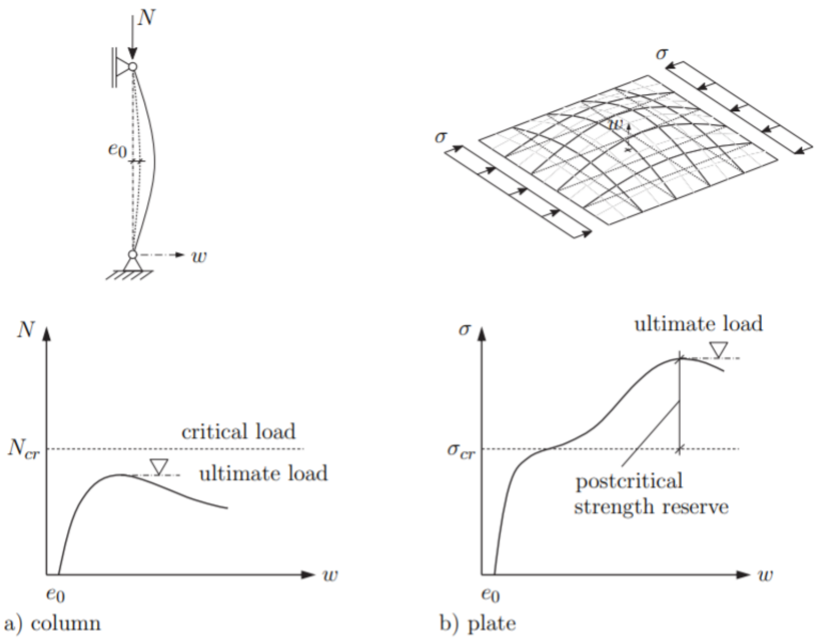

Figure 2.12: Column vs plate buckling [20]

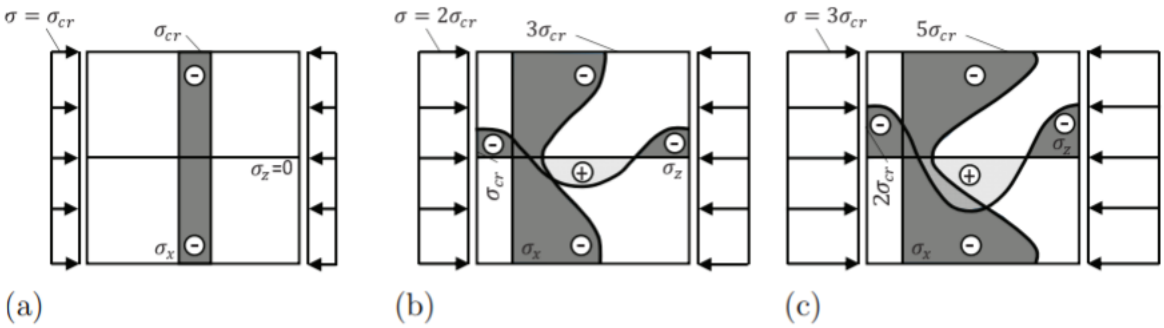

Figure 2.13: Redistribution of stress by formation of tension field [7]

Figure 2.13 show the variation in stress distribution during the loading phase beyond the elastic critical load. Two main observation are the stress redistribution to the loaded edges and secondly the development of tension stresses on edges perpendicular to the loading. Development of tension stresses on the perpendicular edge is dependent on degree of retrained, hence making influence of boundary condition significant.

To quantify the ultimate load capacity of the plate, von Karman [21] established governing equations from nonlinear large deflection plate theory in 1910.These equations allow the in plane and out of plane deformations to be compatible.

$$\frac{\partial^4\phi}{\partial x^4} + \frac{\partial^4\phi}{\partial x^2 * \partial y^2} + \frac{\partial^4\phi}{\partial y^4} = E\left[(\frac{\partial^2\omega}{\partial x * \partial y})^2 - \frac{\partial^2\omega}{\partial x^2}\frac{\partial^2\omega}{\partial y^2}\right] \tag{2.19}$$

$$\frac{\partial^4\omega}{\partial x^4}+2\frac{\partial^4\omega}{\partial x^2\partial y^2}+\frac{\partial^4\omega}{\partial y^4}=\frac{h}{D}\left[\frac{\partial^2\phi}{\partial y^2}\frac{\partial^2\omega}{\partial x^2}+\frac{\partial^2\phi}{\partial x^2}\frac{\partial^2\omega}{\partial y^2}-2\frac{\partial^2\phi}{\partial x\partial y}\frac{\partial^2\omega}{\partial x\partial y}\right] \tag{2.20}$$

$$\left[\frac{\partial^4\omega}{\partial x^4}+2\frac{\partial^4\omega}{\partial x^2\partial y^2}+\frac{\partial^4\omega}{\partial y^4}\right]=N_x\frac{\partial^2\omega}{\partial x^2}+2N_{xy}\frac{\partial^2\omega}{\partial x\partial y}+N_y\frac{\partial^2\omega}{\partial y^2} \tag{2.21}$$

Where,

ϕ = Stress Function

D= Flexural Rigidity

ω = out of plane deflection

As we have seen in Figure 2.13, the stresses redistribute from the middle part to the edges as the middle part of the plate is the buckling risk prone zone. Therefore, yielding occurs along edges as the load is mostly transferred onto these.The strips alongside the simply supported edge carries equal uniform stresses to that at the edges.The effective width of the plate b_e is such that the product of b_e and stresses at the edge is equal to the integration of the total stresses over the actual edge width b.This can be observed in figure 2.14. Therefore, as the stresses at the edge increases, b_e decreases.b_e can be back calculated by equating the critical buckling stresses to the yielding stresses over the effective width, i.e.

$$\sigma_{cr}=k\frac{\pi^2E}{12(1-\upsilon^2)(\frac{b_e}{t})^2}=f_y \tag{2.22}$$

From the above equation, we can get,

$$b_e=\sqrt{\frac{k\pi^2}{12(1-\upsilon^2)}}\sqrt{\frac{E}{f_y}}t=1.90\sqrt{\frac{E}{f_y}}t \tag{2.23}$$

where, $k=4$ and $\upsilon=0.3$

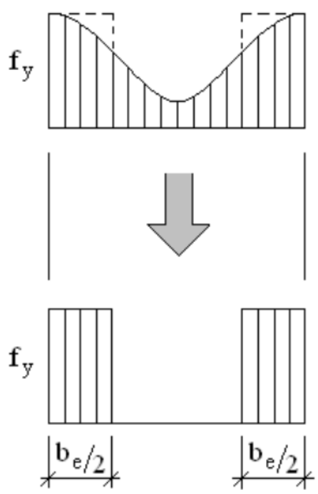

Figure 2.14: Concept of effective width [20]

The point of interest in this concept is the relation the effective width and the stiffness of edges. The equation 2.23 establishes a direct proportionality of the effective width with the square root of Young's modulus and thickness. Therefore the direct proportionality between the stiffness of the plate and the effective width can also be established. Similarly,there is an inverse proportionality of the yield stress to effective width. This means that to compensate for the higher critical buckling stress, the effective stress will be reduce for high strength plates.

2.4 Non-linear theory

In the linear elastic analysis, we assume a perfectly flat plate with no initial stresses. Furthermore, materials are assumed to behave as an ideal elastic material and the stress redistribution beyond the critical buckling stress is accounted for. Hence, nonlinear models were evolved to take into consideration these factors. Initially, von Kármán [21] and Dubas Gehri [2] proposed a set of differential equations to describe the non-linear behavior. Methods such finite difference method, fourier series, and perturbation theory have been used to solve the complex differential equation. Currently, numerical methods like the finite element method (FEM) are more commonly used to robustly solve this task. Apart for FEM other tools are also available to for post-buckling and collapse analysis of plates. These include finite strip method by Lau [22] and generalized beam theory by Scharft [23].

Key consideration while analyzing thin plate by using finite element modelling are the choice of properties and modelling techniques. These include how the shear is modelled in plates, the material stress strain relationship, the yield criterion used, modelling of imperfections, modelling of plate boundaries, the order of the elements and the discretization of the plate in terms of both element density and element aspect ratio. Also, the inclusion of higher order strain terms in the development of the plate stiffness and enforcement of equilibrium on the deformed geometry should be taken into consideration.

3

Methodology and Analysis

This chapter presents the parameters to study stiffened plates with aspect ratios $\alpha = a/b = 1, 2, 3$. The plate modified with a stiffening shape pattern. Extensive paramteric study is performed with circular stiffening unit cells. Their number and dimensions ares varied throughout out the study, to find the most optimized pattern. The plate is simply supported and the loading conditions considered were uni-axial compression, bi-axial compression and pure shear. The investigation further proceeded to check the effect multiple stiffener shapes. From these linear buckling analysis, the initial imperfections were carried to non-linear investigations, to observe the effect of this type of stiffening on ultimate capacity.

3.1 Geometry

The parametric analysis was studied by varying different dimensional parameters of the plate and the circular stiffeners . Each of the variations are listed below. The only constant parameter was the length of the shorter edge (b), which is fixed to be 1 m.

- Plate Dimensions:
  - **Aspect Ratio(a/b):** Plates of aspect ratios 1,2 and 3 were analysed.

  - **Thickness(t):** Considering wide range of application for thin plate, a board thickness range could be analysed. However taking into account the concept of shape stiffening, this thesis is limited to thin plates with very high slenderness (0.05 % - 1 % of b), far above to classified as class lV by euro-code. Plates of thickness 0.5 mm, 1 mm, 2.5 mm, 3 mm, 4 mm, 5 mm, 6 mm, 8 mm, 10 mm were analysed.

- Stiffening Shape Dimensions:
  - **Diameter (D):** An array of diameter for the circular stiffeners were considered from 25 mm - 850 mm (2.5 % - 85% of b). Therefore, the density of the shapes due to smaller diameters is high which reduces as the diameter increases. Diameter of 25 mm, 50 mm, 75 mm, 100 mm, 150 mm, 200 mm, 300 mm, 400 mm, 500 mm, 750 mm, 850 mm are considered

  - **Height (H):** Height of circular stiffener are in range of 2 mm, 3 mm, 4 mm, 6 mm, 8 mm, 10 mm, 20 mm, 30 mm, 40 mm and 50 mm. However keeping in consideration practicality of design, height corresponding to each diameter is kept limited. For each diameter the heights between 2mm - 50 mm are chosen with limitation of 2% to 15% of diameter.

– **Number (n):** The number of shapes along the shorter edge is the decisive parameter. To maintain uniformity, the number of shapes along loaded edges are kept equal to the shapes along unloaded edges for a plate of 1 m × 1 m. The maximum number of circular stiffeners allowed along the shorter edge depends on the dimension of the shape. The total possible circular stiffeners were calculated by dividing the shorter edge length by total length including diameter / side and tolerances.

All the previously mentioned parameters are schematically coded in PYTHON (see Appendix A). The figure 3.2 shows a typical geometry of a stiffened plate. The parameters are summarized in the table 3.1

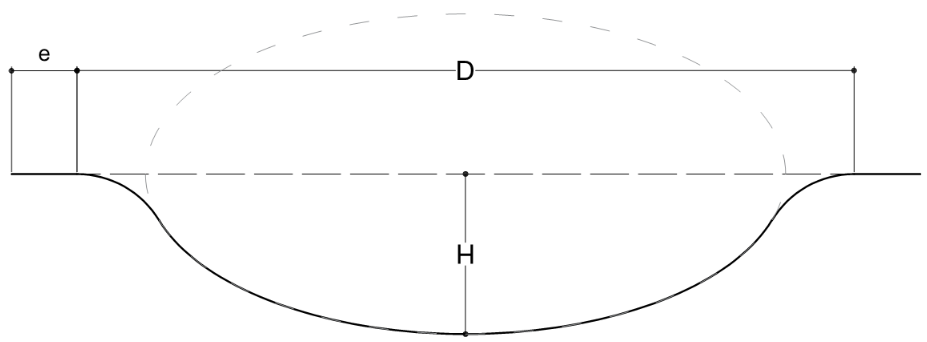

Figure 3.1: Cross-section of circular stiffeners

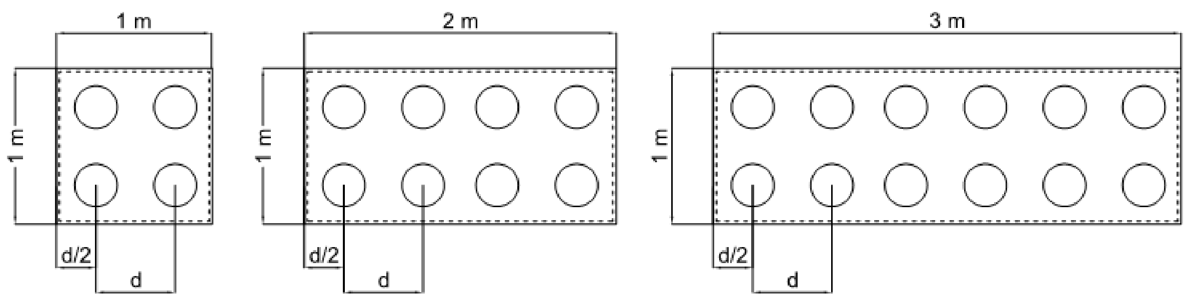

Figure 3.2: Typical geometry of plate

where, d is the distance between the center of shapes and d/2 is the edge distance of the shape.

Table 3.1: Summary of the variables for the parametric study

Diameters (mm)	Range of stiffeners (along shorter edge)									Height of stiffeners (mm)					
25	1	5	9	13	17	21	25	29	33	2	3				
50	1	3	5	7	9	11	13	15	17	2	3	4	6		
75	1	3	5	7	9	11				2	3	4	6	8	10
100	1	2	3	4	5	6	7	8		2	3	4	6	8	10
150	1	2	3	4	5					3	4	6	8	10	20
200	1	2	3	4						4	6	8	10	20	30
300	1	2								6	8	10	20	30	40
400	1	2								8	10	20	30	40	50
500	1									10	20	30	40	50	
750	1									20	30	40	50		
850	1									30	40	50			

A flowchart representing the order and the logic of modelling is presented in the figure 3.3. The choice of parameters abiding to the restrictions is made at every stage to produce around 2062 models per an aspect ratio and per a type of loading. This has allowed for a wide spread research.

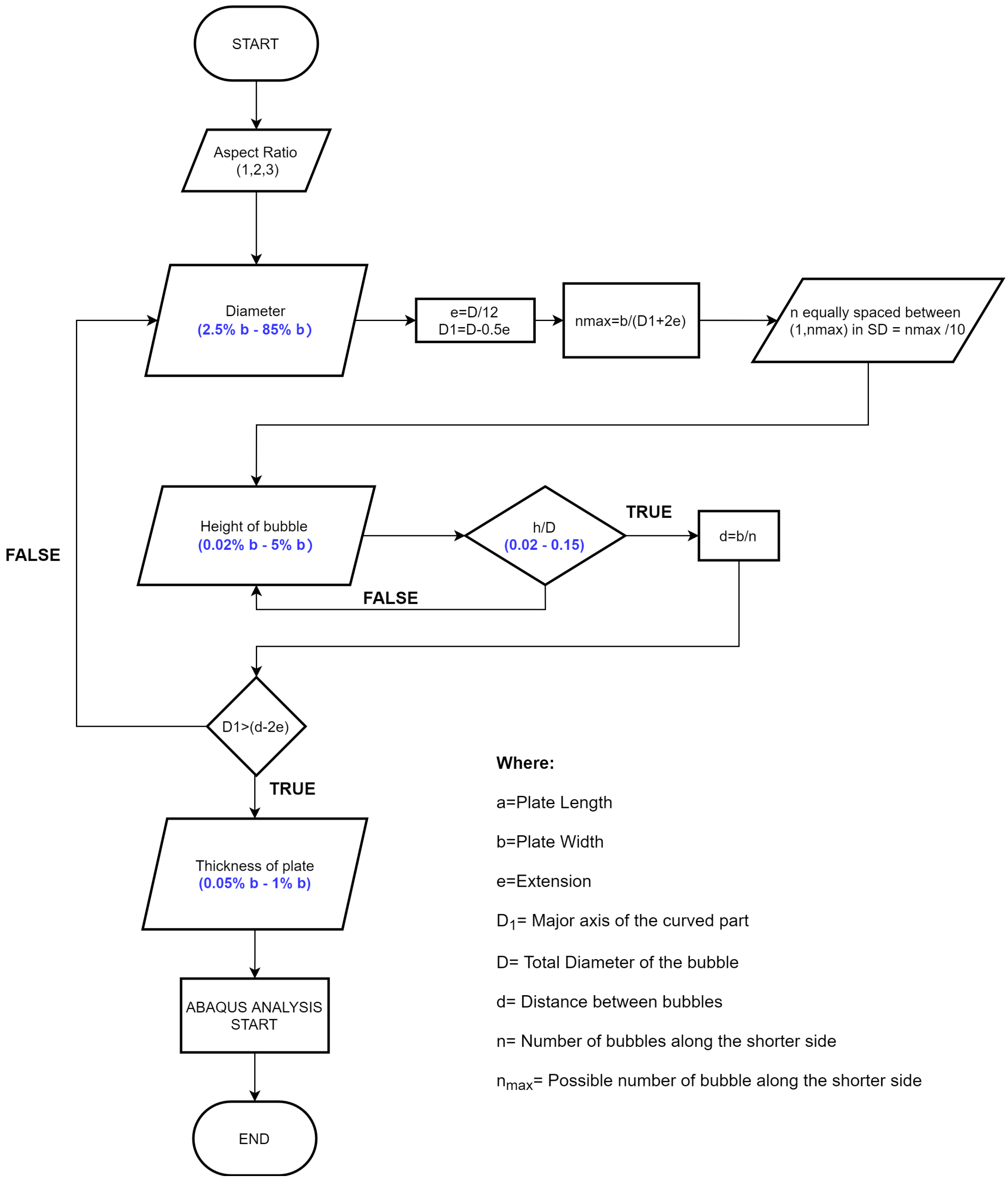

Figure 3.3: Flow of modelling

3.1.1 Shapes

The majority of the thesis was conducted using circular shaped stiffeners. After performing a wide range of analysis, other shapes such as square, capsule (horizontal, vertical and 45°) and triangle were modelled. The typical geometry of these shapes were presented below.

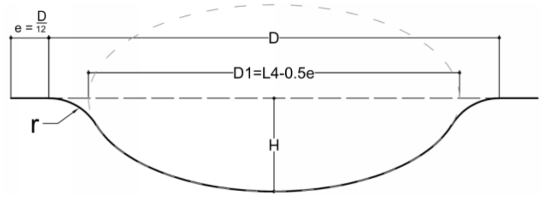

(a) Cross-section of circular stiffener

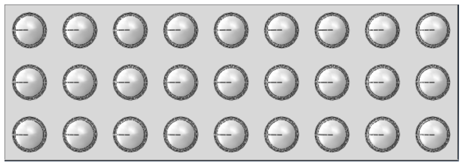

(b) Stiffened plate - Circular stiffener

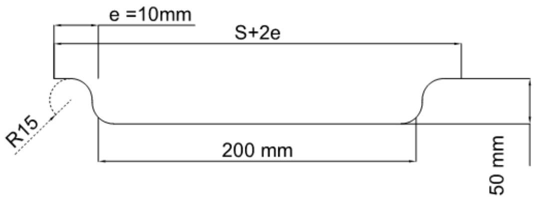

(c) Cross-section of square stiffener

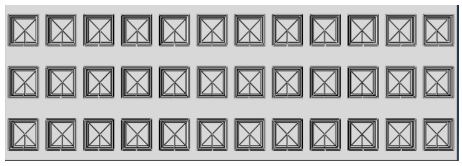

(d) Stiffened plate - Square stiffener

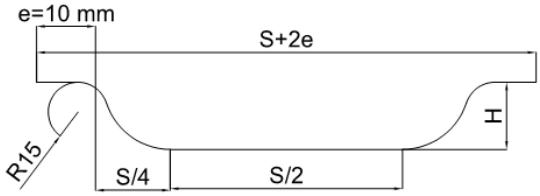

(e) Cross-section of capsule stiffener

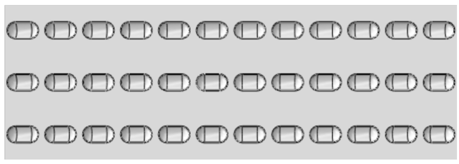

(f) Stiffened plate - Horizontal capsule stiffener

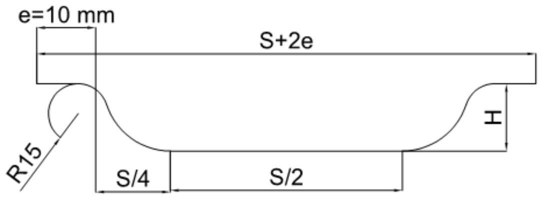

(g) Cross-section of capsule stiffener

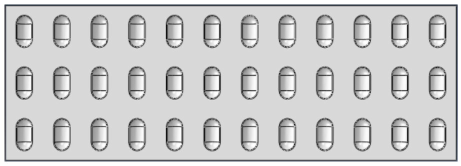

(h) Stiffened plate - Vertical capsule stiffener

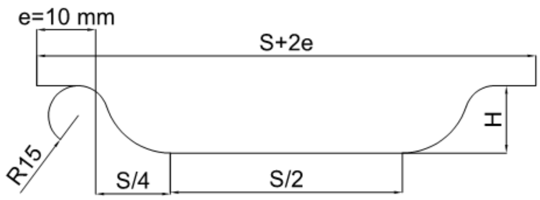

(i) Cross-section of capsule stiffener

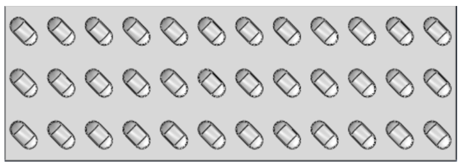

(j) Stiffened plate - Angled capsule stiffener

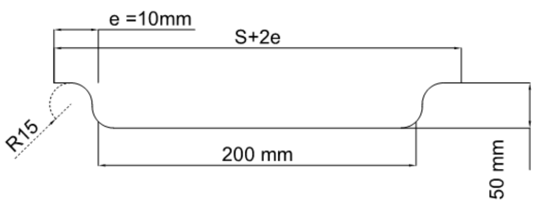

(k) Cross-section of triangle stiffener

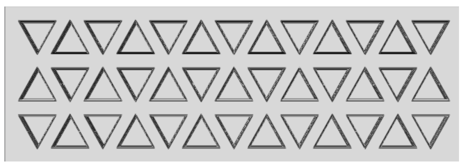

(l) Stiffened plate - Triangular stiffener

Figure 3.4: Cross-section of stiffening unit cells

3.1.1.1 Circular Stiffener

As previously mentioned the major part of the work is performed using circular stiffeners. The typical properties of the shape contain the main dimension Diameter (D), height(h), an extension(e) and the radius of the curved edge(r). These parameters can influence the profile of the bubble can can result in sharp turns, which can lead to local accumulation of stresses. Therefore a standard relationship of the dimensions is required.

- **Height of Stiffener(H):** As mentioned previously, the height range of the stiffeners is considered to be 2% to 15% of the Diameter of Stiffener.
- **Extension(e):** A sensitivity analysis was performed with the extension equal to D/5, D/10, D/12, D/15 and D/20.The Results are shown in the table 3.2.

Table 3.2: Sensitivity analysis of the relationship between extension (e) and diameter (D)

Extension (e)	Eigen Values
D/5	12021
D/10	12038
D/12	12040
D/15	12044
D/20	12047

From these results e = D/12 was chosen to produce the most optimized and best results.

- **Inner Diameter (D1):** The inner diameter is the diameter of the circle without the extension. This is required for the modelling of the shape.Therefore a relation between D1, D and e was to be established. The relations is:

$$D1 = D - me \tag{3.1}$$

A sensitivity analysis was performed with the factor m equal to 0.25, 0.5, 1, 1.5 and 2.5 .The Results are shown in the table 3.3.

Table 3.3: Sensitivity analysis of the relationship between inner diameter (D1) and diameter (D)

Extension Factor (m)	Eigen Values
0.25	12049
0.5	12040
1	12027
1.5	12013
2.5	11989

From these results m = 0.5 was chosen to establish the relationship , D1 = D - 0.5e

- **Edge Radius (r):** The edge radius was chosen to be the height of the stiffener.

The finalized shape of the circular stiffener is shown in the figure 3.5

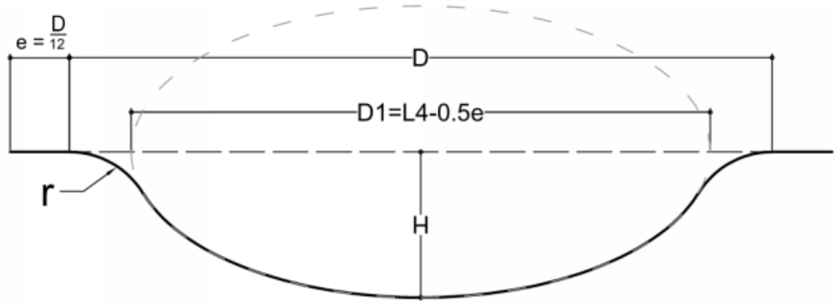

Figure 3.5: Finalised circular cross-section

3.2 Non-dimensional Buckling Parameter - $\overline{P}$

Application of the proposed concept can extend to various plate dimensions, hence there is need to have comparing coefficient independent of plate dimension. Keeping this in consideration, Non-dimensional Buckling Parameter - $\overline{P}$ is used to compare results. Result obtained from linear buckling analysis, is critical buckling load N_{cr} which is converted to non-dimensional parameter using equation 3.2

$$\overline{P} = \frac{N_{cr} \times 12 \times (1 - v^2)}{E} \times \frac{a^2}{t^3} \tag{3.2}$$

where,

N_{cr} is the eigen value (N/m)
v is Poison ratio
a is buckling width (m)
E is Youngs Modulus, (Pa)
t is thickness of the plate (m)

For better understanding of the readers, results and discussions are based on actual dimension of plate and stiffening profile. However for a plate with different scaling factor, results can still be compared using $\overline{P}$. This concept is further elaborated in section 3.5.1

3.3 FE Modelling

Finite Element analysis is becoming increasingly popular for research studies in the present day. Its tool ABAQUS is used to analyse the stiffened thin plates subjected to varied loading situations. The analysis is carried out using ABAQUS/Standard Explicit for both linear buckling analysis and for nonlinear post-buckling analysis .The modelling is carried out with aforementioned restrictions following the flow Chart 3.3. The analysis for all the loading and Aspect ratios is separately conducted in order to point out the similarities and dissimilarities.All the input parameters were carefully chosen and analysed upon to establish an agreeable value to each with the theoretical results.

3.3.1 Material Properties

For the linear buckling analysis, grade of steel is not significant as material response is defined by linear elastic stiffness in original state. Eigenvalue buckling analysis is performed only using elastic modulus and poison ratio. However later in section 3.6, behaviour of modified plate with varying steel grade is also studied using non linear analysis.Three steel grade analysed are S355, S690 and S900 for which material properties and relevant standards are listed in table 3.4.

Table 3.4: Material properties for different classes of steel.

Elastic Modulus (GPa)	Poison Ratio	Standard	Grade	Yield Strength f_y (MPa)	Ultimate Strength f_u (MPa)
210	0.3	EN 10025-2	S355	355	600
		EN 10025-6	S690	690	770
		EN 10025-6	S900	900	980

3.3.2 Element Types and Meshing

Any structural finite elements can be used in an eigenvalue buckling analysis. However, to keep the study efficient and uniform S4R elements are used. S4R is 4-node general-purpose shell, reduced integration with hourglass control, finite membrane strains. S4R is a robust, general-purpose element that is suitable for varying shapes and patterns of stiffening shapes over the extensive parametric study.

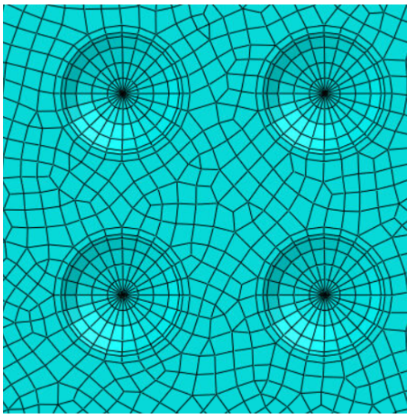

Figure 3.6: Quad dominated sweep meshing

3.3.2.1 Mesh Convergence

Mesh convergence studied is performed to obtain optimum mesh size where we have a good balance between accuracy and computational capacity utilization. A flat plate under uni-axial compression of dimensions 1 m × 3 m × 2.5 mm which is simply supported along all the edges is considered. For the purpose of comparison, the Eigen Value(N/m), critical buckling load to width(N_{cr}/width), is generated for each of the mesh size. Mesh size is chosen where tolerance between two consecutive results falls is less than 0.1%. The study results are presented in table 3.5.

Table 3.5: Mesh Convergence

Mesh Size (mm)	Number of Elements	Eigen Value (N/m)	Tolerance (%)
50	1200	11912	-
40	1875	11894	0.151108126
30	3300	11880	0.117706407
25	4800	11875	0.042087542
20	7500	11870	0.042105263
15	13400	11867	0.025273799
10	30000	11864	0.025280189

This convergence study can be plotted in figure 3.7 to find the most stable and accurate mesh size.The influence of mesh size can be clearly seen on the Eigen Value. As the mesh gets coarser, the solution gets farther from theoretical value, thereby reducing the accuracy. The convergence of the solution can be observed as the number of elements increase. The more appropriate solution is given by the mesh size 20 mm. The graph also shows the compatibility of the Analytical and FEM Eigen Value at the mesh size of 20 mm.

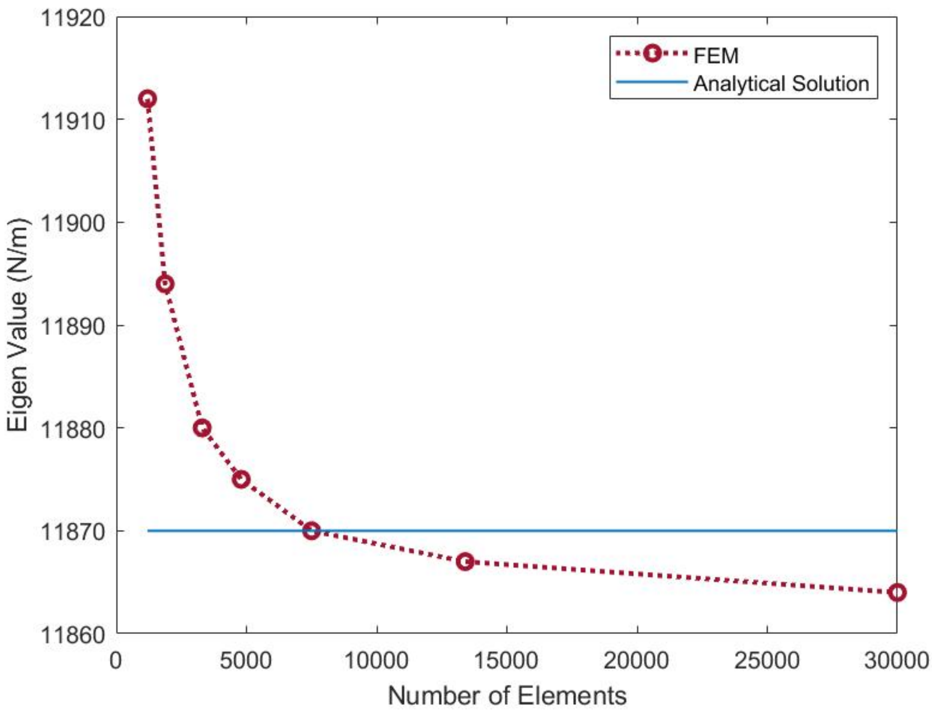

Figure 3.7: Mesh convergence study

3.3.3 Boundary Conditions

Input boundary conditions used are derived from classic plate theory which constraint out of plane deformation on edge length and moment around axis perpendicular to edge length. Additional one more constraint is required to avoid the rigid body motion, which is accomplished by restricting in plane deformation in y direction on one edge.

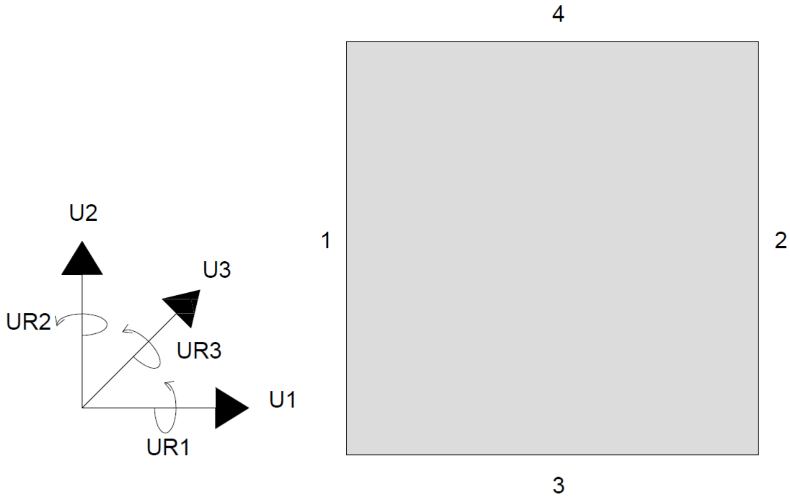

Figure 3.8: Boundary conditions

The boundary Conditions represent a Simply Supported Plate. The boundaries are constrained in the directions mention in table 3.6. These constrains block the movements and rotations of plate in the respective directions in order to maintain equilibrium.

Table 3.6: Modeled boundary constraints

	U1	U2	U3	UR1	UR2	UR3
1	-	-	0	0	-	-
2	-	-	0	0	-	-
3	-	-	0	-	0	-
4	-	0	0	-	0	-

where,

U1 = Longitudinal displacement - x Direction
U2 = Transverse displacement - y Direction
U3 = Out of plane displacement - z Direction
UR1 = Rotation about x axis
UR2 = Rotation about y axis
UR3 = Rotation about z axis

3.4 Verification

In order to verify the modelling technique, a linear buckling analysis was conducted with the previous explained inputs and method. A flat plate of dimensions 1 m × 3 m is considered for the validation of the results from ABAQUS. Critical buckling stresses from ABAQUS and analytical solution are compared to validate the FEM model.

3.4.1 Uni-axial Buckling

As shown in figure 3.9 (a) plate is subjected to uni-axial compressive loads. Results from FEM eigen buckling analysis are compared to closed form solution. The theoretical buckling stress for the flat plate is obtained from the equation 2.11, i.e.

$$\sigma_{cr} = k\frac{\pi^2 E}{12(1-v^2)(\frac{b}{t})^2}$$

where,
k = 4
$E = 210\,GPa$
$v = 0.3$
b =1 m
t = 2.5 mm
The results are tabulated below only.

Table 3.7: Uni-axial buckling stress verification

Method of calculation	Critical buckling stress
ABAQUS	4.745 MPa
Theoretical	4.748 MPa
Difference (%)	0.063

3.4.1.1 Mode Shape

The first mode shape from linear buckling analysis is shown in the figure **??** (b). Mode shape for buckling under uni-axial compression corresponds well with one reported in literature in section. Thus validating the simply supported boundary condition and the modelling technique.

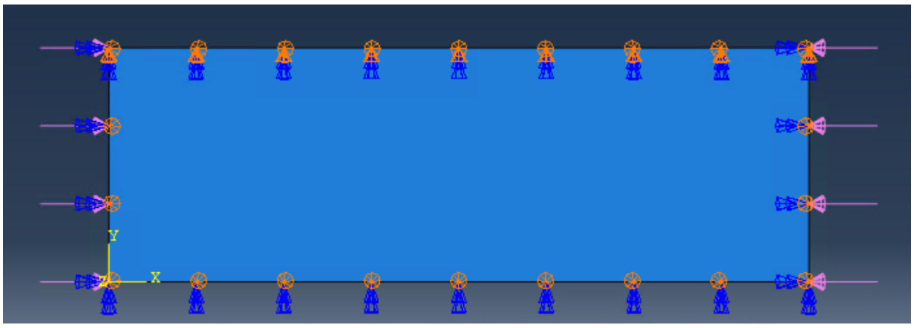

(a) Boundary constraints and loading conditions

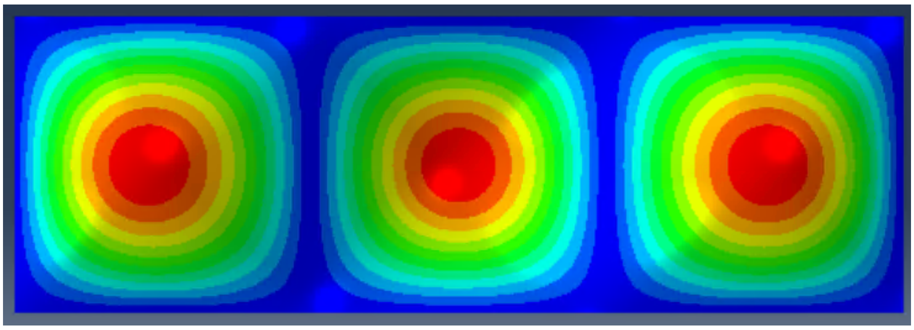

(b) Critical buckling mode shape

Figure 3.9: Buckling of flat plate under uni-axial compression

3.4.2 Bi-axial Buckling

Similar to uni-axial compression a comparison between FEM and closed form solution is performed to validate the model under bi-axial compressive loading. The theoretical buckling stress value for a flat plate under bi-axial compressive load is obtained from the equation 3.8, i.e.

$$\sigma_{cr} = \frac{D\pi^2[m^2 + \phi^2]^2}{a^2 t[m^2 + \beta\phi^2]}$$

where,

m = n =1
$E = 210\,GPa$
$\phi = 3$
$\beta = 1$
a = 3 m
t = 2.5 mm

The results are tabulated below.

Table 3.8: Bi-axial buckling stress verification

α	Thickness (mm)	Theoretical stress (MPa)	ABAQUS stress (MPa)	% Diff
1	2	1.518	1.519	0.066
2		0.949	0.95	0.053
3		0.844	0.844	0.059
1	10	37.96	37.964	0.188
2		23.725	23.73	0.011
3		21.089	21.095	0.021

3.4.2.1 Mode Shape

First buckling mode under bi-axial compressive load is shown in figure 3.10 (b). FEM and theoretical buckling mode (put reference here) also align well for bi-axial compression, hence validating the model for the defined loading.

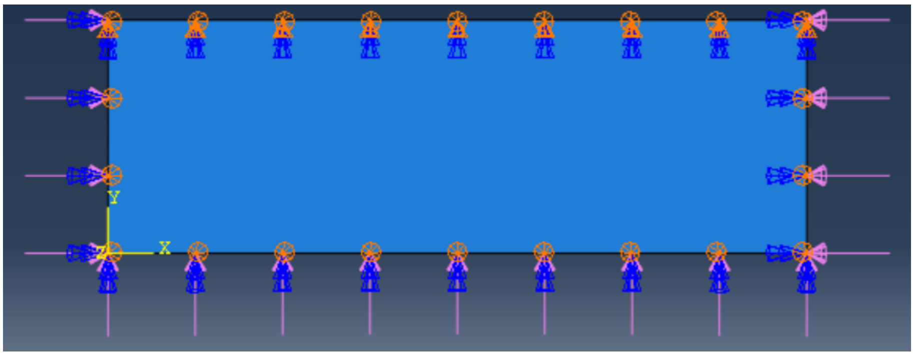

(a) Boundary constraints and Loading conditions

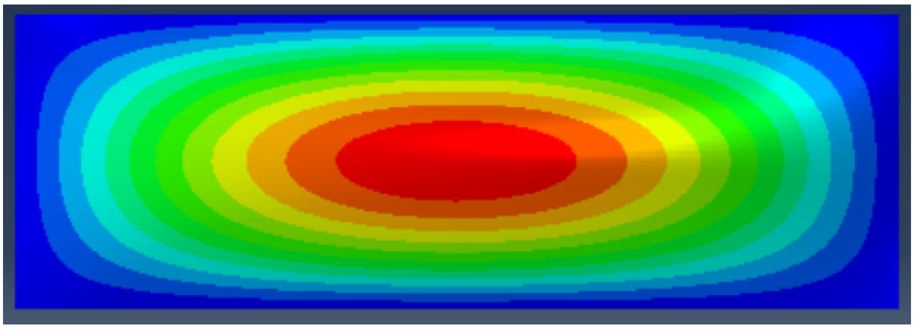

(b) Critical buckling mode shape

Figure 3.10: Buckling of flat plate under bi-axial compression

3.4.3 Shear Buckling

From the figure 2.9 in the literature, effect of aspect ratio on buckling coefficient was already identified by the previous research. Hence model validation under pure shear is performed with aspect ratio 1, 2 and 3. Secondly to study effect of plate thickness on comparison between theoretical and numerical solution two plate thicknesses i.e 2 mm and 10 mm are analysed. Closed form solution is obtained from the equation 2.17, i.e

$$\sigma_{cr} = \frac{D\pi^2[m^2 + \phi^2]^2}{a^2 t[m^2 - \phi^2]}$$

where,

m = n =1
$E = 210\,GPa$
$\phi = 3$
$\beta = 1$
a = 3 m
t = 2 mm and 10 mm

The results are tabulated below.

Table 3.9: Shear buckling stress verification

η	Thickness (mm)	Theoretical stress (MPa)	ABAQUS stress (MPa)	% Diff
1	2	7.099	7.085	0.198
2		4.821	4.981	-3.33
3		4.399	4.444	-1.014
1	10	177.463	177.129	0.188
2		120.523	124.392	-3.21
3		109.979	110.977	-0.908

3.4.3.1 Mode Shape

The first mode shapes from linear buckling analysis are shown in the figure 3.11. Literature also reports similar buckling modes for corresponding aspect ratio. Similar study to validate numerical simulation was conducted by Alinia 2005 [8], where author also reported difference between –0.709% to 2.980%. Hence from the results reported in table 3.9 with error percentage between -3.33% to 0.198% we satisfactorily validate modelling technique.

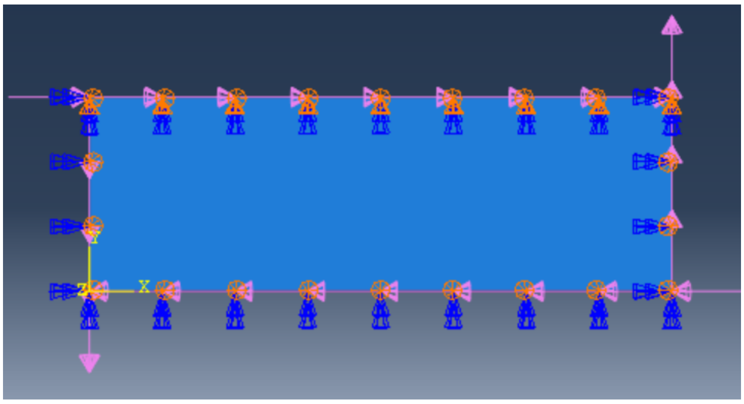

(a) Boundary constraints and Loading conditions

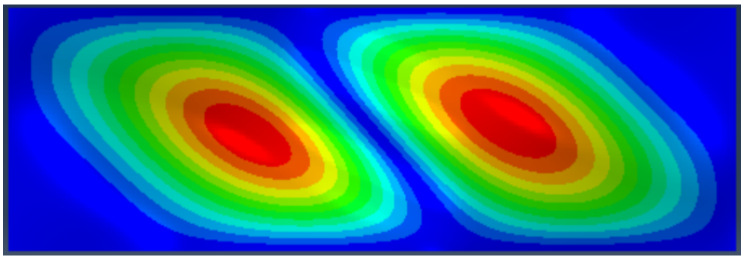

(b) Critical buckling mode shape

Figure 3.11: Buckling of simmply supported flat plate under pure shear

3.5 Pre -Analysis Studies

A preliminary study is conducted to assess the validity of the concept and generalised the conclusions that could be made.

3.5.1 Scale Factor

Effect of magnifying and reducing size of the plate is studied; hence applicability of results can be ensured when similar geometry is used for application with different dimension.

To study this phenomena total of 408 ($68 \times 3 \times 2$) models are analyzed, 68 models each for reduced, normal, and magnified scale factor under uni-axial and shear loading. Later in results chapter its is reported $\overline{P}$ (non-dimensional buckling parameter) is independent of aspect ratio, hence only aspect ratio 1 is analyzed. Study is limited just to circular stiffeners. Geometric properties varied included thickness, length, and width for the plate, and for the stiffener diameter and height are the variables. To keep consistency in analysis mesh size is also the function of scale factor, hence number of elements remain consistent. Scale factor was 0.5 for reduced, 1 for normal and 1.5 for magnified plate. Following figures show graphical comparison between three set of plate sizes.

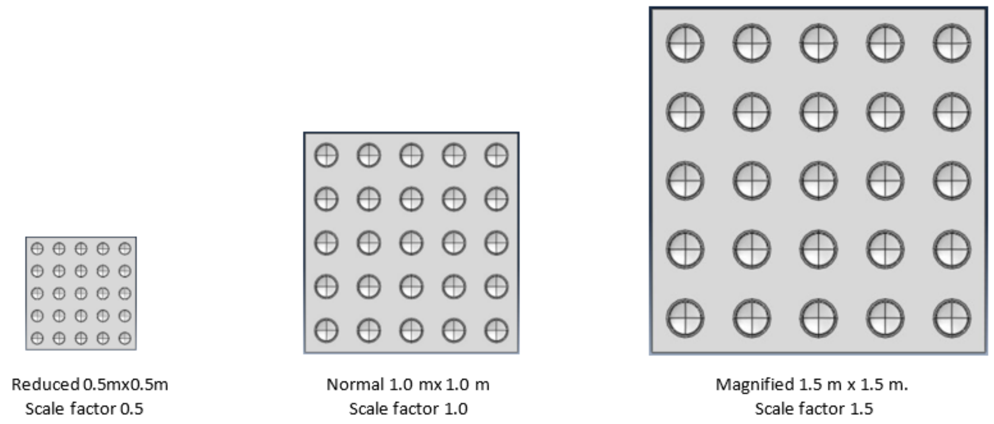

Figure 3.12: Graphical comparison between scale factor 0.5, 1 and 1.5

Inputs are divided into two set 1 and set 2 as shown in table 3.10 and table 3.11 respectively. Each set is further divided into sub sets of thickness and heights.

Table 3.10: Scale factor input parameters set 1 to generate 102 Models

Properties	Normal	Magnified	Reduced
Aspect Ratio	1	1	1
Scale Factor	1	1.5	0.5
Diameter (mm)	50	75	25
Thickness (mm) sub set-1	1	1.5	0.5
Thickness (mm) sub set-2	2.5	3.75	1.25
Height (mm) sub set-1	4	6	2
Height (mm) sub set-2	6	9	3

Table 3.11: Scale factor input parameters set 2 to generate 102 models

Properties	Normal	Magnified	Reduced
Aspect Ratio	1	1	1
Scale Factor	1	1.5	0.5
Diameter (mm)	100	150	50
Thickness (mm) sub set-1	1	1.5	0.5
Thickness (mm) sub set-2	2.5	3.75	1.25
Height (mm) sub set-1	6	9	3
Height (mm) sub set-2	10	15	5

To check whether proposed methodology will yield desired result, method is applied initially to the flat plates with scale factor 0.5, 1 and 1.5 over length, width and thickness. Detailed results are reported in appendix table B.1, B.2 and B.3. After validation of results, study is expanded to stiffened plates.

Results from scale factor validation results reflect that $\overline{P}$ is independent of scale, verifying the proposed methodology. Percentage difference between $\overline{P}$ values for three scales of flat plate dimension varied between -0.05% to 0.0097%. Detailed set of results for flat plate can be found in appendix B.

Followed by validation of methodology, based on inputs in table 3.10 and table 3.11 linear buckling analysis was performed. Table 3.12 and table 3.13 summarise the comparison between normal, reduced and magnified scale factor under normal and shear loading from total of 408 models.

Table 3.12: Summary of scale factor results under uni-axial loading

	NDBP % difference between:	
	Reduced and Normal	Magnified and Normal
Min	-0.045	-0.146
Max	0.114	0.048
Average	0.004	-0.013

Table 3.13: Summary of scale factor results under shear loading

	NDBP % difference between:	
	Reduced and Normal	Magnified and Normal
Min	-0.1229	-0.1682
Max	0.2253	0.0979
Average	0.0072	-0.0023

3.5.2 Direction of Bubble Profile

Buckling of the plates can deform the thin plate in any out of plane direction. Therefore, it is very important to observe the direction of modelling of the stiffening shapes. Therefore a study is performed by including three possible modelling situations.The three potential possibilities of modelling could be:

- All circular stiffeners towards same side
- Adjacent circular stiffeners towards same side
- Corner circular stiffeners same side

These are depicted in the figure 3.13 where(+) means and (-) unit cell facing into and out of the plane of plate respectively.

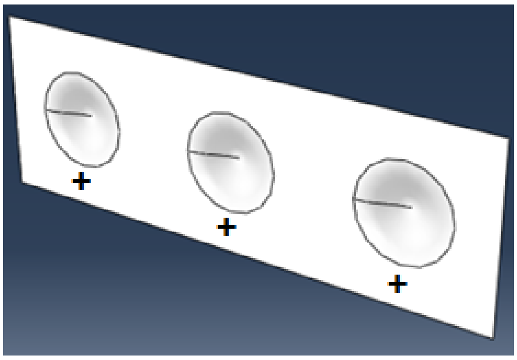

(a) All circular stiffeners into the page

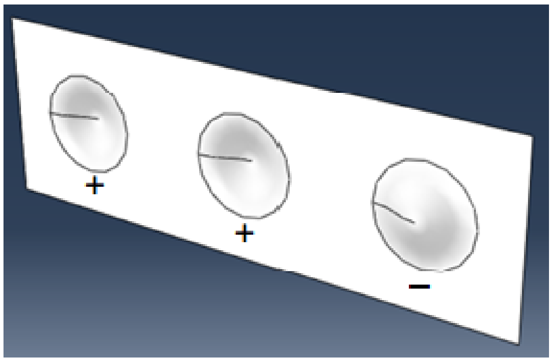

(b) Adjacent circular stiffeners into the page

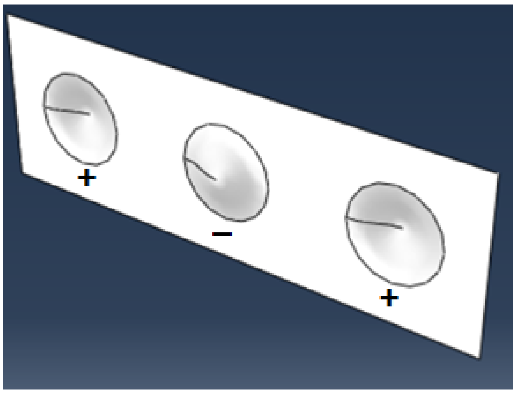

(c) Alternative circular stiffeners into the page

Figure 3.13: Direction of modeling of shapes

In the previous section,we have established that the study is valid for any size of the plate.Therefore, for this particular study, a smaller plate of dimensions 0.1 m × 0.3 m × 2 mm is considered. The study was conducted using circular stiffeners over the stiffener height of 2 mm, 4 mm, 6 mm, 8 mm and 10 mm. The % increase of buckling capacity with respect to flat plate of dimensions 0.1 m × 0.3 m × 2 mm.

Table 3.14: Study of the effect of direction of bubble

Direction of Bubble	Depth	Ncr [kN/m]	Compressive stress [MPa]	% increase of Buckling Capacity
all same side	2	726.327	363.1635	19.84
adjacent same side		721.959	360.9795	19.12
corner same side		718.205	359.1025	18.50
all same side	4	829.433	414.7165	36.85
adjacent same side		819.618	409.809	35.23
corner same side		810.517	405.2585	33.73
all same side	6	899.579	449.7895	48.42
adjacent same side		892.919	446.4595	47.32
corner same side		886.104	443.052	46.20
all same side	8	928.284	464.142	53.16
adjacent same side		928.295	464.1475	53.16
corner same side		928.624	464.312	53.21
all same side	10	945.996	472.998	56.08
adjacent same side		946.003	473.0015	56.08
corner same side		946.27	473.135	56.12

The computed results were also plotted to analyse the sensitivity of the direction.

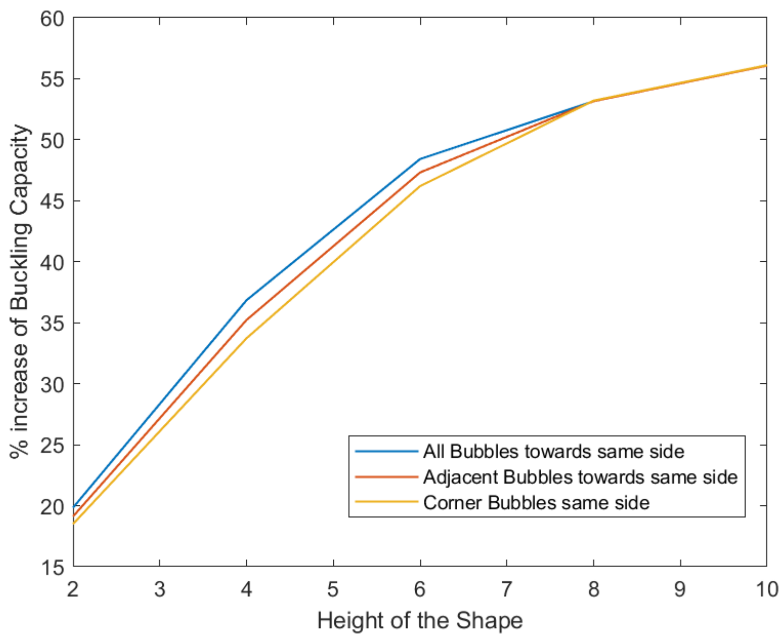

Figure 3.14: Direction of stiffening shape

The most prominent observations are:

- From the graph, we can say that the difference between the three choices is not much.
- At lower depths (2 mm,4 mm,6 mm), all three circular stiffeners to same side is producing better results than any others.

- At depths 8 mm,10 mm, all the choices produce almost equal results.The difference in the % increase varies over 1.34% to 0.04% as the height increases.

Therefore, the winning choice in the three possibilities is modelling all towards the same side. It gives an highest difference in increase of 1.34% which although not prominent, but stands as the most optimal choice. Also, for practical reasons, this gives the best layout.

3.6 Nonlinear Analysis

Primary aim of the thesis is not to study the ultimate capacity of stiffened plate. However, there are various design applications where post buckling strength have notable contribution as opposed to the applications where deflection limits restrict use of post critical strength. Hence insight towards how post critical strength is being affected by stiffening pattern is of vital importance.

This section elaborates on methodology adopted to conduct non-linear analysis on the stiffened plate. Following the methodology explained in section 3.5.1, it is proven that given concept can be scaled up or down for variable geometries. So, using a scale factor of 0.5, model size is reduced making it computationally effective. A $0.5\,\mathrm{m} \times 0.5\,\mathrm{m}$ plate with varying thickness and material properties is analyzed using nonlinear riks analysis to study, post buckling behavior of the stiffened plate. Geometric properties of stiffening pattern consisting of circular stiffeners is tabulated in table 3.15. Graphic illustration of stiffening pattern analysed is shown in figure 3.15.

Table 3.15: Stiffener properties

Aspect Ratio	Diameter as % of plate width	Height as % of plate width	Number of stiffeners along shorter edge
1	15	2	5
Aspect Ratio	Diameter (mm)	Height (mm)	Number of stiffeners along shorter edge
1	75	10	5

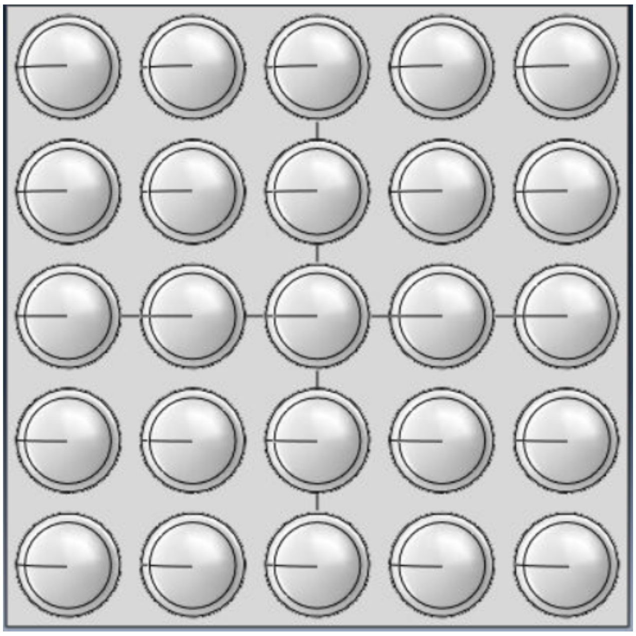

Figure 3.15: Stiffening pattern used in non-linear analysis

The load-deformation curve for stiffened plate is compared to that of a flat plate. First linear buckling mode with an amplitude of 0.1 x thickness of the plate is applied as imperfection. During the non-linear buckling analysis, at a specific load, we might get several solution paths. This point is called the bifurcation point and small imperfections need to be applied to a geometrically perfect structure to open the bifurcation paths and subsequently let the structure buckle. Ideally, a detailed imperfection study must be conducted to see the effect of initial imperfection. However, from the physics of the problem, we can predict that the height of the stiffener will act as a much larger imperfection than one from the mode shape. And the main effect of introduced imperfection will be on the response of the flat plate. So the reason for choosing a smaller amplitude of initial imperfection is to limit the adverse effect of initial imperfection on a flat plate.

4

Results and Discussion

This chapter reports results from the parametric study designed in section 3.1.The PYTHON scripts gets processed by ABAQUS to generate thousands of results to analyze upon and validate the consequences of this novel method. Based on linear buckling analysis of 18549 linear buckling analysis iterations are extracted for number and shape of stiffeners, aspect ratio, the thickness of plate, and loading. The buckling capacity of the stiffened plate is compared to flat buckling capacity and trends are reported based on percentage increase in this chapter.The results were graphically and theoretical analysed in the first part and later proceeded with further analysis. Followed by results from post buckling analysis for a reference stiffening pattern to reflect upon load-deformation behaviour up to collapse load.

Based on results from parametric study over circular stiffeners, further analysis with different shapes is required. Later reported in section 3.4, a greater increase in buckling capacity is observed in the case of square stiffeners, however trends remained similar to as that of circular stiffeners. Hence results for other stiffening shapes are only reported for one reference model.

4.1 Linear Buckling Analysis

A Linear perpetuation buckling analysis was conducted using Lanczos Eigensolver. This method is used for simpler calculation which will converge early. After the extensive study, it was observed that the mode shape of the plate were similar to that of a flat plate in majority of the cases. The Eigen Value denotes the load per meter width of the plate. This value is used to find $\overline{P}$ as discussed in section 3.2. The $\overline{P}$ of the plate is compared to the $\overline{P}$ of the flat plate and % increase of the parameter is considered to estimate the benefit of the present stiffening. Several variations with respect to all the parameters of the Shapes and plate were observed and presented in the following sections.
In order to quantify effect of multiple variable on the buckling capacity, this section report the trends for parametric study with circular stiffeners. In practical implementation of the idea insight into most impacting parameters will enable optimised, use of production resources and merging of stiffened plate in global structure. Refer to the Python script in Appendix A.

4.1.1 %increase of $\overline{P}$ vs Number of Stiffeners

The number of shapes used determine the amount by which the plate is stiffened.The possible number of stiffeners were calculated with with the edge restrictions show in the crossection details. A detailed summarry of the parameters is mention in table 3.1. To observe the dependency of the improvement in Buckling capacity on the number of stiffeners provided a small data set with the properties mentioned in the table 4.1 were selected, which has a good range of variation and comparable parameters. The figure 4.1 illustrates a typical distribution of stiffeners for each iteration.

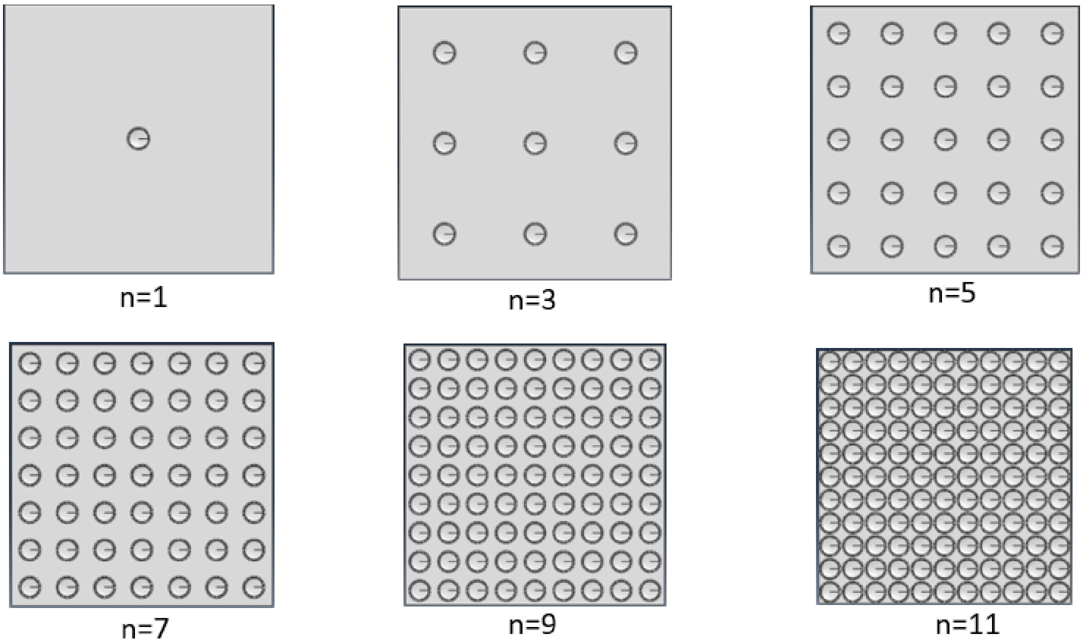

Figure 4.1: Distribution of circular stiffeners

Table 4.1: Chosen set (highlighted in red) for comparison (%increase of $\overline{P}$ vs n)

Diameters (mm)	Range of stiffeners (along shorter edge)									Height of stiffeners (mm)					
50	1	3	5	7	9	11	13	15	17	2	3	4	6		
75	1	3	5	7	9	11				2	3	4	6	8	10

For a deeper understanding, a thin plate with circular stiffeners of diameter 50 mm with a height of 3 mm and the plate thickness of 2.5 mm is considered. The plate is stiffened with a range of 1-17 number of circular stiffeners. Each of these plates are analysed under Uni-axial, Bi-axial and Shear loading conditions. As mentioned earlier,the % increase of $\overline{P}$ for each iteration is calculated. The trends of this particular test are shown in figure 4.2

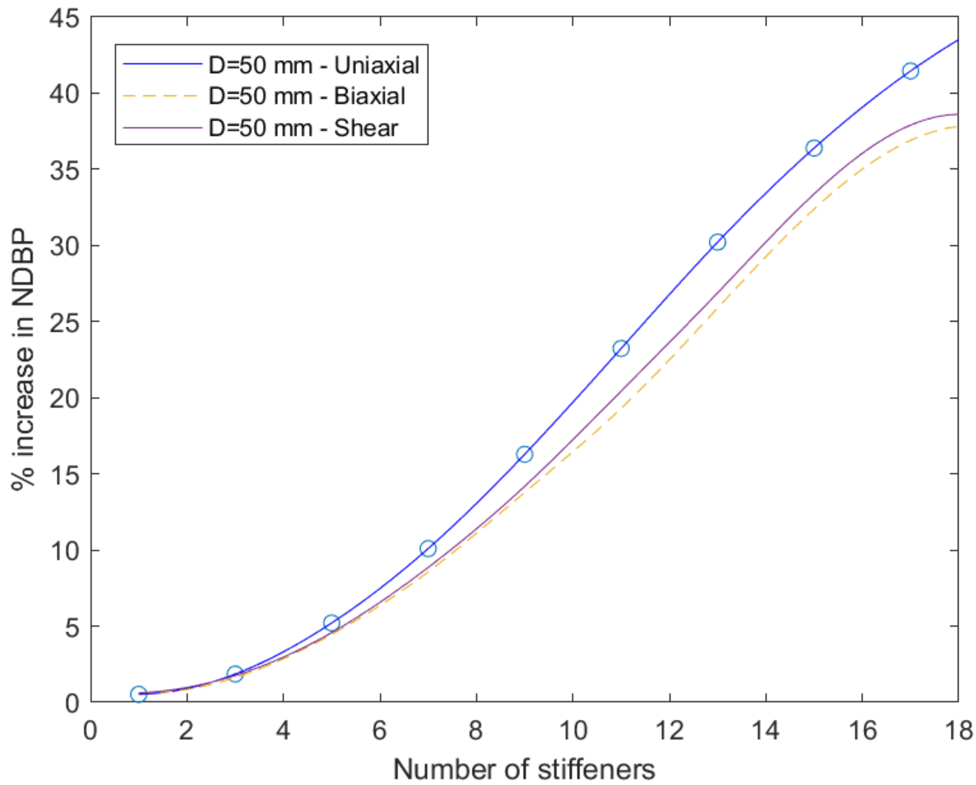

Figure 4.2: Variation of $\overline{P}$ with respect to the number of stiffening shapes (D = 50 mm, t = 2.5 mm , h = 3 mm)

As expected, a trend of significant improvements is observed which varies from 0.5% to 25% with strong indications of the need for higher density of the stiffeners. The other noticeable observation is that a small increase in number of stiffeners leads to a considerable improvement. For example, for this particular plate, the % improvement for 5 number of circular stiffeners is 5.22% and that of 9 number of circular stiffeners is 16.44% and that of 17 number of shapes is 43.29% in the case of uni-axial loading.The positive gradient of the graphs proves this case. We can observe an improved gradient by using higher number of shapes. Similar trends can be observed in the case of Shear and Bi-axial Loading.To generalise the study, these results were extended to aspect ratios 1,2 and 3.These results were represented graphically in the figure 4.3. The graphs are plotted for two diameters 50 mm and 75 mm keeping the height of stiffener i.e. 3 mm and thickness of plate 2.5 mm constant.

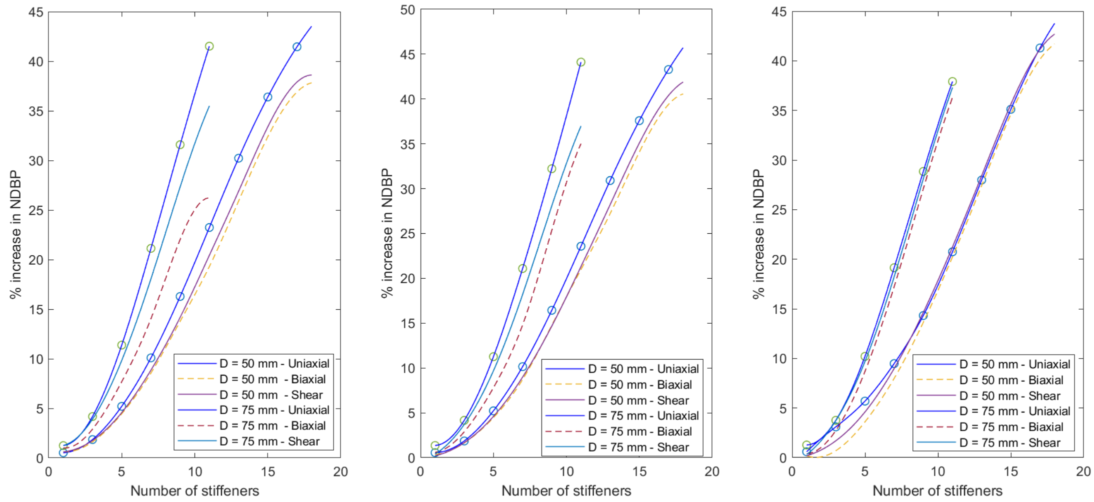

(a) $\alpha = 1$ **(b)** $\alpha = 2$ **(c)** $\alpha = 3$

Figure 4.3: % improvement of $\overline{P}$ (Buckling Capacity) with respect to number of stiffeners for α = 1,2 and 3

From the results presented in graphs 4.3 , the importance of the density of stiffeners irrespective of variation in parameters is observed. These gradient of the graphs increases with increase of diameter.This means that the higher density of higher diameter stiffeners is more beneficial to have drastic improvement of capacity with small change in density. This is expected because higher diameters might disturb the profile more. To conclude, as the number of stiffeners increase, greater is the increase in buckling capacity. Trend remained consistent along all thickness, aspect ratios, loading, height , diameter of stiffeners and aspect ratio of plate.
Recommendation: Higher Diameter with higher density results in higher critical Buckling Load

4.1.1.1 Mode Shapes

The Mode Shapes of the plates of Aspect Ratio 2 with circular stiffeners of diameter 50 mm with increasing number of stiffeners are plotted.The number of stiffeners gradually increased from 1 - 17. We can see that the stiffened plate attains similar Mode shapes to that of a flat plate. The plane of the flat plate is stiffened to act similar to a flat plate.

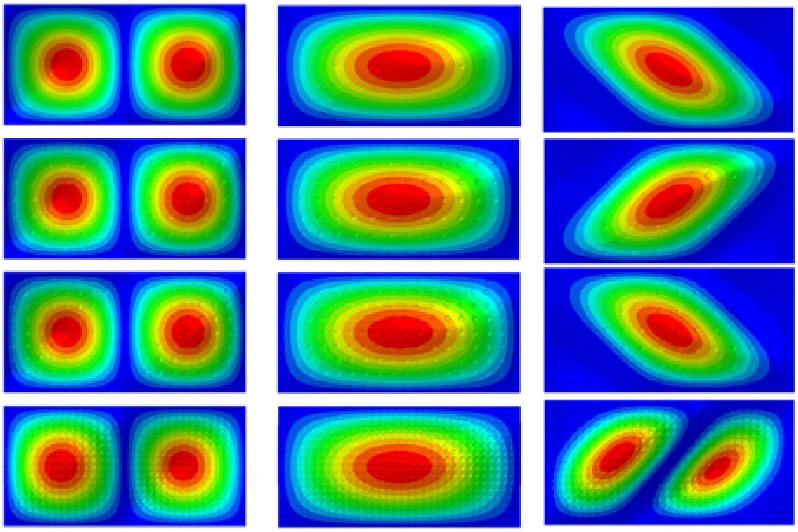

Figure 4.4: Mode shapes of plates stiffened with 50 mm circular stiffeners with n=1,5,9,17

4.1.1.2 %increase of $\overline{P}$ vs %increase of mass of plate

This study provides an insight into the effect on structural self weight and economic aspects due to the present addition of stiffeners.This study does not lead to a very high increase in the mass of the plate. This increase can be obtained from increase in the number of stiffeners.There can be two situations according to the production method:

1. No increase in mass if the production method is similar to embossing or cold forming.
2. Increase in mass if the production method needs the stiffener to be an external attachment.

The increase in mass % as compared to the flat plate depends on the diameter and number of stiffeners.This can range from 0.16% to 185.23% . The higher diameters result in higher % increase. Yet, for the lower diameters with higher density, % increase can be as low as 10%. For example,for diameter 50 mm and number of stiffeners of 17, the increase in mass % is 10.9%. This is very reasonable when compared to the % improvement of 44%.These study results are graphically plotted in figure 4.5

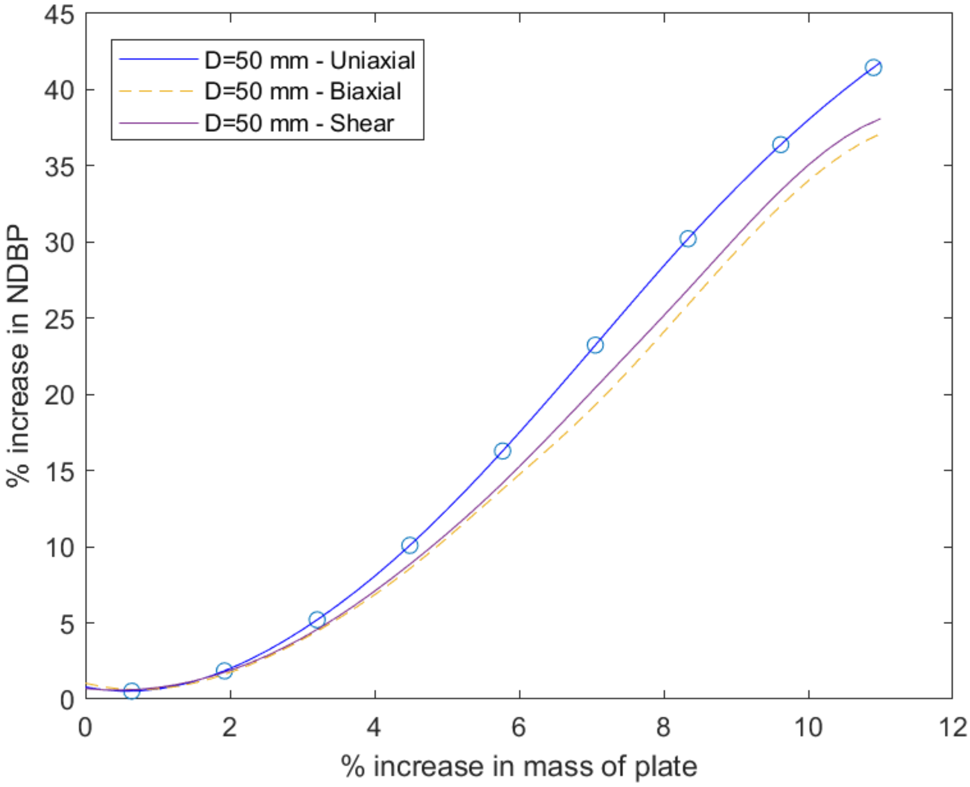

Figure 4.5: Variation of $\overline{P}$ with respect to the % increase of mass of plate (D = 50 mm,t = 2.5 mm, h = 3 mm)

4.1.2 %increase of $\overline{P}$ vs thickness

As reflected from the previous section, % increase in $\overline{P}$ is directly proportional to offset we create to un-stiffened plate. Hence sensitivity analysis with varying thickness can provide insight into how much degree of stiffening is required to attain desired increase in buckling capacity. Keeping this in consideration results are extracted for plate thickness ranging from 0.5 mm to 10 mm. To study this phenomena small data set with diameter (100 mm & 150 mm), 10 mm height of stiffener and 5 stiffeners along the width, is analysed with thickness varying between 0.5 mm and 10 mm. A detailed summary of the parameters is mention in table 4.2. Figure 4.6 graphically show the inputs with diameter 150 mm .

Table 4.2: Chosen set (highlighted in red) for comparison (%increase of $\overline{P}$ of vs t)

Diameters (mm)	Number of stiffeners (along shorter edge)									Height of stiffeners (mm)					
100	1	2	3	4	5	6	7	8		2	3	4	6	8	10
150	1	2	3	4	5					3	4	6	8	10	20

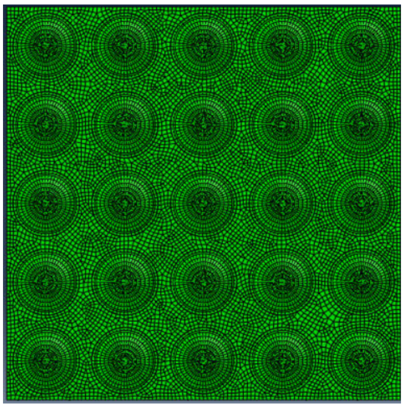

(a) Stiffening Pattern

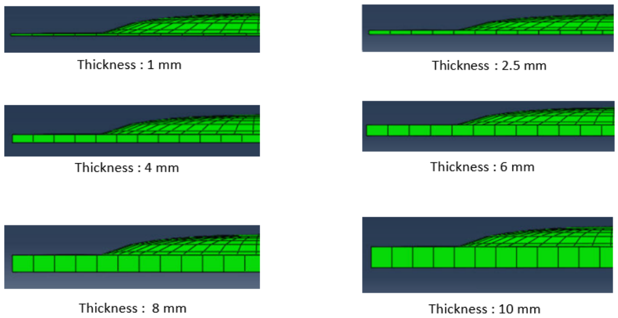

(b) Thickness comparison

Figure 4.6: Graphical representation inputs for thickness comparison with 150 mm diameter and 10 mm of height stiffener

Thinner the plates, more susceptible they are to the buckling failure. Thus any stiffening effort will produce significant increase in buckling capacity. Results with input stated in figure 4.6 are plotted in figure 4.7. We can observe from figure 4.7, for a constant stiffening pattern as the thickness increase, percentage increase in $\overline{P}$ drop drastically. For example, in this particular data , the % improvement for 0.5 mm thickness is 382.26% and for 4 mm thickness is 98.14% and for 10 mm thickness it is 29.77% under uni-axial loading.

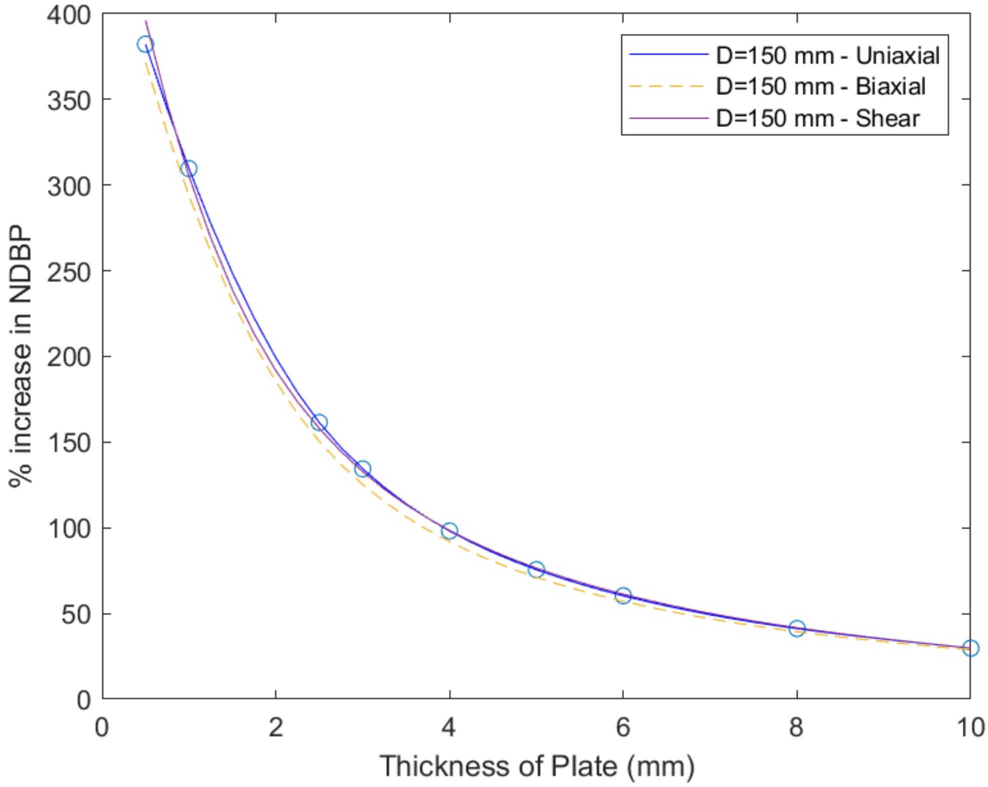

Figure 4.7: Variation of $\overline{P}$ with respect to the thickness of the plate (D = 150 mm, h = 10 mm and n = 5)

.

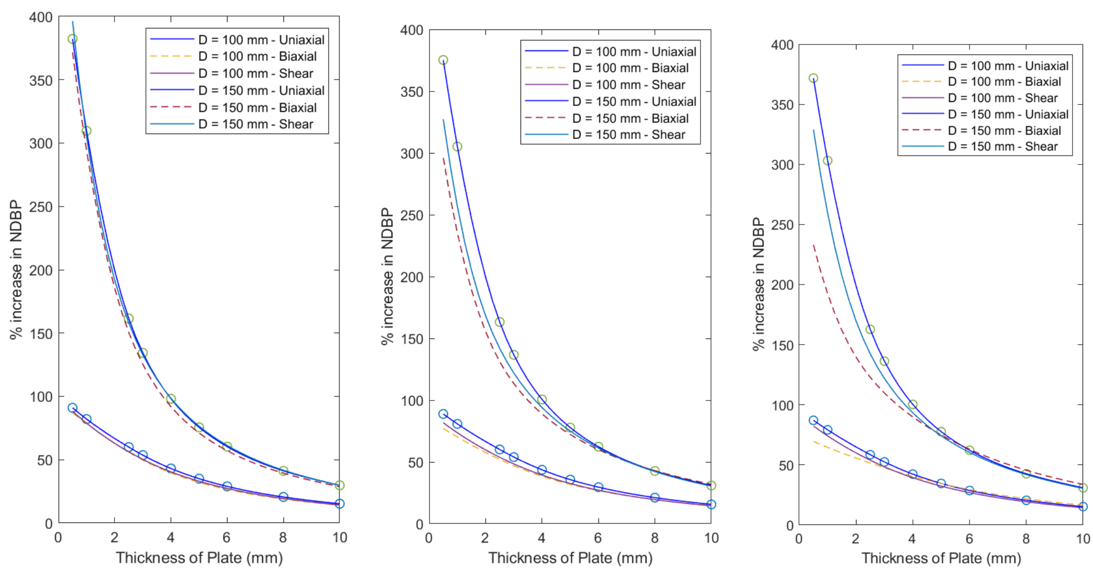

(a) $\alpha = 1$ **(b)** $\alpha = 2$ **(c)** $\alpha = 3$

Figure 4.8: % improvement of $\overline{P}$ (Buckling Capacity) with respect to thickness of the plate for α = 1,2 and 3

To further show the dependency of %increase in $\overline{P}$ vs thickness, result for data set in table 4.2 are plotted in figure 4.8. Overall similar trend can be observed across both diameter, all three aspect ratios and loadings. However another key observation is decreasing slope as the thickness increase. This suggest that effect of thickness variation dilutes with increasing thickness. Which relates to figure 4.6 (b), where plate thickness can be compared to the height of stiffeners. For smaller thickness major contribution to buckling capacity comes from stiffener. Though with higher thickness % contribution from plate thickness to buckling capacity also increase. Thus smaller overall increase in buckling capacity of the plate. This argument does not have numerical base from the extracted result, but is based on physical understanding of thin plate buckling.
Recommendation: Degree of offset relative to plate thickness, affect % increase in buckling capacity.

4.1.3 %increase of $\overline{P}$ vs Diameter of Stiffeners

The diameter of the shape is varied over a range of 25 mm - 850 mm. Nine diameters were considered throughout the analysis. This aspect has a high significance in terms of available surface area of the plate. A higher and smoother distribution of stresses are expected out of this analysis. Table 4.3 gives the details of a selected data set for the presentation of results. The figure 4.9 illustrates the increase in diameter for each iteration.

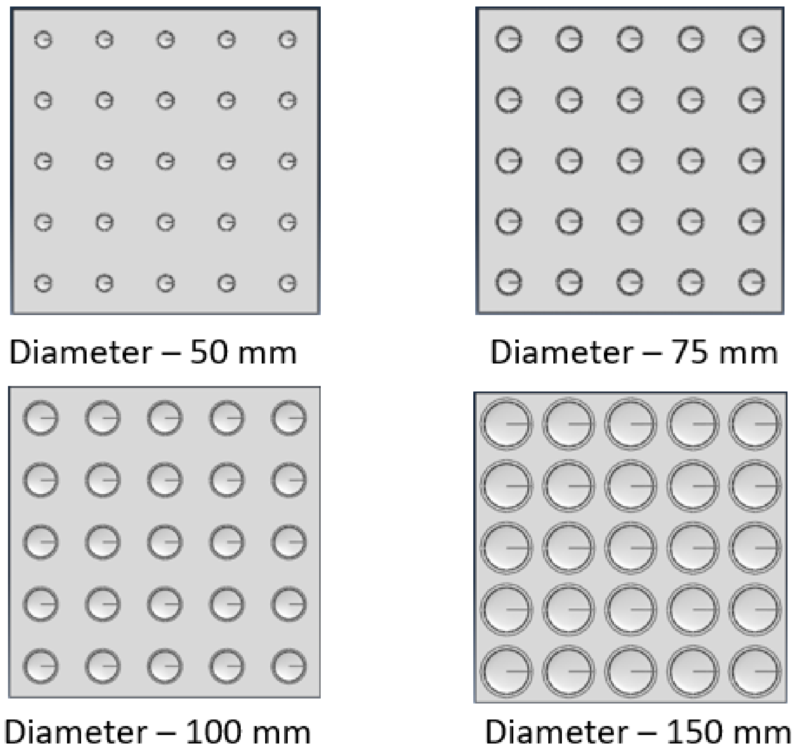

Figure 4.9: Variations of diameters of circular stiffeners

Table 4.3: Chosen set (highlighted in red) for comparison (%increase of $\overline{P}$ vs d)

Diameters (mm)	Range of stiffeners (along shorter edge)									Height of stiffeners (mm)					
25	1	5	9	13	17	21	25	29	33	2	3				
50	1	3	5	7	9	11	13	15	17	2	3	4	6		
75	1	3	5	7	9	11				2	3	4	6	8	10
100	1	2	3	4	5	6	7	8		2	3	4	6	8	10
150	1	2	3	4	5					3	4	6	8	10	20

The plate with circular stiffeners of varying diameters with height 3 mm, 5 number of stiffeners and the plate thickness of 2.5 mm is considered.The improvement in $\overline{P}$ is chosen for the comparison of the results.The variation of $\overline{P}$ with Respect to diameter of stiffening shapes is shown in figure 4.10.

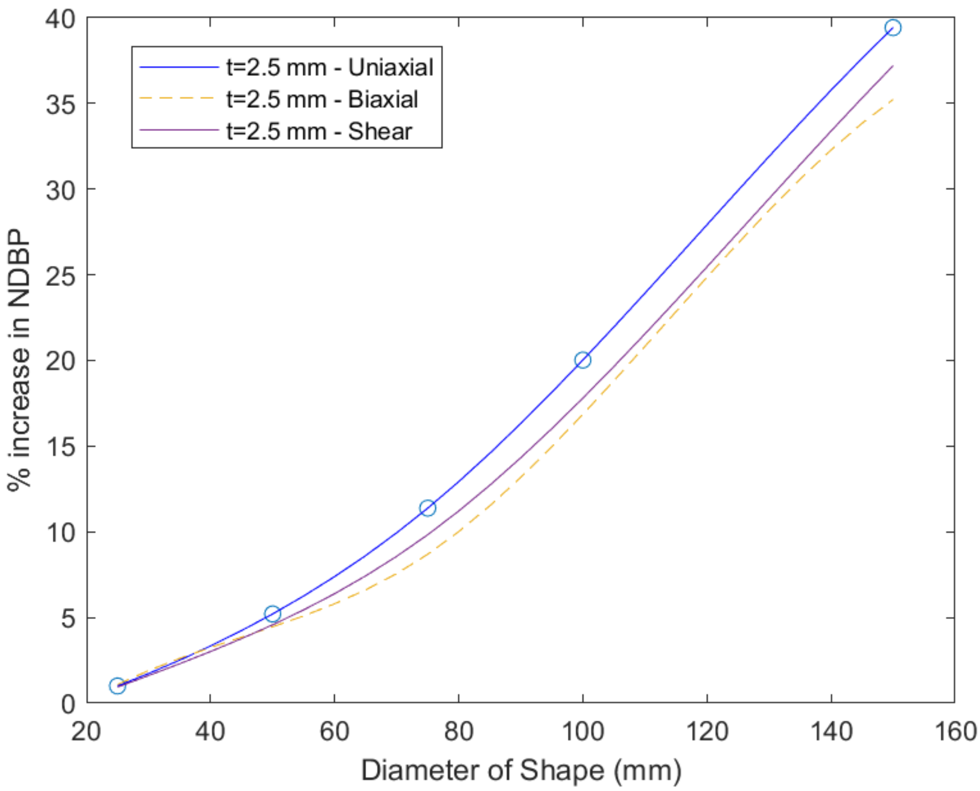

Figure 4.10: Variation of $\overline{P}$ with respect to the diameter of stiffening shapes (n = 5, t = 2.5 mm , h = 3 mm)

The trends are plotted for Uni-axial, Bi-axial and Shear Loading. The preliminary observation which can be made is that the trends remains similar for all types of loading. Yet, the increase of diameter results in approximately 2% higher $\overline{P}$ in case of Uniaxial Loading. The gradient of the curve becomes constant as the diameter increases. These study results show an a range of 0.5% to 39% improvement as the diameter changes from 25 mm to 150 mm. Similar trends can be observed in the cases plotted in figure 4.11.

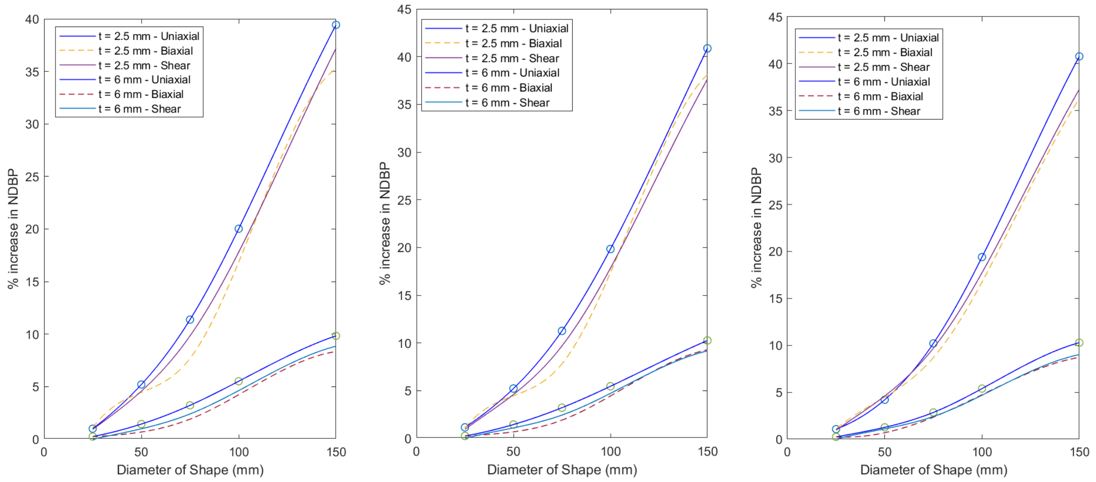

(a) $\alpha = 1$ (b) $\alpha = 2$ (c) $\alpha = 3$

Figure 4.11: % improvement of $\overline{P}$ (Buckling Capacity) with respect to diameters of stiffeners for α = 1,2 and 3

The graphs are plotted primarily two ranges with thickness variations for aspect ratios 1, 2 and 3. The graph is steeper for the plates of lower thickness. The increase in diameter for these lower thickness plate,yielded steeper enhancement of buckling capacity. For higher thicknesses , the slope of the graph is more gradual. Although, there are variations of the trends over varying thicknesses,the improvement patterns are similar for all the ranges of diameters.

Recommendation: A thinner plate can be used for wider range of diameters. Therefore, for thicker plates a larger diameter provide a good improvement in Buckling Load and the vice versa of thinner plates.

4.1.3.1 Mode Shapes

The circular stiffeners are spread uniformly across the surface of the plate. Therefore, this plate can be assumed to be an equivalent orthotropic flat plate. Therefore, although the buckling of the plate is postponed to a higher value of critical load, the first mode shapes with least mechanical energy remain similar to that of a flat plate.

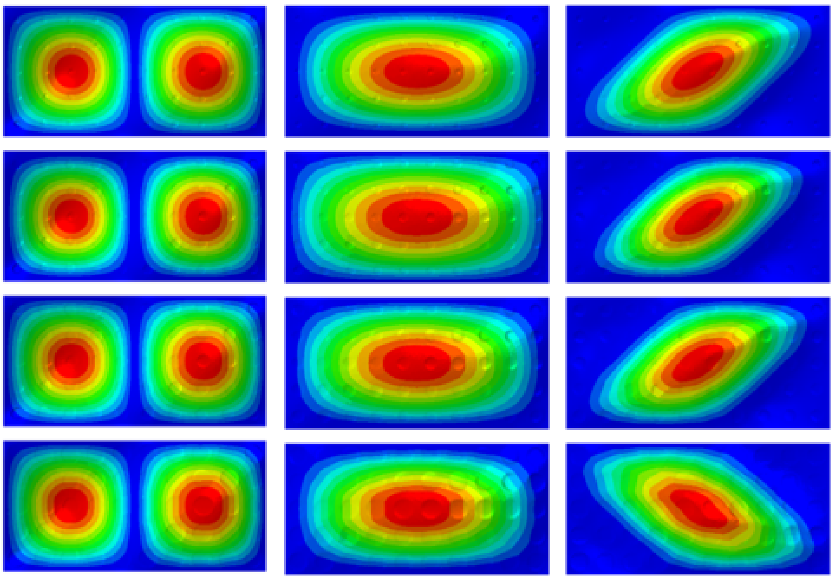

Figure 4.12: Mode shapes of plates stiffened with 7 number circular stiffeners with d=50 mm, 75 mm ,100 mm and 150 mm

4.1.4 $\overline{P}$ %inc vs Height

Height of stiffener is a crucial production aspect, thus insight of how this parameter will effect the plate behaviour is vital. To investigate the improvement in the buckling capacity by increasing the height of stiffener results from a small data set are plotted in figure 4.15. Summary of inputs for this data set are tabulated in table 4.4. From the two diameters (100 mm and 75 mm) chosen, a pictorial representation of models with 100 mm diameter is shown in the figure 4.13

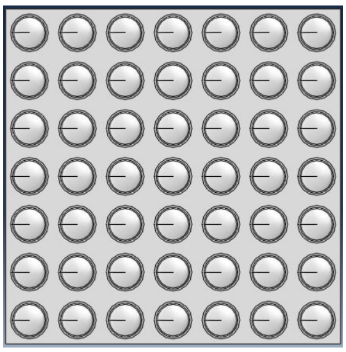

(a) Stiffening pattern

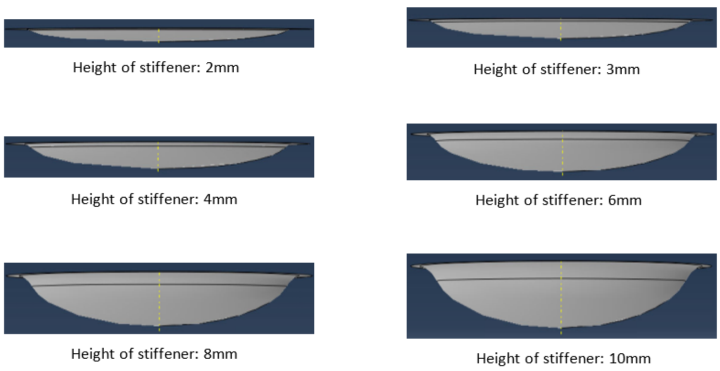

(b) Height comparison

Figure 4.13: Pictorial representation of models for height comparison with 100 mm diameter

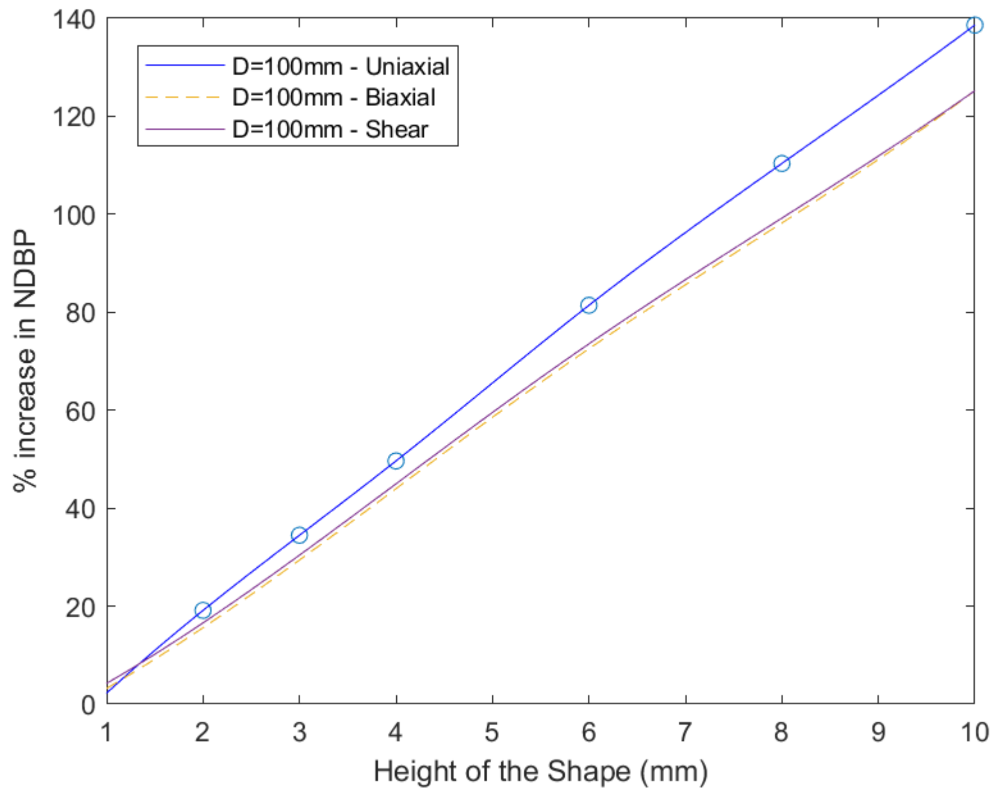

Figure 4.14: Variation of $\overline{P}$ with respect to the diameter of stiffening shapes (D = 100 mm, n = 7, t = 2.5 mm)

Table 4.4: Chosen set (highlighted in red) for comparison (%increase of $\overline{P}$ vs h)

Diameter (mm)	Number of stiffeners (along shorter edge)									Height of stiffeners (mm)					
75	1	3	5	7	9	11				2	3	4	6	8	10
100	1	2	3	4	5	6	7	8		2	3	4	6	8	10

Similar to previous sections, selected models are analysed under uni-axial, bi-axial and shear loading with aspect ratio of 1,2 and 3. Plate thickness of 2.5 mm and 7 number of stiffeners along shorter edge, remain constant.

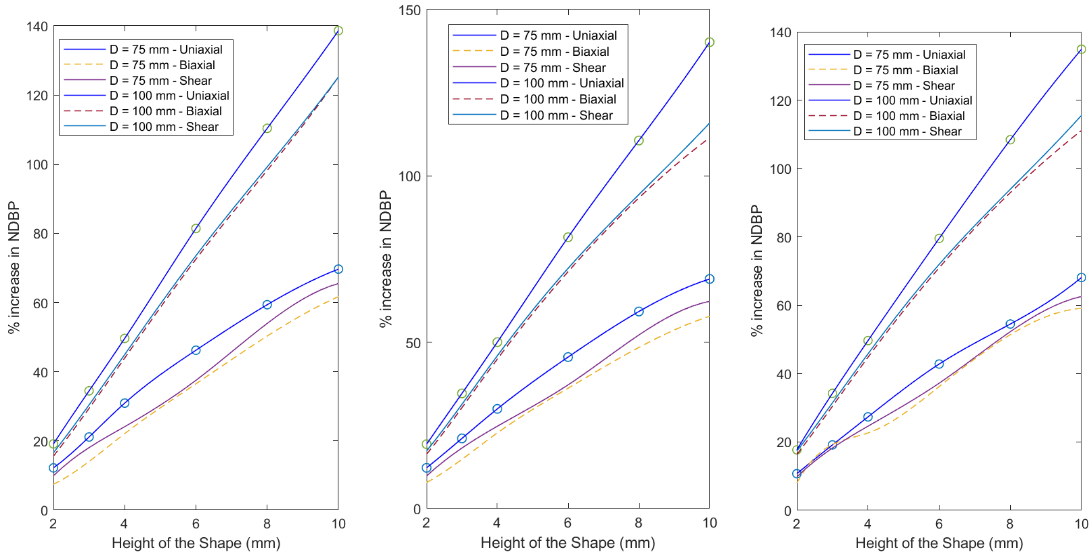

(a) $\alpha = 1$ **(b)** $\alpha = 2$ **(c)** $\alpha = 3$

Figure 4.15: % improvement of $\overline{P}$ (Buckling Capacity) with respect to height of stiffeners for α = 1,2 and 3

As height of stiffeners increase % increase in $\overline{P}$ as compared to flat plate also increase. For example in figure 4.15 (a) with 75 mm diameter under uni-axial compression as height of stiffener increase from 3 mm to 10 mm, %increase $\overline{P}$ also increase from 21.13% to 69.67%. Similar trend can be observed with other loadings and diameters across all aspect ratios.

Another key observation from the graphs in figure 4.15 indicates that increasing height of stiffener for higher diameter lead to greater increase in $\overline{P}$. Argument is supported by relatively steeper slope with increasing height of stiffeners for 100 mm diameter. Quantitatively, an increase of stiffener height from 3 mm to 10 mm lead to % increase in $\overline{P}$ of from 34.47% to 138.62% as compared to 21.13% to 69.67% for diameter 75 mm.

Recommendation: Degree of offset increase with increasing height of stiffener. Based on limitations of production method and avoiding local yielding at edge of the stiffening shape, higher heights are recommended.

Although we observe enhanced buckling capacity by increasing the height of stiffening shape, these offset from the plane of the plate can also act as initial imperfection. Leading to induced moments and out of plane stresses as illustrated in figure 4.16 (b). Effect of these inherit imperfection amplify under higher loads, which are expected when concept is applied thicker plates.

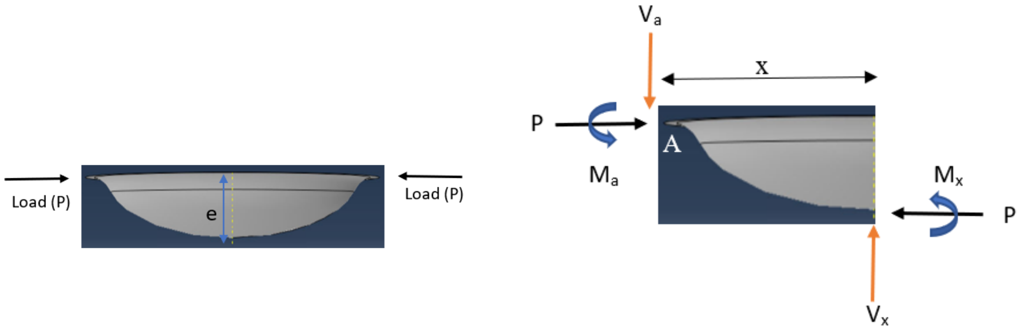

(a) Height as imperfection (b) Effect of imperfection

Figure 4.16: Height of plate acting as imperfection, leading to induced moment and out of the plane stresses

4.1.4.1 Mode Shapes

The first buckling mode shape for plate modified with 7 number of 100 mm circular stiffeners is shown in in figure 4.17. In terms of buckling mode shape behaviour of modified is similar to a flat plate. Although with increasing height of stiffener the buckling capacity increases, still the mode shapes remain almost same. Disturbance to buckling mode by introduction of unit cells, is big to altogether change the buckling mode.

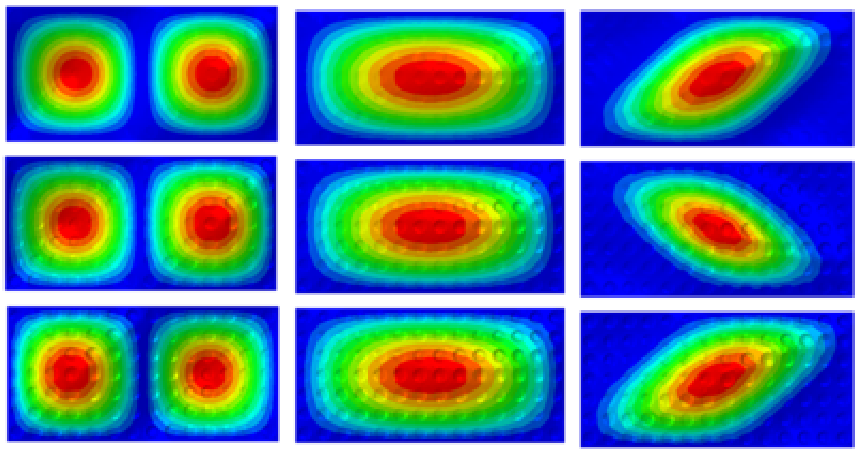

Figure 4.17: Mode shapes of plates stiffened with 7 number of 100 mm circular stiffeners with h = 2 mm, 6 mm and 10 mm

4.2 Recommended plate configuration

The analysis performed in the previous sections not only validate the concept of this work,but also establish the most optimised pattern that can be chosen, for a required increase of buckling capacity. Out of 18558 iteration, about 80% of the results show an improvement over 40%.

A further refining analysis is performed by sorting out the results with more than 40% improvement. The % improvement of these results vary from 40% - 1200% of improvement in elastic buckling load. This study was performed by comparing all the dimensional parameters to one another. Some interesting revelations are observed.

- The maximum improvement should be observed by taking all the parameters into consideration.
- The density of the Stiffeners plays a major role. Higher diameters with lower density produces lower improvement than lower diameters with higher density. For example a plate with 9 number of 75 mm diameter stiffeners with height 10 mm gives 321.96% of improvement where as a plate with 6 number of 100 mm diameter stiffeners with height 10 mm gives 164.94% of improvement.
- The height of the stiffener is an other important parameter. A Higher diameter stiffener with lower height gives lower improvement that a lower diameter stiffener with higher height.For example a plate with 5 number of 150 mm diameter stiffeners with height 30 mm gives 278.94% of improvement where as a plate with 6 number of 75 mm diameter stiffeners with height 10 mm gives 78.9% of improvement.
- Higher diameters are best suitable for higher thickness and lower diameter for lower thickness. The range of thickness is increased with increase in diameters. For example, the highest diameter of 400 mm produces a results ranging from 341% to 25% over the thickness range of 0.5 mm - 10 mm. The lower diameter of 100 mm produces an improvement range of 541% to 20% over a thickness range of 0.5 mm to 10 mm. The reduction in the % improvement becomes steeper as the diameter decreases,thereby, reducing the range of thicknesses for lower diameters.

By considering all these factors, the diameters are divided into smaller ranges to identify the most optimized layout of the stiffeners for each range.The ranges are:

Table 4.5: Recommended stiffener parameters

Range of Diameters (mm)	Minimum Height Multiplication Factor (a)	Thickness Range (mm)
25-75	0.12	0.5-1
75-150	0.08	0.5-3
150-300	0.07	0.5-5
300-500	0.1	0.5-8
500-850	0.1	0.5-10

Table 4.6: Study results of optimized patterns analysis

Range of Diameters (mm)	a	t	minimum increase (%)	Diameter - Height - Number of Stiffeners	maximum increase (%)	Diameter - Height - Number of Stiffeners
25-75	0.12	0.5	262%	25 mm - 3 mm - 33	1143.63%	75 mm - 10 mm - 11
		1	112%	25 mm - 3 mm - 33	583.43%	75 mm - 10 mm - 11
75-150	0.08	0.5	533.96%	75 mm - 6 mm - 11	1143.63%	75 mm - 10 mm - 11
		3	78.92%	75 mm - 6 mm - 11	278.94%	150 mm - 30 mm - 5
150-300	0.07	0.5	127.92%	300 mm - 20 mm - 2	645.05%	150 mm - 20 mm - 5
		5	75.55%	150 mm - 10 mm - 5	167.31%	150 mm - 20 mm - 5
300-500	0.1	0.5	84.73%	500 mm - 40 mm - 1	151.61%	300 mm - 40 mm - 2
		8	72.43%	500 mm - 40 mm - 1	114.16%	300 mm - 40 mm - 2
500-850	0.1	0.5	84.73%	500 mm - 50 mm - 1	389.68%	850 mm - 50 mm - 1
		1	72.00%	500 mm - 50 mm - 1	320.31%	850 mm - 50 mm - 1

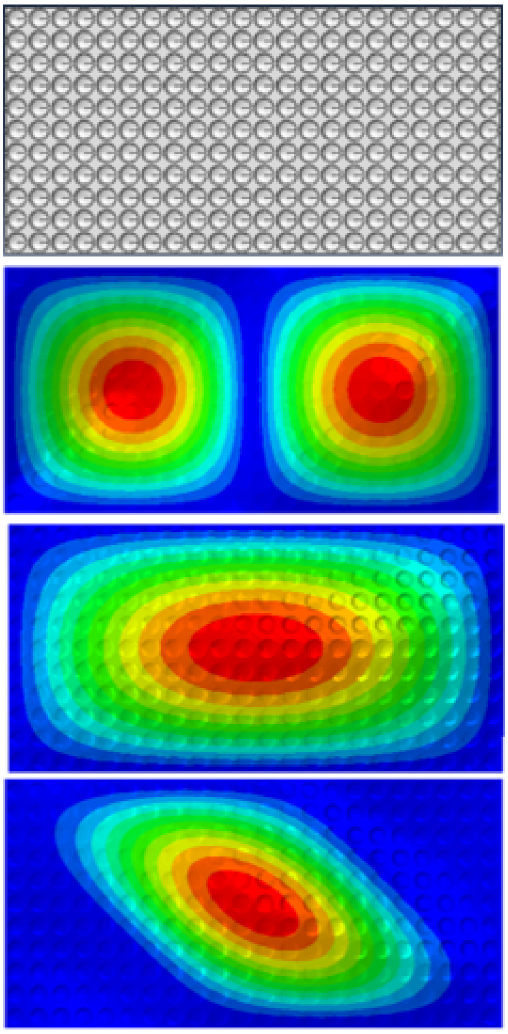

Figure 4.18: A stiffened thin plate of $\alpha = 2$ with the most optimized pattern and its mode shapes due to uni-axial , bi-axial and shear loading

The table 4.6 presents the maximum and minimum improvement that can expected if a range is selected for the minimum and maximum thicknesses. All the observations mentioned earlier are reflected in this results. From this analysis, we can also find the most optimized pattern of the entire study is obtained when stiffeners of diameter 75 mm, height 10 mm and 11 number of stiffeners along the shorter side are used. The detailed analysis of the optimized pattern is presented in figure 4.18

4.3 Nonlinear Post Buckling Analysis

Based on the methodology explained in section 3.6, 0.5 m × 0.5 m plate is analysed using static riks analysis. Summary of input and distribution of stiffening pattern can be found in table 3.15 and figure 3.15 respectively. This section reports results from non linear analysis to draw comparison between the behaviour of stiffened and the flat plate. With constant stiffening pattern, 15 model are generated to be analysed

Summary of the results can be found in table 4.7, which are followed by the load vs deformation curves in figure 4.19. Each of the load vs deformation graph corresponds to a specific thickness. Within each graph, comparison between the stiffened and flat plate with varying material models is plotted. With constant stiffening pattern, 15 model are generated to be analysed. Load curves vs deformation in form of non dimensional parameter can be found in appendix C

Table 4.7: Non-linear analysis results

Thickness	1 mm	2 mm	3 mm	4 mm	5 mm
Thickness as % of plate width	0.2	0.4	0.6	0.8	1
Linear Buckling Analysis					
Linear Buckling load Stiffened Plate (kN)	13.34	73.39	191.03	379.71	654.54
Linear Buckling load: Flat Plate (kN)	3.04	24.27	81.99	194.32	379.45
$\overline{P}$: Stiffened Plate	173.42	119.26	91.98	77.13	68.07
$\overline{P}$: Flat Plate	39.47	39.47	39.47	39.47	39.46
% increase between stiffend and flat plate	**339.36**	**202.14**	**133.02**	**95.41**	**72.50**
Non Linear Analysis					
Material	*S355*				
Ultimate load Stiffened Plate (kN)	28.73	96.08	230.00	389.08	580.09
Ultimate load: Flat Plate (kN)	23.64	96.08	225.83	417.99	671.70
$\overline{P}$: Stiffened Plate at "Ultimate Load"	373.44	172.94	110.74	79.03	60.33
$\overline{P}$: Flat Plate at "Ultimate Load"	307.37	156.13	108.73	84.90	69.86
% increase between stiffend and flat plate	**21.49**	**10.77**	**1.84**	**-6.92**	**-13.64**
Material	*S690*				
Ultimate load Stiffened Plate (kN)	38.22	14.40	321.28	564.79	864.85
Ultimate load: Flat Plate (kN)	33.80	133.98	306.40	560.26	901.91
$\overline{P}$: Stiffened Plate at "Ultimate Load"	496.90	234.10	154.69	114.72	89.94
$\overline{P}$: Flat Plate at "Ultimate Load"	439.35	217.72	147.53	113.80	93.80
% increase between stiffened and flat plate	**13.10**	**7.53**	**4.86**	**0.81**	**-4.11**
Material	*S900*				
Ultimate load Stiffened Plate (kN)	42.05	16.27	361.59	643.00	1016.57
Ultimate load: Flat Plate (kN)	38.39	154.49	168.29	634.54	997.34
$\overline{P}$: Stiffened Plate at "Ultimate Load"	546.70	264.49	174.10	130.61	105.72
$\overline{P}$: Flat Plate at "Ultimate Load"	499.06	251.04	168.29	128.89	103.72
% increase between stiffend and flat plate	**9.55**	**5.36**	**3.45**	**1.33**	**1.93**

.

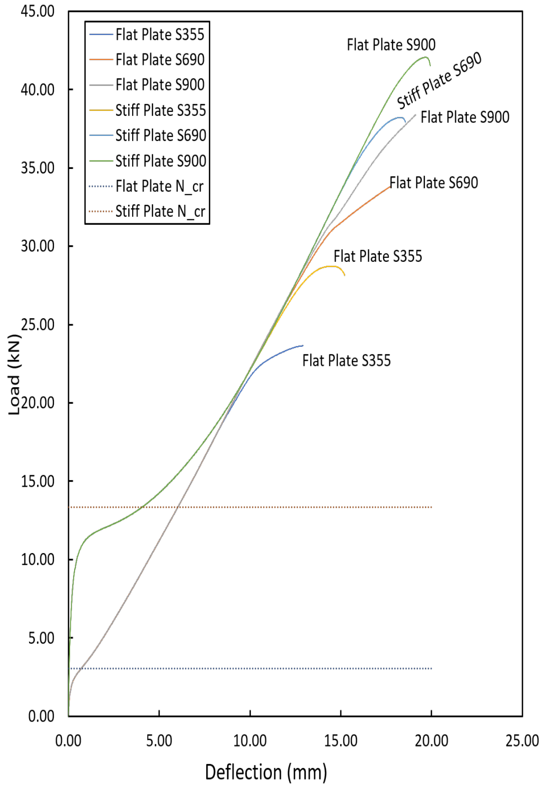

(a) Plate thickness = 1 mm

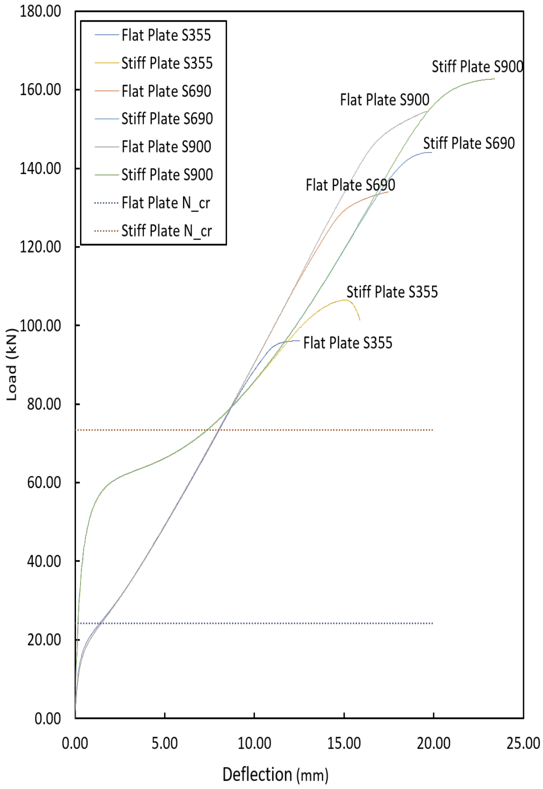

(b) Plate thickness = 2 mm

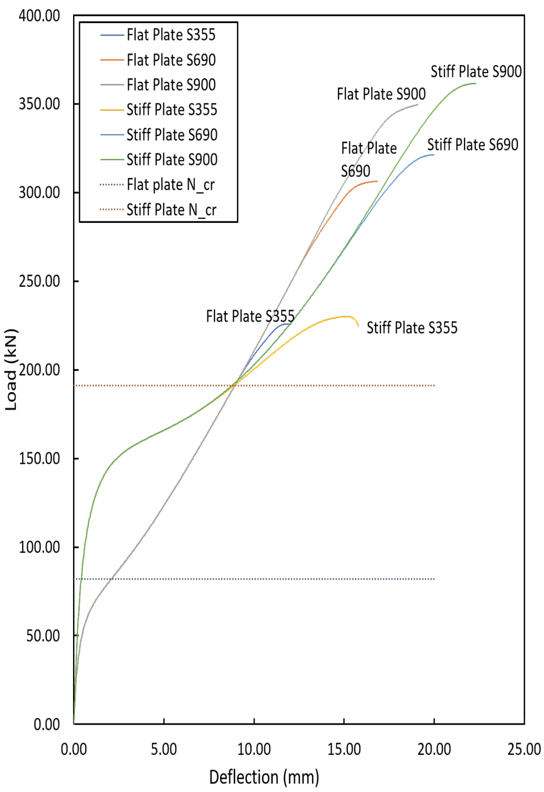

(c) Plate thickness = 3 mm

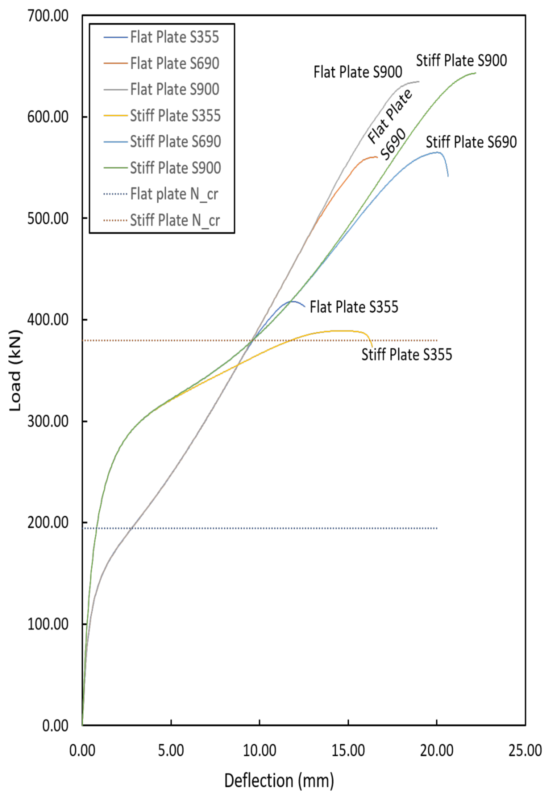

(d) Plate thickness = 4 mm

Figure 4.19: Continued...

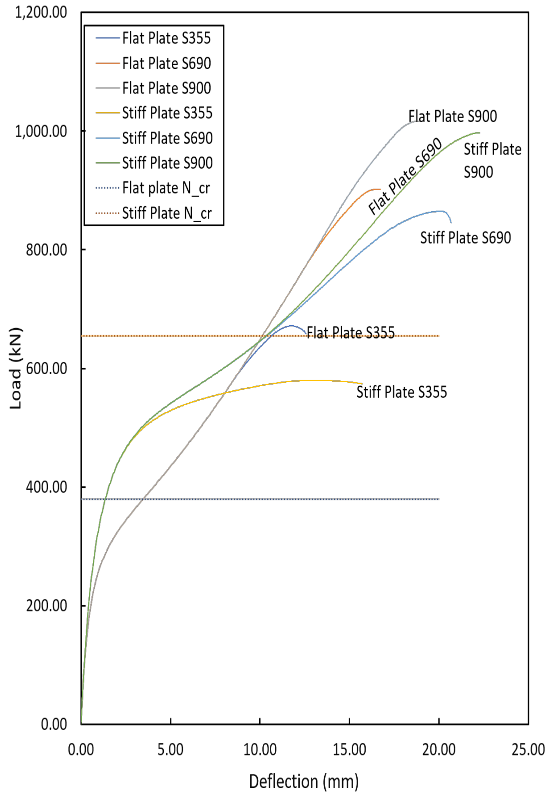

(e) Plate thickness = 5 mm

Figure 4.19: Load vs out of plane deflection response of flat and stiffened plate for varying thickness and steel grade under uni-axial compressive loads.

Load deformation curves clearly show positive effect of stiffening pattern on the bifurcation load. Aligning well with the results from linear buckling analysis, and verifying the patterns observed in the linear buckling analysis.

For thin plate transition from pre-buckling and post buckling behaviour is not clearly defined. So buckling capacity is calculated by using 2% offset method. In this method firstly initial slope of load vs deformation curve is calculated.Then a line with this slope is shifted toward right by 2% of the maximum deflection. The load at intersection between this line and load-deformation curve is defined as buckling load. Figure 4.20 shows how buckling load of 52 kN and 123 kN is calculated for flat and stiffened plate respectively. Results are calculated from stiffening pattern shown in figure 3.15 with thickness of 3 mm using S690 material model.

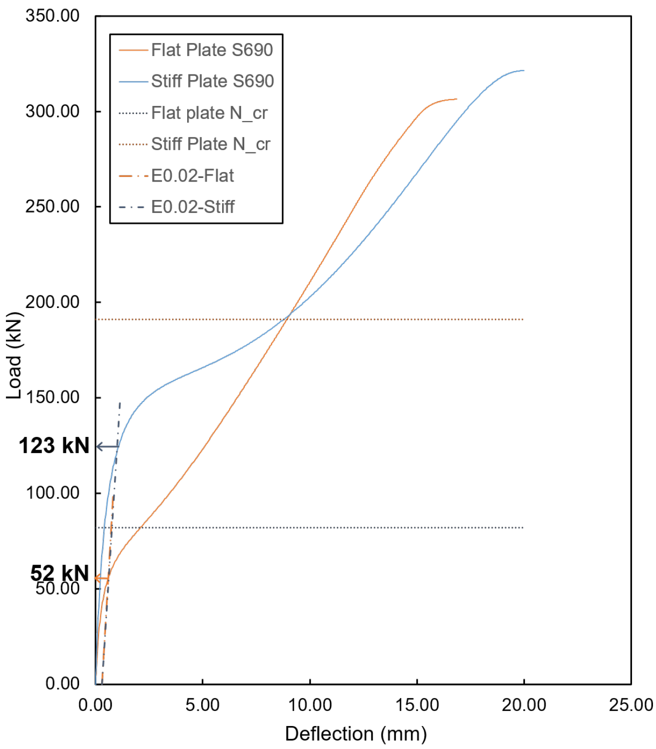

Figure 4.20: Load vs Deformation curve for thickness 3 mm and S690 material model to calculate yielding load (t = 0.6% of plate width)

Table 4.8 shown comparison between critical buckling load from linear and non linear analysis. Two of the key conclusions are:

- % increase in buckling capacity between stiffened and flat plate is similar using linear (132.99%) and non linear analysis (136.54%).
- Reduction in buckling load, introduced by geometric and material non linearity is affecting stiffened (36.58%) and flat (35.61%) plate by similar proportion.

Table 4.8: Buckling load from linear and non-linear analysis for t = 3 mm (0.6% of plate width) using S690 material model.

	Buckling Load Flat Plate (kN)	Buckling Load Stiff Plate (kN)	% Difference between Stiff and Flat plate
Eigen Buckling Analysis	81.99	191.03	132.99%
Post Buckling Analysis	52	123	136.54%
% Difference between Eigen and Post Buckling Analysis	36.58%	35.61%	

The figure 4.21 compare deflection and stress distribution for flat and stiffened plate at respective buckling loads. Similarly figure 4.22 compare deflection and stress distribution for flat and stiffened plate at respective ultimate collapse load. In both figures we can observe similar deflection patterns for flat and stiffened plate. However, distribution of stresses completely changes by introduction of stiffening pattern. In fig 4.21 (c) for flat plate stresses are concentrated at the centre of the plate. Where as in fig 4.21 (d) for stiffened plate we observe stiffeners resisting accumulation of stresses at centre and spreading them across the plate. Comparably, for the flat plate at ultimate load stress are concentrated at edges where load is applied and stiffened plate has much more uniform distribution instead (figure 4.22 (c) vs (d)).

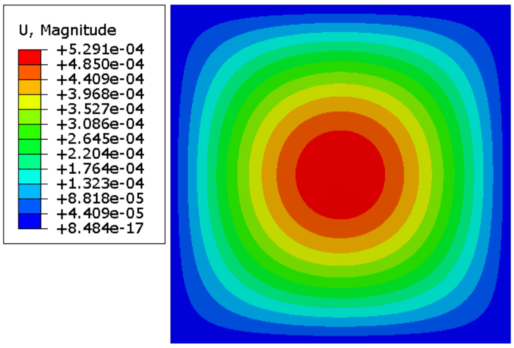

(a) U3 flat plate at buckling load

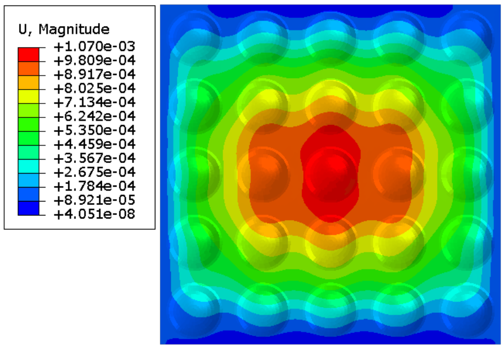

(b) U3 stiff plate at buckling load

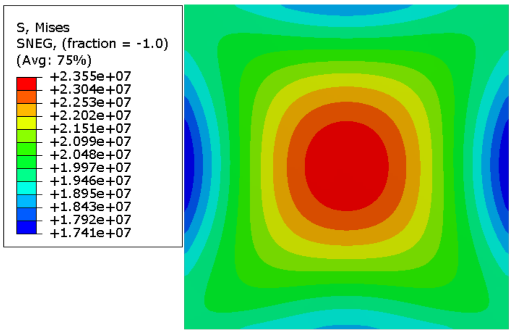

(c) Stress flat plate at buckling load

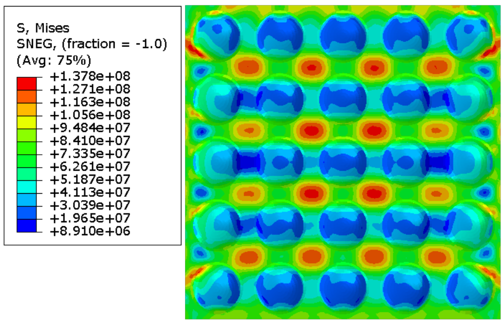

(d) Stress stiff plate at buckling load

Figure 4.21: Comparison between stiff and flat plate using out of the plane deflection and stresses at buckling load of 123 kN and 52 kN respectively

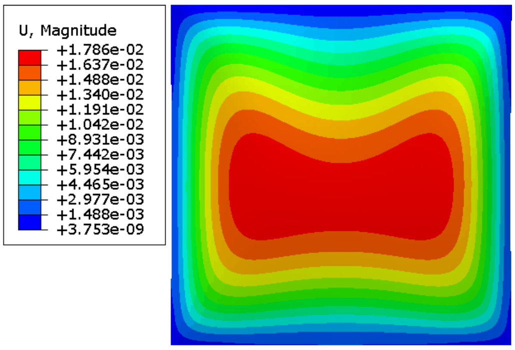

(a) U3 flat plate at ultimate load

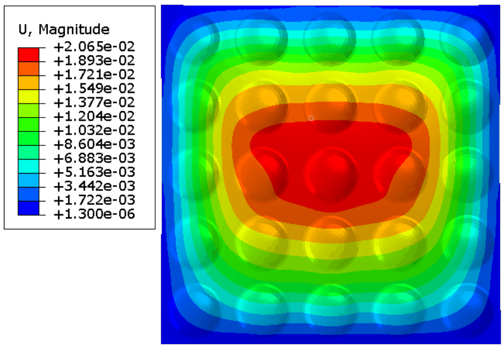

(b) U3 stiff plate at ultimate load

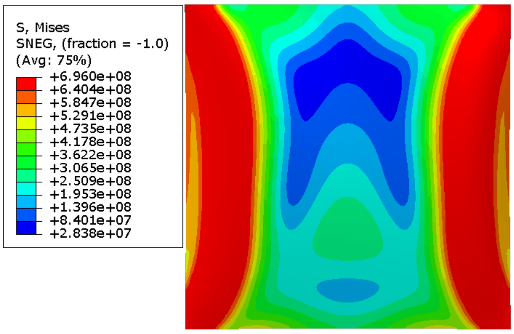

(c) Stress flat plate at ultimate load

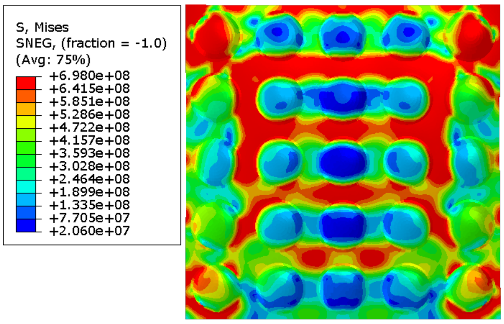

(d) Stress stiff plate at ultimate load

Figure 4.22: Comparison between stiff and flat plate using out of the plane deflection and stresses at ultimate load of 321.28 kN and 306.40 kN respectively.

The stiffening patterns significantly increase the buckling capacity of the thin plates but the exact mechanism behind this improvement needs further research. Numerical models derived from extensive parametric study would be required to accurately quantify contribution of each parameter towards the behavior of stiffened plates. However, stress distribution plots suggest that relatively more uniform distribution of stresses is leading to enhanced buckling behavior.

Although introducing patterns is leading to uniform distribution of stresses, they will also act as imperfections within the plate. Adverse effect of imperfections will amplify with increasing load, hence application of proposed concept should be critically analyzed for thicker plates. As the loads at bifurcation and in post buckling range might rise significantly for thicker plate.

Despite the fact that number of models studied are very limited to confidently draw the conclusions, few of the key observations from the comparison of stiffened plate and flat plate results are:

- For thickness range under consideration bifurcation load is independent of material yield strength. So, if design loads are not expected to go beyond bifurcation load of stiffened plate, the concept is applicable to all material classes.

- Using higher material class for stiffened plate in lower thickness range (0.2%-0.4%) can increase the post buckling strength has compared to that of flat plate.
- In intermediate thickness range of (0.6%) material class starts playing role in utilization of ultimate strength for stiffened plate in comparison to flat plate. As an example, for the case studied with material class S355 there is only 1.84% difference in ultimate load of stiffened and flat plate. However, this difference increases 4.86% with S690 material model.
- Effect of stiffeners acting as inherit imperfection increase with increasing load, as percentage difference between ultimate strength of stiffened and flat plate decrease with higher material class. Trend can be consistently observed in thickness range (0.2%-0.4%).

4.4 Shape of the Stiffener

The third part of the thesis focuses on the various shapes of stiffeners. The shape of the stiffener acts as a secondary surface for distribution of stress and provides an increase width and length at its location thereby providing higher surface area.As discussed in section 3.4, these can also act as an additional imperfection. Each shape has to be optimized and analysed for its appropriate dimensional properties in order to provide a smoother and practical transition to avoid stress concentrations. For this analysis, various shapes are considered. They are:

1. Circular Stiffeners
2. Square Shaped Stiffeners
3. Capsule shaped Stiffeners
4. Triangular Stiffeners

The cross-sections of these section is show in the chapter 3 in the figure 3.4.Linear Buckling Analysis is conducted to compare different shapes of the stiffeners.To keep the distribution constant and the results comparable, a new set of density parameters were considered. The analysis was performed on a plate of dimensions 1 m × 3 m × 5 mm. All types of loading conditions were used.The properties of the study were tabulated below.

Table 4.9: Circular Stiffeners

Shape	Circle (m)
Major axis	0.2
Minor axis	0.1
height	0.05
number	36

Table 4.10: Triangular Stiffeners

Shape	Equilateral Triangle (m)
Height of triangle	0.2
Height of shape	0.05
Number of stiffeners	39

Table 4.11: Square Stiffeners

Shape	Square (m)
Side	0.2
Height	0.05
Number	36

Table 4.12: Capsule Stiffeners - Horizontal

Shape	Capsule (m)
Direction	Horizontal
Major axis	0.2
Minor axis	0.1
Height	0.05
Number	36

Table 4.13: Capsule Stiffeners - Vertical

Shape	Capsule (m)
Direction	Vertical
Major axis	0.2
Minor axis	0.1
Height	0.05
Number	36

Table 4.14: Capsule Stiffeners - 45 Degrees

Shape	Capsule
Direction	45 degrees
Major axis	0.2
Minor axis	0.1
Height	0.05
Number	36

The results of the linear Buckling analysis were generated and the the %increase in $\overline{P}$ is compared for all the shapes. This is plotted in a bar graph 4.23 to show the comparison of each shape.

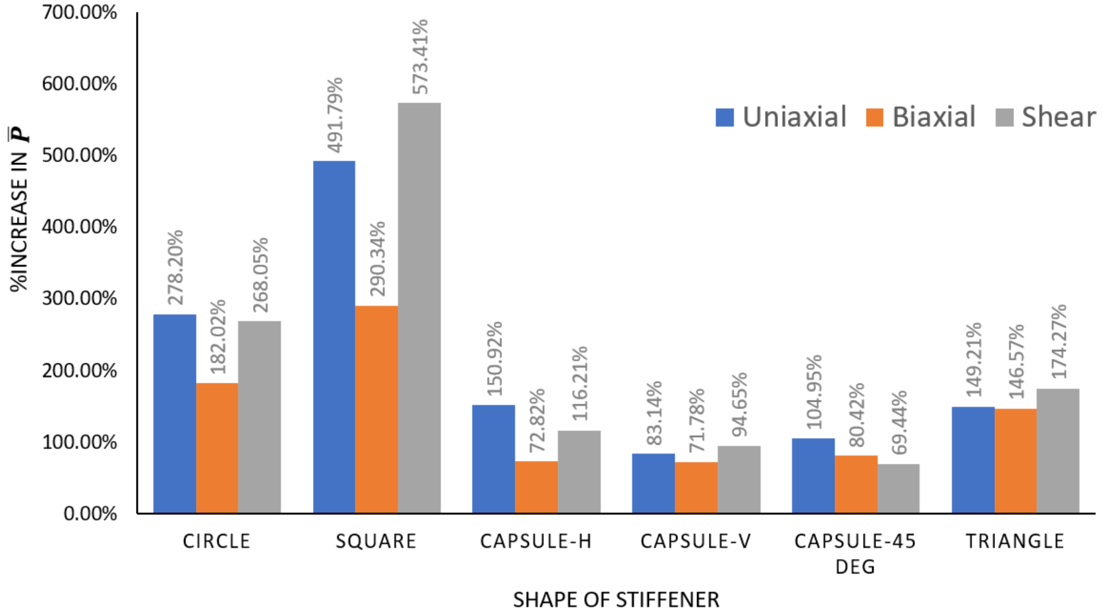

Figure 4.23: Comparison of the Shapes of the Stiffeners

The results of the study gives a trend of Square > Circle > Triangle > Horizontal Capsule > Vertical Capsule > Inclined 45 deg Capsule.The efficiency of the square is expected due to the provision of these shapes,enables the flat area of the plate to act as longitudinal and transverse stiffeners and also providing the highest surface area.

4.4.0.1 Mode Shapes

The judgement of the most beneficial shape can also be assessed by looking at their mode shapes.These are show in figures 4.24 - 4.29

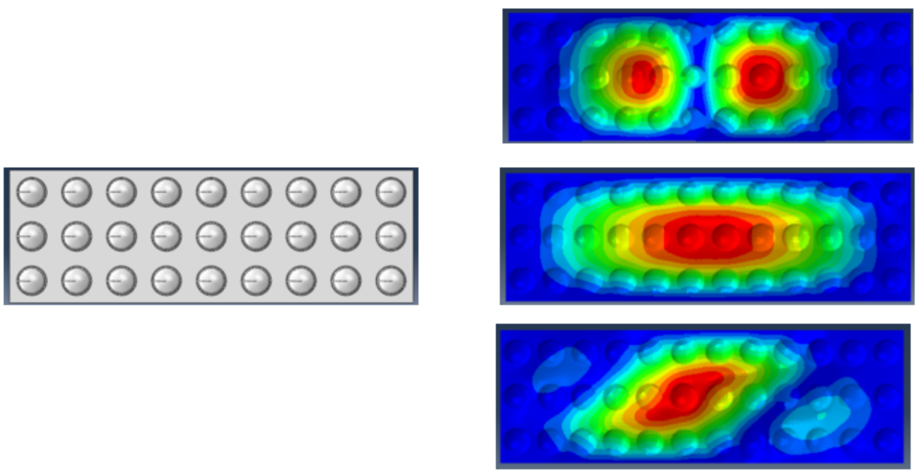

Figure 4.24: Circular stiffeners

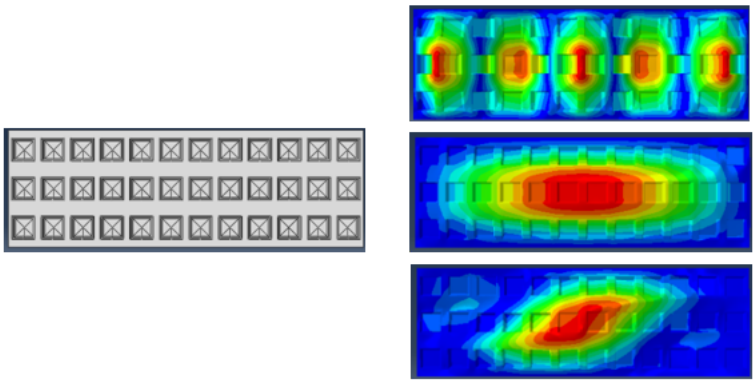

Figure 4.25: Square stiffeners

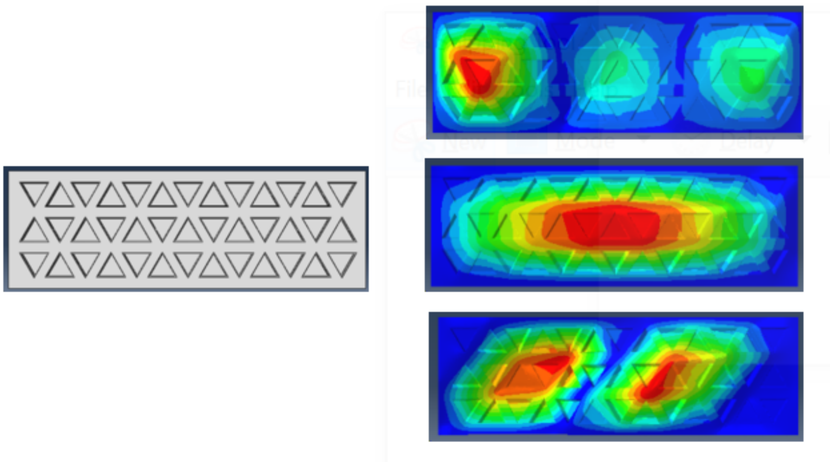

Figure 4.26: Triangular stiffeners

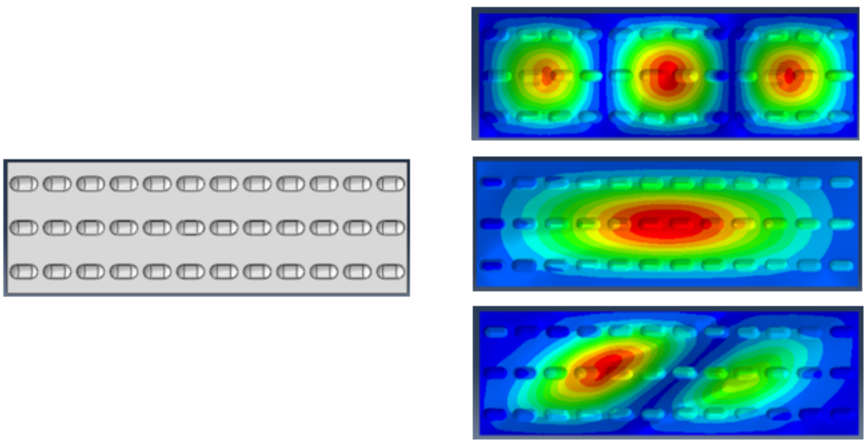

Figure 4.27: Capsule stiffeners - Horizontal

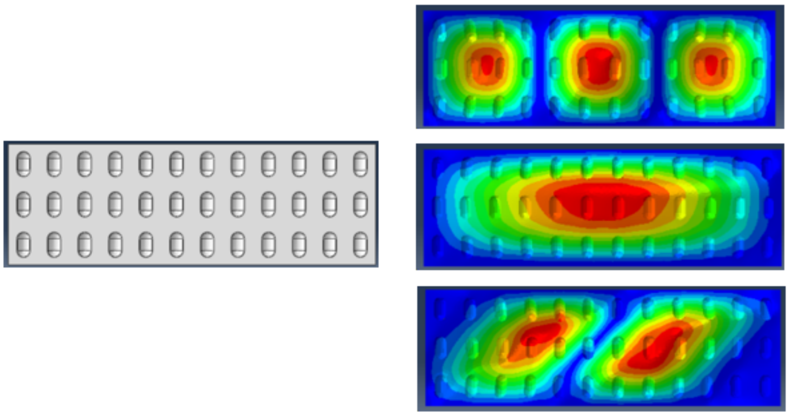

Figure 4.28: Capsule stiffeners - Vertical

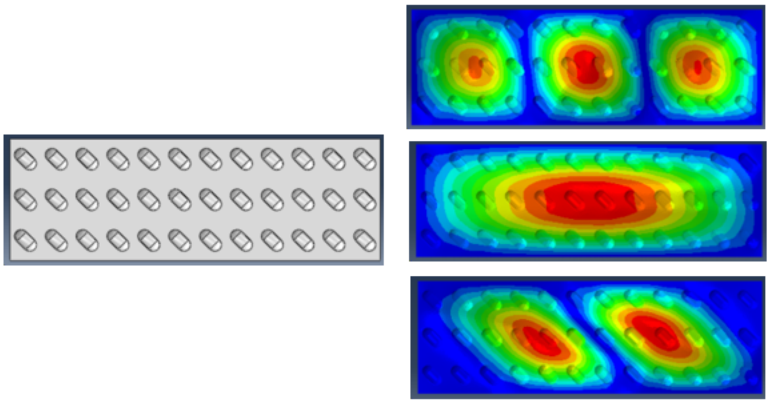

Figure 4.29: Capsule stiffeners -Inclined

From the modes shaped we can see that the buckled area of the plate with square shaped stiffeners less compared to other stiffener shapes. For the plates with capsule shaped unit cell and triangular unit cell, the mode shapes remain similar to flat plate. For the plates with circular shaped unit cells, the mode shape has shifted to second mode shape of that of flat plate. For the plates with square stiffeners,the mode shape resembles that of a 5 half sine curves. Therefore, mitigating the local buckling failure to a greater extent. These mode shapes are sensitive to the dimensions of the stiffeners shapes and should not be considered to be similar in all cases. Yet, this provides a validation to the best shape among all the analysed shapes.

5

Conclusion

5.1 Conclusion

In this master's thesis, stiffening patterns were introduced on the surface of thin plates (0.5 - 1% of plate width) to study their effect on critical buckling load. The table 5.1 draws a comparison between how stiffening patterns can be compared to increasing thickness in terms of buckling capacity. By introducing a stiffening pattern to a 2.5 mm thickness plate we can achieve a buckling load greater than 4 mm thickness plate, without any increase in the mass. There are not many applications for thin plates without any stiffening method. Thus comparison must only be used to see how significantly percentage increase in buckling capacity can impact, rather as weight reduction.

Table 5.1: Perspective towards enhanced buckling capacity by the implementation of the proposed concept with circular stiffeners of D = 150 mm, n = 5, h = 20 mm on 1 m × 1 m plate

	Stiffening method	Thickness (mm)	Critical Buckling Load (N)	% increase in buckling load	Mass of the plate (kg)	% increase in mass
Original Plate	-	2.5	11864	-	20.125	-
Stiffer Plate	Increasing Thickness	4	48593	309.58%	32.2	60%
	Stiffening Pattern	2.5	50376	324.00%	20.125	0%

The preliminary investigation included finding the optimal direction of stiffeners and the validity of the work upon varying plate dimensions. Followed by extensive parametric linear buckling analysis of a plate with various patterns of circular stiffeners by using ABAQUS and python scripting. Sensitivity analysis is performed to identify the stiffener's edge curvature and other parameters for the parametric study.

Conclusion from linear buckling analysis with circular stiffeners:
The least diameter of 25 mm of thickness 0.5 mm thickness with a highest density of 33 number of stiffeners produced 260% of improvement which is very commendable even though its effect with a lower density is not significant. The dimensional parameters of the stiffened plate have an interdependent effect on each other and on % increase in NDBP. This can be seen in table 5.2. To elaborate:

- The parameter which stands out is the Density or Number of stiffeners that could be used which is also governed by the plate dimensions and diameter/Side of the stiffener.For example, by increase the number from 1 to 7 for diameter 75 mm, an increase of 72% can be observed.

- The number of stiffeners that can be accommodated depends on the diameter of the stiffener. The diameter has a advantageous effect on the improvement of buckling capacity. Yet its increase results in reduction of the density. Therefore the selection must be made carefully.
- As observed from the graphs 4.11 and 4.8, a thicker plate yields good results only with higher diameters. This stiffening is most suitable for thinner plates of thickness in the range of 0.5 mm to 2.5 mm.
- The next parameter is the height of the stiffener which also has a positive influence on the improvement. Yet, choice of height must be made keeping in view of the production, visual and practical aspects.
- Selection of the suitable stiffening must be carefully made. For example, selection of 7 number stiffeners with diameter 75 mm yields 90% additional improvement when compared to 1 stiffener of 100 mm.
- The lower diameter of 75 mm can also accommodate further more stiffeners (maximum of 11) when compared to 100 mm (maximum of 7). Therefore, the choice of pattern governs the buckling capacity.

Table 5.2: Summarized comparison of parameters from linear Buckling Analysis

	h = 3 mm				h= 6 mm			
	t= 0.5 mm		t= 5 mm		t= 0.5 mm		t= 5 mm	
D (mm)	n = 1	n =7	n = 1	n =7	n = 1	n =7	n = 1	n =7
75	1.79%	74.48%	0.65%	7.72%	1.96%	93.73%	1.23%	21.78%
100	3.13%	171.87%	1.17%	12.05%	3.37%	246.25%	2.21%	34.97%

The most reasonable choices , keeping in mind the influence of all parameters, the diameters were divided into 5 categories which are presented in table 4.5. The expected minimum and maximum improvements of these categories are presented in table 4.6. From these, the most optimized pattern of the linear Buckling Study was observed to be obtained when stiffeners of diameter 75 mm, height 10 mm and 11 number of stiffeners along the shorter side are used. This study was later extended to analysis of other shapes such as square, triangle and capsule. Results show that the thin plate stiffened with square stiffeners yield highest buckling capacity.

Non-linear Riks analysis was used to study the behavior of stiffened plate till collapse load and its correlation with material yield strength over varying thicknesses. Other stiffening shapes like square, triangular, and capsule are also analyzed. Due to time constraints, non-linear analysis and analysis with additional profiles were limited to one stiffening pattern.

Conclusion from non-linear analysis and analysis of other shapes:

- Geometric and material non linearity is affecting buckling load of flat and stiffened plate by similar proportion, so linear buckling analysis can be used to study % increase in buckling capacity.
- Dense pattern of square stiffeners can lead to highest percentage increase in buckling capacity. However, shape must be optimised to avoid any stress concentration.

5.2 Future work

This master's thesis scratches the surface of the novel concept for improving the buckling capacity of thin-walled structures. The potential impact towards increased buckling capacity by creating an augmented surface looks very promising. Opening doors for future research within the domain of thin-walled structures. The possibility to optimize stiffening pattern as to how thin plate fits into the global structures coupled with added aesthetic value is remarkable. Although, current mass-production methods for such a concept are limited in terms of flexibility offered to make application-adaptive patterns. Work from future researches will pave the way toward practical implementation of the idea.

Future research in following domains could be of high value:

- Develop an artificial neural network (ANN) based model to estimate the buckling capacity of thin plates stiffened with particular shape.
- Conduct experimental testing for a optimal stiffener pattern, followed by comparison with FE model. This will help to validate the results and provide future researcher with grounds to explore other shapes.
- Explore combination of surface stiffening with external stiffeners to produce efficient lightweight members.
- Cost benefit analysis to find balance between production expense and strengthening offered.

Bibliography

[1] Gardner L, Nethercot DA. Structural stainless steel design: A new approach. Struct Eng. 2004 Nov 2;82:21–8.

[2] Dubas P, Gehri E. Behaviour and Design of Steel Plated Structures. Applied Statics and Steel Structures, Swiss Federal Institute of Technology; 1986. 252 p.

[3] Arbocz J, Babcock ChD. Prediction of Buckling Loads Based on Experimentally Measured Initial Imperfections. In: Budiansky B, editor. Buckling of Structures. Berlin, Heidelberg: Springer; 1976. p. 291–311. (International Union of Theoretical and Applied Mechanics).

[4] Bryan GH. On the Stability of a Plane Plate under Thrusts in its own Plane, with Applications to the "Buckling" of the Sides of a Ship. Proc Lond Math Soc. 1890;s1-22(1):54–67.

[5] Timoshenko SP, Gere JM. Theory of Elastic Stability. Courier Corporation; 2009. 562 p.

[6] Betten J, Shin CH. Elastic-plastic buckling analysis of rectangular plates subjected to biaxial loads. Forsch Ingenieurwes. 2000;6.

[7] Zizza, A. Buckling Behaviour of Unstiffened and Stiffened Steel Plates Under Multi-axial Stress States. Inst Für Konstr Entwurf. 2016;

[8] Appendix C: Plate Buckling Under Biaxial Compression and Shear. In: Mechanics of Optimal Structural Design [Internet]. John Wiley Sons, Ltd; 2009 [cited 2021 Jun 5]. p. 537–41.

[9] EN 1993-1-5. Eurocode 3 - Design of steel structures - Part 1-5: Plated structural elements; 2006

[10] Batdorf SB, Houbolt C. Critical combinations of shear transverse direct stress for an infinitely long flat plate with edges elastically restrained against rotation. :8.

[11] Stowell EZ, Schwartz EB. Critical stress for an infinitely long flat plate with elastically restrained edges under combined shear and direct stress.

Washington, D.C: National Advisory Committee for Aeronautics; 1943. 1 p. (Wartime Report / National Advisory Committee for Aeronautics).

[12] Osadebe, N. N Ibearugbulem, Owus M. Buckling analysis of axially compressed SSSS thin rectangular plate using Taylor-Mclaurin shape function. Int J Civ Struct Eng. 2011;2(2).

[13] Nwoji U, Onah H, Mama B, Ike C, IKWUEZE E. Elastic buckling analysis of simply supported thin plates using the double finite fourier sine integral transform method. 2017 Sep 1;01.

[14] Riahi F. Buckling Stability Assessment of Plates with Various Boundary Conditions Under Normal and Shear Stresses. Eng Technol Appl Sci Res. 2017 Oct 15;7:2056–61.

[15] Jana P, Bhaskar K. Stability analysis of simply-supported rectangular plates under non-uniform uniaxial compression using rigorous and approximate plane stress solutions. Thin-Walled Struct. 2006 May 1;44(5):507–16.

[16] Neale KW. Effect of Imperfections on the Plastic Buckling of Rectangular Plates. J Appl Mech. 1975 Mar 1;42(1):115–20.

[17] Luo Y, Zhan J, Liu P. Buckling assessment of thin-walled plates with uncertain geometrical imperfections based on non-probabilistic field model. Thin-Walled Struct. 2019 Dec 1;145:106435.

[18] Chinnaraj K, Ramasamy P. Analytical Prediction of Residual Stresses in Cold Formed Steel Sections with Elastic - Perfectly Plastic Material Model. 2017.

[19] Anon. Effect of Initial Imperfection;2021

[20] Al-Emrani, M. and Åkesson, B. Steel Structures. Göteborg: Chalmers University of Technology. 2020

[21] Tauchert TR. Large Plate Deflections, von Kármán Theory, Statical Problems. In: Hetnarski RB, editor. Encyclopedia of Thermal Stresses [Internet]. Dordrecht: Springer Netherlands; 2014 [cited 2021 Jun 5]. p. 2697–704.

[22] Lau SCW, Hancock GJ. Buckling of thin flat-walled structures by a spline finite strip method. Thin-Walled Struct. 1986 Jan 1;4(4):269–94.

[23] Schardt R . Extension of the Engineer's Theory of Bending to the Analysis of Folded Plate Structures. Der Stahlbau;1966. 35, 161–171.

A
Appendix

The appendix A provides the general code to carry out the modelling and further analysis in ABAQUS. This Python code must be run as script in ABAQUS. Each iteration is counted with an iteration variable which also forms its model name. For example, a stiffened plate with $\alpha = 3$ and 10 mm thick with 11 number of circular stiffeners of diameter 75 mm and height of 6 mm will get a name of "Model-B-3-11-4-9". Unique names are obtained to each models and the future Eigen Value linear buckling analysis is performed. This code generates input files which can be submitted to obtain the analysis results.

```
# -*- coding: mbcs -*-
from part import *
from material import *
from section import *
from assembly import *
from step import *
from interaction import *
from load import *
from mesh import *
from optimization import *
from job import *
from sketch import *
from visualization import *
from connectorBehavior import *
import regionToolset
import math


############# Iteration Variables ##############
# a in loop for a/b
# o in loop for height
# p in loop for diameter
# q in loop for thickness
##########################################

############# Width of plate ##############
b=1
############# Length of plate ##############
```

```
for a in [1,2,3]:
  b=1
  p = 0
  ############# Diameter of Stiffener ##############
  for L4 in [0.025,0.05, 0.075, 0.1, 0.15, 0.2, 0.3, 0.4, 0.5, 0.75,
      0.85]:

    p = p + 1

    e = L4/12 # extension
    L3 = float(L4)-0.5*float(e)
    nmax = round(float(b) / float(float(L3)+ 2 * e))

    ############# Number of Stiffeners ##############
    for n in range(1, int(nmax_y) + 1, int(math.ceil(nmax_y / 10))):
      o = 0

      ############# Height of Stiffener ##############
      for h in
          [0.002,0.003,0.004,0.006,0.008,0.01,0.02,0.03,0.04,0.05]:
        o = o + 1

        # total number of bubbles
        nb = (a / b) * (n ** 2) + 1
        print(nb)

        # distance between extrusion
        d = float(b) / float(n)
        print(float(d))

        if L3 > (d - 2 * e): break
        print(d - 2 * e)


        #-----------------------------------------

        Hs1 = 2 * float(h) / 3
        Hs2 = float(h)

        #-----------------------------------------
        elps_x = float(L3)/float(2)
        elps_y = float(h)
        F_x = elps_x - float(e)/3
        F_y = math.sqrt((1 - (float(F_x ** 2) / float(elps_x ** 2)))
           * elps_y ** 2)
        print(F_x, F_y)
```

```
#------------------------------------------
# point on instance to be translated
i_x = -(L3 / 2 + e)
i_y = 0
i_z = 0
# point on plate where the instance should be translated to
p_x = d / 2 - L3 / 2 - e
p_y = d / 2
p_z = 0
# translation vector coordinates
v_x = round((p_x - i_x), 6)
v_y = round((p_y - i_y), 6)
v_z = round(0, 6)


############## Thickness of Plate ##############
q = 0
for t in [0.0005, 0.001,0.0025,
    0.003,0.004,0.005,0.006,0.008,0.01]:

  q = q + 1
  # x coordinate of first bubble
  centre_x = d / 2
  # y cooordinate of first bubble
  centre_y = d / 2

  mdb.Model(modelType=STANDARD_EXPLICIT, name='Model-B-%d-%d-%
      d-%d-%d' % (a, p, n, o, q))

  mdb.models['Model-B-%d-%d-%d-%d-%d' % (a, p, n, o, q)].
      ConstrainedSketch(name='__profile__', sheetSize=10)
  mdb.models['Model-B-%d-%d-%d-%d-%d' % (a, p, n, o, q)].
      sketches['__profile__'].rectangle(
    point1=(0.0, 0.0),
    point2=(a, b))

  for i in range(1, nb):
    mdb.models['Model-B-%d-%d-%d-%d-%d' % (a, p, n, o, q)].
        sketches[
      '__profile__'].CircleByCenterPerimeter(
      center=(
        centre_x, centre_y), point1=(centre_x + r + e,
            centre_y))
    if centre_y < b - d:
      centre_y = centre_y + d
    else:
```

```
    centre_x = centre_x + d
    centre_y = d / 2

mdb.models['Model-B-%d-%d-%d-%d-%d' % (a, p, n, o, q)].Part(
    dimensionality=THREE_D, name='Part-1', type=
DEFORMABLE_BODY)
mdb.models['Model-B-%d-%d-%d-%d-%d' % (a, p, n, o, q)].parts
    ['Part-1'].BaseShell(sketch=mdb.models[
                                'Model-B-%d-%d-%d-%d-%d' % (a,p,
                                    n, o,q)].sketches['
                                   __profile__'])
del mdb.models['Model-B-%d-%d-%d-%d-%d' % (a, p, n, o, q)].
    sketches['__profile__']

mdb.models['Model-B-%d-%d-%d-%d-%d' % (a, p, n, o, q)].
    ConstrainedSketch(name='__profile__', sheetSize=2*L3)
mdb.models['Model-B-%d-%d-%d-%d-%d' % (a, p, n, o, q)].
    sketches['__profile__'].sketchOptions.setValues(
  decimalPlaces=3)
mdb.models['Model-B-%d-%d-%d-%d-%d' % (a, p, n, o, q)].
    sketches['__profile__'].ConstructionLine(point1=(0.0,
                                    -L3), point2=(0.0, L3))
mdb.models['Model-B-%d-%d-%d-%d-%d' % (a, p, n, o, q)].
    sketches['__profile__'].FixedConstraint(entity=
                                mdb.models['Model-B-%d-%d-%d-%d
                                    -%d' % (a, p, n, o, q)].
                                    sketches[
                                   '__profile__'].geometry[2])
mdb.models['Model-B-%d-%d-%d-%d-%d' % (a, p, n, o, q)].
    sketches['__profile__'].EllipseByCenterPerimeter(
  axisPoint1=(elps_x, 0.0), axisPoint2=(0.0, elps_y), center
      =(0.0, 0.0))
mdb.models['Model-B-%d-%d-%d-%d-%d' % (a, p, n, o, q)].
    sketches['__profile__'].Line(point1=(elps_x, 0.0),
    point2=(
  elps_x + e, 0.0))
mdb.models['Model-B-%d-%d-%d-%d-%d' % (a, p, n, o, q)].
    sketches['__profile__'].HorizontalConstraint(
  addUndoState=False, entity=
  mdb.models['Model-B-%d-%d-%d-%d-%d' % (a, p, n, o, q)].
      sketches['__profile__'].geometry[5])
mdb.models['Model-B-%d-%d-%d-%d-%d' % (a, p, n, o, q)].
    sketches['__profile__'].autoTrimCurve(curve1=
                              mdb.models['Model-B-%d-%d-%d-%d-%
                                  d' % (a, p, n, o, q)].
                                  sketches[
```

```
                                '__profile__'].geometry[3],
                                   point1=(
  0, elps_y))
mdb.models['Model-B-%d-%d-%d-%d-%d' % (a, p, n, o, q)].
    sketches['__profile__'].autoTrimCurve(curve1=
                              mdb.models['Model-B-%d-%d-%d-%d-%
                                 d' % (a, p, n, o, q)].
                                 sketches[
                                '__profile__'].geometry[6],
                                   point1=(
  0, elps_y))
mdb.models['Model-B-%d-%d-%d-%d-%d' % (a, p, n, o, q)].
    sketches['__profile__'].FilletByRadius(curve1=
                               mdb.models['Model-B-%d-%d-%d-%d
                                  -%d' % (a, p, n, o, q)].
                                  sketches[
                                 '__profile__'].geometry[5],
                                    curve2=
                               mdb.models['Model-B-%d-%d-%d-%d
                                  -%d' % (a, p, n, o, q)].
                                  sketches[
                                 '__profile__'].geometry[7],
                               nearPoint1=(
                                 elps_x+e/2, 0),
                               nearPoint2=(F_x,-1*F_y), radius=
                                  Hs2)
mdb.models['Model-B-%d-%d-%d-%d-%d' % (a, p, n, o, q)].Part(
    dimensionality=THREE_D, name='Part-2', type=
DEFORMABLE_BODY)
mdb.models['Model-B-%d-%d-%d-%d-%d' % (a, p, n, o, q)].parts
    ['Part-2'].BaseShellRevolve(angle=360.0,
                             flipRevolveDirection=OFF, sketch=
                             mdb.models['Model-B-%d-%d-%d-%d-%d
                                ' % (a, p, n, o, q)].sketches[
                               '__profile__'])
del mdb.models['Model-B-%d-%d-%d-%d-%d' % (a, p, n, o, q)].
    sketches['__profile__']



mdb.models['Model-B-%d-%d-%d-%d-%d' % (a, p, n, o, q)].
    Material(name='Material-1')
mdb.models['Model-B-%d-%d-%d-%d-%d' % (a, p, n, o, q)].
    materials['Material-1'].Elastic(
  table=((210000000000.0,
      0.3),))
```

```
mdb.models['Model-B-%d-%d-%d-%d-%d' % (a, p, n, o, q)].
    HomogeneousShellSection(
  idealization=NO_IDEALIZATION,
  integrationRule=SIMPSON,
  material='Material-1',
  name='Section-1',
  nodalThicknessField='',
  numIntPts=5,
  poissonDefinition=DEFAULT,
  preIntegrate=OFF,
  temperature=GRADIENT,
  thickness=t, thicknessField='',
  thicknessModulus=None,
  thicknessType=UNIFORM,
  useDensity=OFF)
mdb.models['Model-B-%d-%d-%d-%d-%d' % (a, p, n, o, q)].parts
    ['Part-1'].SectionAssignment(offset=0.0,
                         offsetField='',offsetType=
                            MIDDLE_SURFACE,region=Region(
                            faces=mdb.models['Model-B-%d-%d-%
                            d-%d-%d'% (a,p,n,o,q)].parts[ '
                            Part-1'].faces.
                            getSequenceFromMask(mask=('[#1 ]'
                            ,),)) ,sectionName='Section-1',
                            thicknessAssignment=FROM_SECTION)
mdb.models['Model-B-%d-%d-%d-%d-%d' % (a, p, n, o,
  q)].parts['Part-2'].SectionAssignment(offset=0.0,
     offsetFiel d='',offsetType=MIDDLE_SURFACE,region=Region
     (faces=mdb.mo dels['Model-B-%d-%d-%d-%d-%d' % (a, p,c,n
     ,o,q)]. parts['Part-2'].faces.getSequenceFromMask(mask
     =('[#7 ]',),)),sectionName='Section-1',
     thicknessAssignment=FROM_ SECTION)

mdb.models['Model-B-%d-%d-%d-%d-%d' % (a, p, n,          o,
    q)].rootAssembly.DatumCsysByDefault(CARTESIAN)
mdb.models['Model-B-%d-%d-%d-%d-%d' % (a, p, n, o,q      )].
    rootAssembly.Instance(dependent=OFF,name='Part-1-1',part
     =mdb.models['Model-B-%d-%d-%d-%d-%d' % (a,p, n, o,q)].
    parts['Part-1'])
mdb.models['Model-B-%d-%d-%d-%d-%d' % (a, p, n, o, q)].
    rootAssembly.Instance(dependent=OFF,name='Part-2-1',part
    =mdb.models['Model-B-%d-%d-%d-%d-%d' % (a, p, n, o, q)].
    parts[
                                     'Part-2'])
mdb.models['Model-B-%d-%d-%d-%d-%d' % (a, p, n, o, q)].
    rootAssembly.rotate(angle=90.0,axisDirection=(0.15, 0.0,
```

```
                                             0.0),axisPoint=(0.0,
                                                 0.0, 0.0),
                              instanceList=('Part-2-1',))

mdb.models['Model-B-%d-%d-%d-%d-%d' % (a, p, n, o, q)].
    rootAssembly.translate(instanceList=('Part-2-1',),
                                      vector=(v_x, v_y, v_z))
mdb.models['Model-B-%d-%d-%d-%d-%d' % (a, p, n, o, q)].
    rootAssembly.LinearInstancePattern(
  direction1=(1.0, 0.0,
        0.0),
  direction2=(
    0.0, 1.0, 0.0),
  instanceList=(
    'Part-2-1',),
  number1=n * (a / b),
  number2=n, spacing1=d,
  spacing2=d)

mdb.models['Model-B-%d-%d-%d-%d-%d' % (a, p, n, o, q)].
    rootAssembly.InstanceFromBooleanMerge \
  (domain=GEOMETRY,
   instances=mdb.models['Model-B-%d-%d-%d-%d-%d' % (a, p, n,
        o, q)].rootAssembly.instances.values(),
   keepIntersections=ON,
   name='Merged_plate', originalInstances=DELETE)

mdb.models['Model-B-%d-%d-%d-%d-%d' % (a, p, n, o, q)].
    rootAssembly.makeIndependent(instances=(
  mdb.models['Model-B-%d-%d-%d-%d-%d' % (a, p, n, o, q)].
      rootAssembly.instances['Merged_plate-1'],))

plateAssembly = mdb.models['Model-B-%d-%d-%d-%d-%d' % (a, p,
     n, o, q)].rootAssembly
plateInstance = plateAssembly.Instance(name='Merged_plate-1'
    , part=mdb.models[
  'Model-B-%d-%d-%d-%d-%d' % (a, p, n, o, q)].parts[
  'Merged_plate'])

mdb.models['Model-B-%d-%d-%d-%d-%d' % (a, p, n, o, q)].
    BuckleStep(name='Step-1', numEigen=3, previous=
'Initial', vectors=15)

# For Boundary Conditions
# Left edge
left_edge = plateInstance.edges.findAt(((0, float(b) / 2.0,
```

```
    0),))
left_edge_region = regionToolset.Region(edges=left_edge)
# right edge
right_edge = plateInstance.edges.findAt(((a, float(b) / 2.0,
     0),))
right_edge_region = regionToolset.Region(edges=right_edge)
# top edge
top_edge = plateInstance.edges.findAt(((float(a) / 2.0, b,
    0),))
top_edge_region = regionToolset.Region(edges=top_edge)
# bottom edge
bottom_edge = plateInstance.edges.findAt(((float(a) / 2.0,
    0, 0),))
bottom_edge_region = regionToolset.Region(edges=bottom_edge)

# for loads
left_surf = plateInstance.edges.findAt(((0, float(b) / 2.0,
    0),))
plateAssembly.Surface(side1Edges=left_surf, name='Surf-1')
# for right
right_surf = plateInstance.edges.findAt(((a, float(b) / 2.0,
     0),))
plateAssembly.Surface(side1Edges=right_surf, name='Surf-2')
# for bottom
right_surf = plateInstance.edges.findAt(((float(a)/2.0, 0,
    0),))
plateAssembly.Surface(side1Edges=right_surf, name='Surf-3')

# Load Application

##### Changes with type of Loading #####
## Uniaxial Loading: As Shown in the code
## Biaxial Loading: Apply to all edges
## Shear Loading: Apply to all edges (1 for adjacent edges
    and -1 for remaining edges)

# left surf
mdb.models['Model-B-%d-%d-%d-%d-%d' % (a, p, n, o, q)].
    ShellEdgeLoad(createStepName='Step-1',
                                distributionType=UNIFORM,
                                    field='',localCsys=None,
                                    magnitude=1.0,name='Load
                                    -1',region=plateAssembly.
                                    surfaces['Surf-1'])

# right Surf
```

```
mdb.models['Model-B-%d-%d-%d-%d-%d' % (a, p, n, o, q)].
    ShellEdgeLoad(createStepName='Step-1',
                                    distributionType=UNIFORM,
                                        field='',localCsys=None,
                                        magnitude=1.0,name='Load
                                        -2',region=plateAssembly.
                                        surfaces['Surf-2'])


# Boundary Conditions
# left edge
mdb.models['Model-B-%d-%d-%d-%d-%d' % (a, p, n, o, q)].
    DisplacementBC(amplitude=UNSET, buckleCase=
PERTURBATION_AND_BUCKLING, createStepName='Step-1',
    distributionType=UNIFORM, fieldName='', fixed=OFF,
    localCsys=None, name='BC-left',region=left_edge_region,
    u1=UNSET,u2=UNSET,u3=0.0, ur1=0.0, ur2=UNSET,ur3=UNSET)
# right edge
mdb.models['Model-B-%d-%d-%d-%d-%d' % (a, p, n, o, q)].
    DisplacementBC(amplitude=UNSET, buckleCase=
PERTURBATION_AND_BUCKLING, createStepName='Step-1',
    distributionType=UNIFORM, fieldName='', fixed=OFF,
    localCsys=None, name='BC-right',region=right_edge_region
    , u1=UNSET,u2=UNSET,u3=0.0, ur1=0.0, ur2=UNSET,ur3=UNSET
    )

# top edge

mdb.models['Model-B-%d-%d-%d-%d-%d' % (a, p, n, o, q)].
    DisplacementBC(amplitude=UNSET, buckleCase=
PERTURBATION_AND_BUCKLING, createStepName='Step-1',
    distributionType=UNIFORM, fieldName='', fixed=OFF,
    localCsys=None, name='BC-3', region=top_edge_region, u1=
    UNSET,u2=UNSET,u3=0.0, ur1=UNSET, ur2=0.0,ur3=UNSET)

# bottom edge
mdb.models['Model-B-%d-%d-%d-%d-%d' % (a, p, n, o, q)].
    DisplacementBC(amplitude=UNSET, buckleCase=
PERTURBATION_AND_BUCKLING, createStepName='Step-1',
    distributionType=UNIFORM, fieldName='', fixed=OFF,
    localCsys=None, name='BC-4',region= bottom_edge_region,
    u1=UNSET,u2=0.0, u3=0.0, ur1=UNSET, ur2=0.0, ur3=UNSET)

# change mesh size if needed (ms = Mesh Size)

ms=0.03
```

```
mdb.models['Model-B-%d-%d-%d-%d-%d' % (a, p, n, o, q)].
    rootAssembly.setMeshControls(regions=
  mdb.models['Model-B-%d-%d-%d-%d-%d' % (a, p, n, o, q)].
      rootAssembly.instances[
    'Merged_plate-1'].faces.getSequenceFromMask(
    ('[#ffffffff:10 #f ]',), ), technique=SWEEP)
mdb.models['Model-B-%d-%d-%d-%d-%d' % (a, p, n, o, q)].
    rootAssembly.seedPartInstance(
  deviationFactor=0.1
  , minSizeFactor=0.1, regions=(
    mdb.models['Model-B-%d-%d-%d-%d-%d' % (a, p, n, o, q)].
        rootAssembly.instances[
      'Merged_plate-1'],),
  size=ms)
mdb.models['Model-B-%d-%d-%d-%d-%d' % (a, p, n, o, q)].
    rootAssembly.generateMesh(regions=(
  mdb.models['Model-B-%d-%d-%d-%d-%d' % (a, p, n, o, q)].
      rootAssembly.instances[
    'Merged_plate-1'],))

mdb.Job(atTime=None, contactPrint=OFF, description='',
    echoPrint=OFF,
    explicitPrecision=SINGLE, getMemoryFromAnalysis=True,
        historyPrint=OFF,
    memory=90, memoryUnits=PERCENTAGE, model='Model-B-%d-%d
        -%d-%d-%d' % (a, p, n, o, q),
    modelPrint=OFF,
    multiprocessingMode=DEFAULT, name='Job-B-%d-%d-%d-%d-%d'
         % (a, p, n, o, q),
    nodalOutputPrecision=SINGLE,
    numCpus=1, numGPUs=0, queue=None, resultsFormat=ODB,
        scratch='', type=
    ANALYSIS, userSubroutine='', waitHours=0, waitMinutes=0)
mdb.jobs['Job-B-%d-%d-%d-%d-%d' % (a, p, n, o, q)].
    writeInput()
#mdb.jobs['Job-%d-%d-%d-%d-%d' % (a, p, n, o, q)].submit(
    consistencyChecking=OFF)

#mdb.jobs['Job-%d-%d-%d-%d-%d' % (a, p, n, o, q)].
    waitForCompletion()
```

Listing A.1: General Python Code for Eigen Value Analysis

B

Appendix

Detailed results from scale factor study in section 3.5.1 are reported in this appendix. In table B.1, B.2 and B.3 results from comparison of flat with different scale factor are compared. Flat plate results are followed by results of modified plate under uni-axial and shear loading.

Table B.1: Scale factor (0.5) study results for flat plate under uni-axial loading

Length	**Width**	**Thickness (mm)**	**Eigen Value (N/m)**	$\overline{P}$
0.5	0.5	0.25	47.482	39.51
0.5	0.5	0.5	379.85	39.50
0.5	0.5	1.25	5935	39.50
0.5	0.5	1.5	10256	39.50
0.5	0.5	2	24309	39.50
0.5	0.5	2.5	47475	39.50
0.5	0.5	3	82032	39.50
0.5	0.5	3.5	130255	39.49
0.5	0.5	4	194416	39.49
0.5	0.5	4.5	276788	39.49
0.5	0.5	5	379642	39.48

Table B.2: Scale factor (1.0) study results for flat plate under uni-axial loading

Length	**Width**	**Thickness (mm)**	**Eigen Value (N/m)**	$\overline{P}$
1	1	0.5	94.916	39.49
1	1	1	759.32	39.48
1	1	2.5	11864	39.48
1	1	3	20501	39.48
1	1	4	48593	39.48
1	1	5	94903	39.48
1	1	6	163982	39.48
1	1	7	260378	39.47
1	1	8	388636	39.47
1	1	9	553297	39.47
1	1	10	758900	39.46

Table B.3: Scale factor (1.5) study results for flat plate under uni-axial loading

Length	**Width**	**Thickness (mm)**	**Eigen Value (N/m)**	$\overline{P}$
1.5	1.5	0.75	142.36	39.48
1.5	1.5	1.5	1138.9	39.48
1.5	1.5	3.75	17794	39.48
1.5	1.5	4.5	30748	39.48
1.5	1.5	6	72882	39.48
1.5	1.5	7.5	142341	39.48
1.5	1.5	9	245949	39.47
1.5	1.5	10.5	390530	39.47
1.5	1.5	12	582899	39.47
1.5	1.5	13.5	829869	39.46
1.5	1.5	15	1138240	39.46

Following tables report, results from scale factor study under uni-axial and shear loading based on methodology explained in section 3.5.1. $\overline{P}$ values are calculated based on below mentioned equation, where plate thickness and width are multiplied by scale factor.

$$\overline{P} = \frac{N_{cr} \times 12 \times (1 - v^2)}{E} \times \frac{(S.F \times a)^2}{(S.F \times t)^3}$$

Properties of Normal					Eigen Values			$\overline{P}$		
Plate width (m)	**Dia (m)**	**Number of stiffener**	**Height of stiffener (m)**	**Thick -ness (m)**	**Reduced (N/m)**	**Magnified (N/m)**	**Normal (N/m)**	**Redu -ced**	**Magn -ified**	**Nor -mal**
1	0.05	1	0.004	0.001	382.99	1148	765.41	39.83	39.80	39.80
1	0.05	1	0.004	0.0025	5977.2	17913	11946	39.78	39.74	39.76
1	0.05	1	0.006	0.001	383.29	1149	766.04	39.86	39.83	39.83
1	0.05	1	0.006	0.0025	5982.8	17932	11957	39.82	39.79	39.79
1	0.05	3	0.004	0.001	394.5	1184.7	788.74	41.03	41.07	41.01
1	0.05	3	0.004	0.0025	6065	18210	12126	40.37	40.40	40.36
1	0.05	3	0.006	0.001	397.37	1192.8	794.52	41.33	41.35	41.32
1	0.05	3	0.006	0.0025	6117.9	18378	12232	40.72	40.77	40.71
1	0.05	5	0.004	0.001	421.58	1271.1	842.74	43.84	44.06	43.82
1	0.05	5	0.004	0.0025	6290.2	18940	12573	41.87	42.02	41.84
1	0.05	5	0.006	0.001	430.51	1297.2	861.11	44.77	44.97	44.78
1	0.05	5	0.006	0.0025	6443.6	19438	12884	42.89	43.13	42.88
1	0.05	7	0.004	0.001	465.09	1415.4	929.45	48.37	49.07	48.33
1	0.05	7	0.004	0.0025	6617.6	20050	13221	44.05	44.48	44.00
1	0.05	7	0.006	0.001	486.25	1474.7	978.39	50.57	51.12	50.88
1	0.05	7	0.006	0.0025	6935.1	21066	13959	46.16	46.74	46.46
1	0.05	9	0.004	0.001	529.91	1631.9	1058.1	55.11	56.57	55.02
1	0.05	9	0.004	0.0025	7049	21452	14074	46.92	47.59	46.84
1	0.05	9	0.006	0.001	575.58	1758.3	1162.1	59.86	60.95	60.43
1	0.05	9	0.006	0.0025	7608.3	23305	15364	50.64	51.71	51.13
1	0.05	11	0.004	0.001	624.05	1936.3	1226.1	64.90	67.13	63.76
1	0.05	11	0.004	0.0025	7550.3	23088	14977	50.25	51.22	49.84
1	0.05	11	0.006	0.001	724.21	2195.3	1441.9	75.32	76.10	74.98
1	0.05	11	0.006	0.0025	8429.5	25974	17036	56.11	57.63	56.70

1	0.05	13	0.004	0.001	752.85	2321.9	1461.2	78.30	80.49	75.98
1	0.05	13	0.004	0.0025	8158.3	24752	16122	54.30	54.92	53.65
1	0.05	13	0.006	0.001	959.23	2831.5	1877	99.76	98.16	97.60
1	0.05	13	0.006	0.0025	9429.4	28776	19003	62.76	63.84	63.24
1	0.05	15	0.004	0.001	906.25	2755.9	1745.6	94.25	95.54	90.77
1	0.05	15	0.004	0.0025	8933.7	26310	17652	59.46	58.37	58.75
1	0.05	15	0.006	0.001	1246.3	3690.3	2454.6	129.62	127.93	127.64
1	0.05	15	0.006	0.0025	10707	31564	21039	71.27	70.03	70.02
1	0.05	17	0.004	0.001	1058.5	3085.7	2108.3	110.08	106.97	109.63
1	0.05	17	0.004	0.0025	9603.5	27679	18581	63.92	61.41	61.84
1	0.05	17	0.006	0.001	1516.7	4263.6	2993.6	157.74	147.80	155.67
1	0.05	17	0.006	0.0025	11780	33694	22930	78.41	74.76	76.31
1	0.1	1	0.006	0.001	391.74	1175.6	783.65	40.74	40.75	40.75
1	0.1	1	0.006	0.0025	6105.3	18308	12205	40.64	40.62	40.62
1	0.1	1	0.01	0.001	393.25	1179.4	786.3	40.90	40.89	40.89
1	0.1	1	0.01	0.0025	6124.3	18364	12244	40.76	40.74	40.75
1	0.1	2	0.006	0.001	408.99	1229.5	818.98	42.53	42.62	42.59
1	0.1	2	0.006	0.0025	6254.3	18855	12554	41.63	41.83	41.78
1	0.1	2	0.01	0.001	413.72	1240.6	826.8	43.03	43.01	42.99
1	0.1	2	0.01	0.0025	6365.4	19147	12754	42.37	42.48	42.45
1	0.1	3	0.006	0.001	448.2	1358.9	903.66	46.61	47.11	46.99
1	0.1	3	0.006	0.0025	6645.9	20260	13459	44.24	44.95	44.79
1	0.1	3	0.01	0.001	461	1389.4	925.21	47.94	48.17	48.11
1	0.1	3	0.01	0.0025	6930.3	21040	13992	46.13	46.68	46.57
1	0.1	4	0.006	0.001	510.86	1571.7	1041.6	53.13	54.49	54.16
1	0.1	4	0.006	0.0025	7209	22342	14790	47.98	49.57	49.22
1	0.1	4	0.01	0.001	539.49	1642.8	1091.2	56.11	56.95	56.74

1	0.1	4	0.01	0.0025	7797.8	24055	15945	51.90	53.37	53.06
1	0.1	5	0.006	0.001	610.74	1906.8	1258.3	63.52	66.10	65.43
1	0.1	5	0.006	0.0025	7922.1	25124	16559	52.73	55.74	55.11
1	0.1	5	0.01	0.001	677.2	2065.7	1368.8	70.43	71.61	71.18
1	0.1	5	0.01	0.0025	9048.3	28529	18829	60.23	63.30	62.66
1	0.1	6	0.006	0.001	749.14	2427.4	1595	77.91	84.15	82.94
1	0.1	6	0.006	0.0025	8779.8	28484	18713	58.44	63.20	62.28
1	0.1	6	0.01	0.001	891.54	2791.3	1844.9	92.72	96.77	95.93
1	0.1	6	0.01	0.0025	10676	34711	22772	71.06	77.01	75.79
1	0.1	7	0.006	0.001	948.96	3187.9	2078.3	98.69	110.51	108.07
1	0.1	7	0.006	0.0025	9893.2	31963	20913	65.85	70.92	69.60
1	0.1	7	0.01	0.001	1269.8	4062.2	2686.4	132.06	140.82	139.69
1	0.1	7	0.01	0.0025	12899	42051	27408	85.86	93.30	91.21
1	0.1	8	0.006	0.001	1290	4091.6	2677	134.16	141.84	139.20
1	0.1	8	0.006	0.0025	11151	34916	22901	74.22	77.47	76.21
1	0.1	8	0.01	0.001	2000.1	6027.4	4004.6	208.01	208.95	208.24
1	0.1	8	0.01	0.0025	15528	48439	31704	103.35	107.47	105.51

Table B.4: Scale factor study results under uni-axial loading

Properties of Normal					Eigen Values			$\overline{P}$		
Plate width (m)	**Dia (m)**	**Number of stiffener**	**Height of stiffener (m)**	**Thick -ness (m)**	**Reduced (N/m)**	**Magnified (N/m)**	**Normal (N/m)**	**Redu -ced**	**Magn -ified**	**Nor -mal**
1	0.05	1	0.004	0.001	893.86	2681.5	1787.7	92.96	92.96	92.96
1	0.05	1	0.004	0.0025	13919	41755	27838	92.64	92.64	92.64
1	0.05	1	0.006	0.001	894.96	2684.8	1789.9	93.08	93.07	93.07
1	0.05	1	0.006	0.0025	13941	41822	27882	92.79	92.79	92.79
1	0.05	3	0.004	0.001	924.62	2773.7	1849.2	96.16	96.15	96.16
1	0.05	3	0.004	0.0025	14195	42583	28390	94.48	94.48	94.48
1	0.05	3	0.006	0.001	930.94	2792.6	1861.9	96.82	96.81	96.82
1	0.05	3	0.006	0.0025	14332	42993	28663	95.39	95.39	95.39
1	0.05	5	0.004	0.001	991.21	2973.7	1982.4	103.09	103.09	103.08
1	0.05	5	0.004	0.0025	14784	44352	29568	98.40	98.40	98.40
1	0.05	5	0.006	0.001	1009.8	3029.5	2019.6	105.02	105.02	105.02
1	0.05	5	0.006	0.0025	15166	45499	30333	100.94	100.95	100.95
1	0.05	7	0.004	0.001	1105.1	3315.4	2210.3	114.93	114.93	114.94
1	0.05	7	0.004	0.0025	15700	47103	31402	104.50	104.51	104.51
1	0.05	7	0.006	0.001	1148.2	3445	2296.5	119.41	119.43	119.42
1	0.05	7	0.006	0.0025	16507	49522	33013	109.87	109.87	109.87
1	0.05	9	0.004	0.001	1277.7	3833.9	2555.5	132.88	132.91	132.89
1	0.05	9	0.004	0.0025	16899	50703	33799	112.48	112.49	112.48
1	0.05	9	0.006	0.001	1369.9	4108.8	2739.8	142.47	142.44	142.47
1	0.05	9	0.006	0.0025	18359	55078	36719	122.20	122.20	122.20
1	0.05	11	0.004	0.001	1523.8	4572.7	3048.3	158.48	158.52	158.51
1	0.05	11	0.004	0.0025	18299	54908	36604	121.80	121.82	121.82
1	0.05	11	0.006	0.001	1713.8	5143	3428.9	178.24	178.29	178.30
1	0.05	11	0.006	0.0025	20667	62016	41337	137.56	137.59	137.57

1	0.05	13	0.004	0.001	1849.3	5551.9	3699.1	192.33	192.47	192.35
1	0.05	13	0.004	0.0025	19749	59295	39500	131.45	131.56	131.46
1	0.05	13	0.006	0.001	2238	6715.4	4475.7	232.75	232.80	232.74
1	0.05	13	0.006	0.0025	23179	69512	46377	154.28	154.22	154.34
1	0.05	15	0.004	0.001	2214.1	6656.1	4438.2	230.27	230.74	230.79
1	0.05	15	0.004	0.0025	21041	63200	42141	140.05	140.22	140.25
1	0.05	15	0.006	0.001	2939.9	8808.7	5878	305.75	305.37	305.66
1	0.05	15	0.006	0.0025	25468	76391	50898	169.52	169.49	169.39
1	0.05	17	0.004	0.001	2514.3	7561.6	5032.6	261.49	262.14	261.70
1	0.05	17	0.004	0.0025	22036	66207	44093	146.67	146.89	146.74
1	0.05	17	0.006	0.001	3502.5	10510	6996.4	364.26	364.35	363.81
1	0.05	17	0.006	0.0025	27256	81779	54511	181.42	181.44	181.41
1	0.1	1	0.006	0.001	920.67	2762	1841.3	95.75	95.75	95.75
1	0.1	1	0.006	0.0025	14272	42817	28544	94.99	95.00	94.99
1	0.1	1	0.01	0.001	924.59	2773.8	1849.2	96.16	96.16	96.16
1	0.1	1	0.01	0.0025	14355	43065	28710	95.55	95.55	95.55
1	0.1	2	0.006	0.001	996.71	2990	1993.4	103.66	103.65	103.66
1	0.1	2	0.006	0.0025	15124	45371	30248	100.67	100.66	100.67
1	0.1	2	0.01	0.001	1010.8	3032.3	2021.6	105.12	105.12	105.12
1	0.1	2	0.01	0.0025	15477	46429	30954	103.01	103.01	103.01
1	0.1	3	0.006	0.001	1068.3	3204.7	2136.5	111.10	111.10	111.10
1	0.1	3	0.006	0.0025	15901	47699	31799	105.84	105.83	105.83
1	0.1	3	0.01	0.001	1092.9	3278.2	2185.5	113.66	113.64	113.65
1	0.1	3	0.01	0.0025	16522	49561	33041	109.97	109.96	109.96
1	0.1	4	0.006	0.001	1223.5	3670.1	2446.9	127.24	127.23	127.24
1	0.1	4	0.006	0.0025	17466	52396	34931	116.25	116.25	116.25
1	0.1	4	0.01	0.001	1276.3	3828.6	2552.5	132.74	132.72	132.73

1	0.1	4	0.01	0.0025	18733	56196	37466	124.69	124.68	124.69
1	0.1	5	0.006	0.001	1479.1	4437.9	2958.4	153.83	153.85	153.84
1	0.1	5	0.006	0.0025	19689	59070	39378	131.05	131.06	131.05
1	0.1	5	0.01	0.001	1595.6	4787.8	3191.5	165.94	165.98	165.96
1	0.1	5	0.01	0.0025	22188	66572	44378	147.68	147.70	147.69
1	0.1	6	0.006	0.001	1879.3	5638	3759.5	195.45	195.45	195.49
1	0.1	6	0.006	0.0025	22445	67338	44894	149.39	149.40	149.41
1	0.1	6	0.01	0.001	2145.1	6431.1	4291.6	223.09	222.94	223.16
1	0.1	6	0.01	0.0025	27069	81196	54141	180.17	180.15	180.18
1	0.1	7	0.006	0.001	2478.8	7433.8	4958.3	257.80	257.71	257.83
1	0.1	7	0.006	0.0025	25404	76205	50809	169.09	169.07	169.09
1	0.1	7	0.01	0.001	3113.5	9338.1	6228.1	323.80	323.72	323.86
1	0.1	7	0.01	0.0025	33145	99426	66294	220.61	220.59	220.63
1	0.1	8	0.006	0.001	3235.7	9705	6470.9	336.51	336.44	336.49
1	0.1	8	0.006	0.0025	27967	83909	55934	186.15	186.17	186.15
1	0.1	8	0.01	0.001	4681	14036	9361.6	486.82	486.58	486.80
1	0.1	8	0.01	0.0025	38830	116508	77660	258.45	258.49	258.45

Table B.5: Scale factor study results under shear loading

C

Appendix

In this appendix results from post buckling analysis in section 4.3 are presented in form of Non dimensional parameter ($\overline{P}$). Thickness and out of plane deflections are reported in percentage of plate width. Results from this study can be used by other researcher for comparison when plate is analysed with different plate geometry.

.

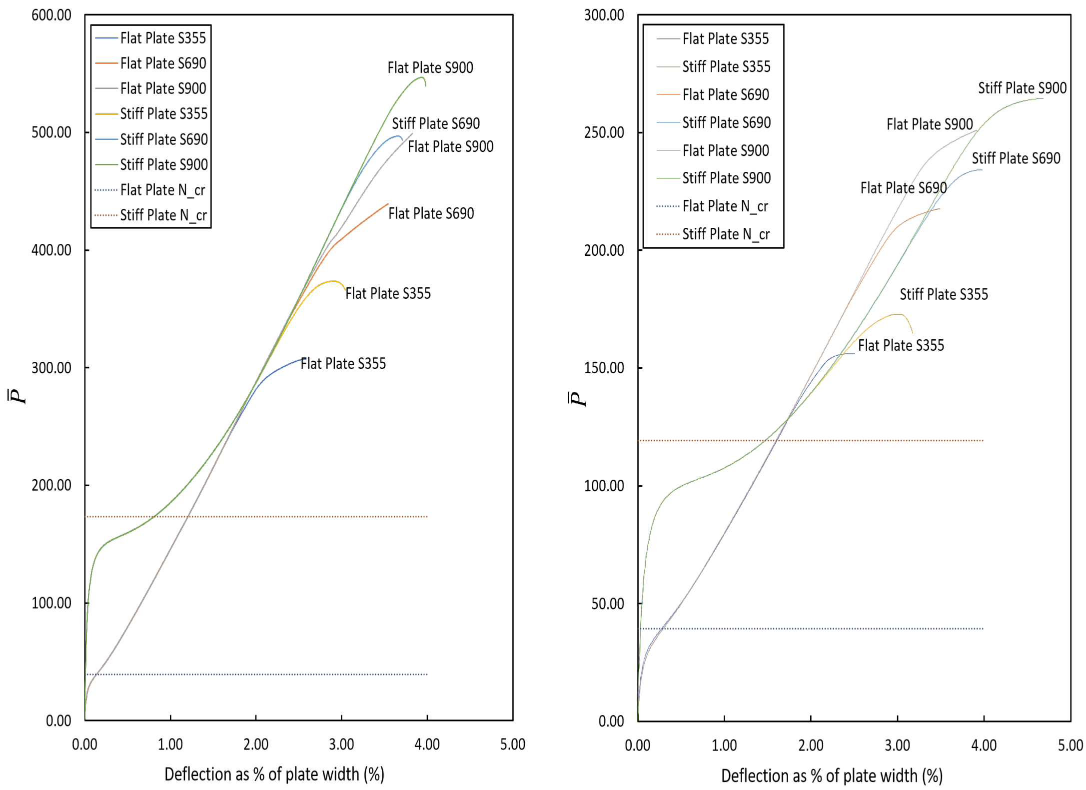

(a) Thickness = 0.2 % of plate width **(b)** Thickness = 0.4 % of plate width

Figure C.1: Continued...

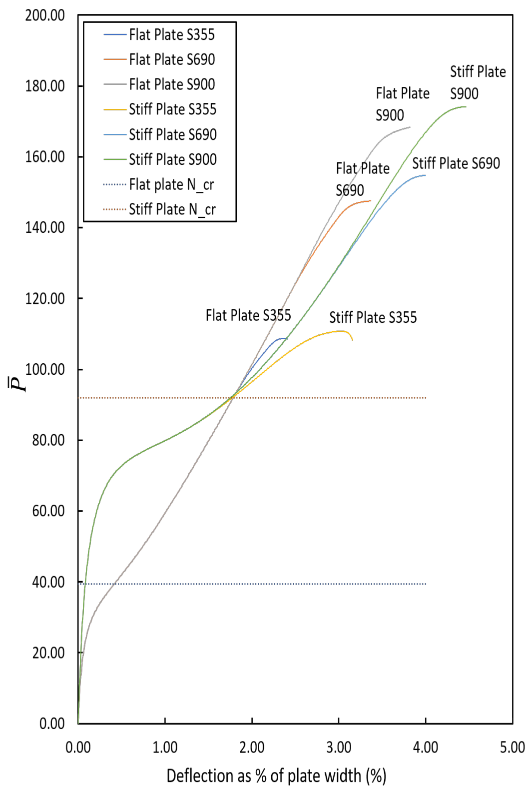

(c) Thickness = 0.6 % of plate width

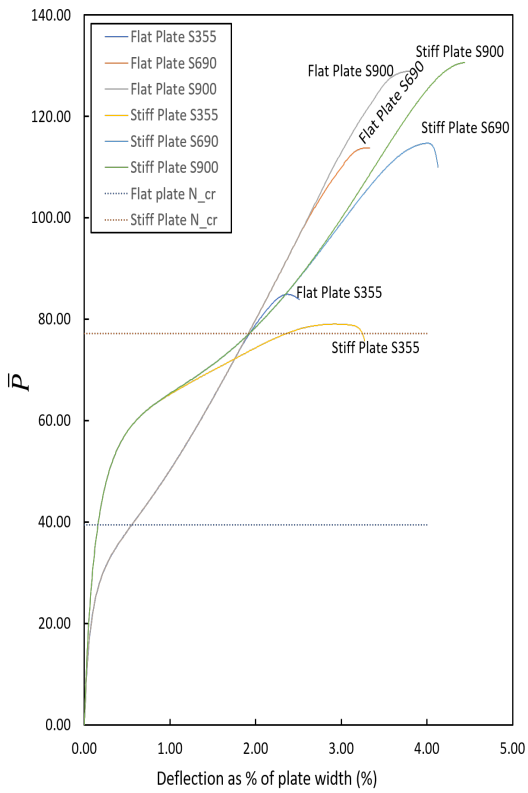

(d) Thickness = 0.8 % of plate width

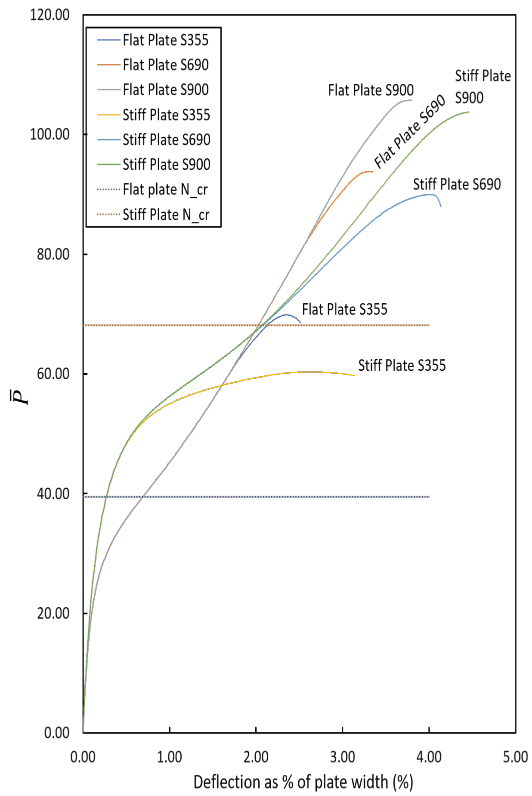

(e) Thickness = 1 % of plate width

Figure C.1: Non-dimensional parameter ($\overline{P}$) vs out of plane deflection response of flat and stiffened plate for varying thickness and steel grade under uni-axial compressive loads.

DEPARTMENT OF ARCHITECTURE AND CIVIL ENGINEERING
CHALMERS UNIVERSITY OF TECHNOLOGY
Gothenburg, Sweden
www.chalmers.se

CHALMERS
UNIVERSITY OF TECHNOLOGY